

**An Investigation into the Temperature Distribution
Resulting from Cutting of Compact Bone
Using a Reciprocating Bone Saw**

A thesis submitted for the degree of
Master of Engineering

by

Hamid Khalili Parsa
B.Sc.

Department of Mechanical and Electronic Engineering
Institute of Technology, Sligo

Supervisors
Mr. Ger Reilly
Dr. Brendan McCormack

September 2006

To

My Dearest Ever

Hadi, Sedigheh, Hamed and Mozghan

Abstract

Surgical procedures such as osteotomy and hip replacement involve the cutting of bone with the aid of various manual and powered cutting instruments including manual and powered bone saws. The basic mechanics of bone sawing processes are consistent with most other material sawing processes such as for wood or metal. Frictional rubbing between the blade of the saw and the bone results in the generation of localised heating of the cut bone. Research studies have been carried out which consider the design of the bone saw which deals with specifics of the saw teeth geometry and research which examines the effect of drilling operations on heating of the bone has shown that elevated temperatures will occur from frictional overheating. This overheating in localised areas is known to have an impact on the rate of healing of the bone post operation and the sharpness life of the blade.

The purpose of this study was to measure the temperature at three zones at fixed intervals of 3mm, 6mm, and 9mm away from the cutting zone. It should be noted that it was the first time that this measurement technique was used to measure the temperature gradient through the bone specimen thereby establishing the extent to which clinicians are experiencing thermal injury during sawing of bone while using a reciprocating saw. The effect of various cutting feed rate on temperature elevation was also investigated in this research.

The results showed that there will be a region of bone at least 9mm either side of the cutting blade experiencing thermal injury as temperatures in this region exceeded the threshold temperature of 44°C for necrosis (cell death).

Declaration

This thesis describes original work which has not been submitted for a degree at any other university or college. The investigations were carried out in the Department of Mechanical and Electronic Engineering, Institute of Technology, Sligo under the supervision of Mr. Ger Reilly.

Hamid Khalili Parsa

Hamid Khalili Parsa

September 2006

Acknowledgements

It is a pleasure to acknowledge the help and support of Mr. Ger Reilly and Dr Brendan McCormack for their encouragement and advice in all stages of the research.

I would like to thank Mr. Andrew Macey for his support and allowing me to use the bone saw and saw blades.

Thanks to Gordon Muir for machining jigs and preparing the bone specimen during this research.

The support and help from Professor Hossein Valizadeh is appreciated especially since he is responsible for introducing me to the Institute of Technology, Sligo.

Many special thanks to my Irish colleagues who tolerated all my questions and supported me in all aspects during the research: John, Eamonn, Cormac, Shane, and Anthony. The support of non-Irish colleagues is also appreciated: Ashkan, Saeid, Bahman and Chan. Thank you all!

My thanks to all of the staff of the engineering workshop Ray, John, Seamus and Sam. I would also appreciate all engineering secretaries: Carmel, Mary and Margaret.

I would like to acknowledge the Council of Directors Strand I Research Program for funding this research.

My sincere appreciation to my dearest Mozghan Samiee who has been truthfully patient during my three years of research, tolerated my good or bad moods and giving me courage always to finish this research.

Finally, I would like to thank my father and mother for all their support and encouragement throughout my entire education.

Publications Resulting from this Research

Khalili Parsa, H.; Reilly, G. A.; McCormack, B. A. O. Cutting rate effect on temperature during cortical bone sawing. Proceeding of the 12th Annual Conference of the Section of Bioengineering of the Royal Academy of Medicine in Ireland, January 2006, p30

Khalili Parsa, H.; Reilly, G. A.; McCormack, B. A. O. Scanning Electron Microscopy (SEM) of saw blade wear and evaluation of thermal injury during cortical bone cutting. Proceedings of the 6th Annual Multidisciplinary Research Conference at Sligo General Hospital, Ireland, November 2005, p21

Khalili Parsa, H.; Reilly, G. A.; McCormack, B. A. O. An experimental technique for measurement of heat generated during bone sawing. Proceedings of the 19th Conference of European Society for Biomaterials combined with European Society of Biomechanics, Sorrento, Italy, September 2005, P59

Khalili Parsa, H.; Reilly, G. A.; McCormack, B. A. O.; Macey, A. An investigation of the extent of the heat affected zone in cortical bone sawing. Proceedings of the 11th Annual Conference of the Section of Bioengineering of the Royal Academy of Medicine in Ireland, January 2005, p53

Khalili Parsa, H.; Reilly, G. A.; McCormack, B. A. O.; Macey, A. Investigation of frictional heat generated in serrated cutting of bone. Proceedings of the 5th Annual Multidisciplinary Research Conference at Sligo General Hospital, Ireland, November 2004, p15

Contents

Abstract	i
Declaration	ii
Acknowledgements	iii
Publications Resulting from this Research	iv
Contents	v
Table of Figures	ix
List of Tables	xii
Chapter 1: Introduction	1
1.0 Background to Surgical Cutting Process	1
1.1 Types of Surgical Process	2
1.2 Aspects of Bone Sawing	2
1.2.1 Sawing Techniques.....	2
1.2.2 Procedures where Saws are Used.....	5
1.3 Heat, Irrigation and Cutting Forces	5
1.4 Commentary on what this Project will Focus on	6
Chapter 2: Literature Review	7
2.0 Overview	7
2.1 What is Bone?	7
2.1.1 Long Bones	7
2.1.2 Short Bones	8
2.1.3 Flat Bones	9
2.1.4 Irregular Bones	9
2.2 Structure of Bone Tissue	9
2.2.1 Cortical Bone.....	10
2.2.2 Cancellous Bone.....	11
2.2.3 Lamellar and Woven Bone.....	12
2.2.4 Primary and Secondary Bone.....	13

2.2.5	Bone Cells	15
2.2.6	Modelling and Remodelling of Bone	15
2.3	Properties of Bone	17
2.3.1	Stress and Strain	18
2.3.2	What is Heat?	20
2.3.3	Mechanical Properties of Cortical Bone	22
2.3.4	Thermal Properties of Bone	24
2.4	Thermal Injury in Bone During Cutting of Bone.....	26
2.5	Bone Osteotomy	28
2.6	Studies on Bone Cutting	29
2.7	Bone Sawing	30
2.7.1	Effects of Cutting Forces on Temperature.....	31
2.7.2	Effect of Cutting Speed on Temperature	32
2.7.3	Effects of Irrigation on Temperature	32
2.7.4	Effect of Saw Design on Temperature.....	33
2.7.5	Wear of Saw Blades.....	35
2.7.6	Oscillating Saw Blade Geometry	36
2.7.7	Geometry of Oscillating Saw Teeth	38
2.8	Drilling of Bone	40
2.8.1	Effects of Drilling Force on Temperature.....	41
2.8.2	Effects of Drilling Speed on Temperature	42
2.8.3	Effects of Irrigation on Temperature	43
2.9	Bur Cutting.....	43
2.9.1	Effects of Bur Cutting Forces on Temperature	43
2.9.2	Effects of Bur Cutting Speed on Temperature	43
2.9.3	Effects of Irrigation on Temperature	44
2.10	Effect of Depth of Cut on Temperature.....	44
Chapter 3: Materials and Methods		47
3.0	Selection of Components	47
3.1	Selection of the Appropriate Temperature Transducer	47
3.1.1	The Principle of Operation of Thermocouples.....	48
3.1.2	Thermocouples Types.....	49

3.1.3	Thermocouple Selection for Measuring Heat in Bone	49
3.1.4	Thermocouple Type T	52
3.2	Introduction to Data Loggers.....	53
3.2.1	Data Logger SQ2020	53
3.2.2	SquirrelView Software	54
3.3	Selection and use of Thermocouple Bonding Adhesive.....	55
3.4	Experimental Methods	56
3.5	Experiment 1	56
3.5.1	Preparation of Bone Specimens	56
3.5.2	Bone Clamping Fixture.....	57
3.5.3	Preparation of Thermocouple Holes.....	58
3.5.4	Drilling the Holes	59
3.5.5	Time Required for Drilling each Hole.....	59
3.5.6	Problems during Drilling	60
3.5.7	Thermocouples' Zones Relative to the Cutting Zone.....	60
3.6	Thermocouple Preparation	61
3.7	Data Logger Set-up	63
3.8	Bone Saw.....	64
3.8.1	Saw Blade	65
3.9	Experimental Procedure	65
3.10	Sawing Procedure in Experiment 1	68
3.10.1	Problems During Sawing Procedure.....	70
3.11	Experiment 2	71
3.11.1	Bone Specimen Preparation	71
3.12	Saw Blade Inspection	74
3.12.1	Blade Inspection by Shadow Graph	74
3.12.2	Using SEM for Examination of the Blades.....	75
3.12.3	Test Set up for SEM	75
3.13	Preparation of Experimental Data for Result Analysis	76
3.13.1	Bone Removal Volume.....	76
3.13.2	Rate of Bone Removal.....	78

Chapter 4: Results and Discussions	79
4.1 Overview	79
4.2 Typical Temperature Measurement Graph	79
4.3 Experiment 1 Results	84
4.3.1 Average Maximum Temperatures in each Zone	84
4.3.2 Total Time that Temperatures Exceeded 44°C	88
4.3.3 Rate of Temperature Increase	89
4.4 Experiment 2 Results	91
4.4.1 Average Maximum Temperatures in each Zone	91
4.4.2 Total Time that Temperatures Exceeded 44°C	93
4.4.3 Effect of Cutting Rates on Temperature Response	93
4.4.4 Force Measurement	96
4.4.5 Comparison of Different Forces at Different Cutting Rates	97
4.5 Blade SEM Observation Results	99
4.6 Threshold for Necrosis	102
Chapter 5: Conclusions and Future Work	104
References.....	107
Appendix A (Experiment 1 Graphs)	
Appendix B (Experiment 2 Graphs)	
Appendix C (Technical Sheets)	

Table of Figures

Figure 1.1: Reciprocating blade	3
Figure 1.2: Oscillating saw blade	3
Figure 1.3: Schematic of saggital saw blade	3
Figure 1.4: Circular bone saw and blades	4
Figure 1.5: Typical modern hand saw	4
Figure 1.6: Gigli saw	5
Figure 2.1: Illustration of a typical long bone in humerus	8
Figure 2.2: Hierarchical structural organisation of bone	10
Figure 2.3: Sketch of a typical long bone	11
Figure 2.4: Morphology of cancellous bone	12
Figure 2.5: Lamellar bone structure	12
Figure 2.6: The formation of plexiform bone	13
Figure 2.7: Plexiform bone	14
Figure 2.8: Illustration of Haversian systems and interstitial lamellae	14
Figure 2.9: Remodelling sequence in cortical bone showing the cutting cone	17
Figure 2.10: Typical remodelling process in cancellous bone	17
Figure 2.11: Conventional definition of stress	18
Figure 2.12: Normal strain	18
Figure 2.13: Stress-strain curve of bone	19
Figure 2.14: Different types of stress	20
Figure 2.15: A perfectly insulated block	21
Figure 2.16: Proportional relation of heat transfer with insulation	21
Figure 2.17: A block without insulation	22
Figure 2.18: Exponential relation of heat transfer with no insulation	22
Figure 2.19: Illustration of the cutting modes relative to predominant osteon direction	29
Figure 2.20: Orthogonal cutting illustration	30
Figure 2.21: Temperature recorded on saw blade	31
Figure 2.22: Illustration of double saw blade	33
Figure 2.23: Different temperature response in 2 different saw blades	34
Figure 2.24: Different saw blade design	34
Figure 2.25: Oscillating saw blade dimensions	37

Figure 2.26: Measurement of tooth offset.....	37
Figure 2.27: Oscillating saw tooth arrangement.....	38
Figure 2.28: Dimension of oscillating saw teeth.....	39
Figure 2.29: Illustration of different rake angles.....	39
Figure 2.30: Temperature at different location from drilling site.....	40
Figure 3.1: Schematic layout of typical heat measurement experiment.....	47
Figure 3.2: Thermocouple type T.....	52
Figure 3.3: Illustration of thermocouple type T international color code.....	52
Figure 3.4: Rear view of PHOENIX connectors.....	53
Figure 3.5: SQ2020 data logger.....	54
Figure 3.6: SquirrelView Assistant window.....	54
Figure 3.7: Bone clamping fixture.....	57
Figure 3.8: Drill template and its dimensions.....	58
Figure 3.9: Drilled holes.....	59
Figure 3.10: Thermocouples position relative to the sawing line in Experiment 1.....	61
Figure 3.11: Thermocouples type T glued and inserted into the drilled holes.....	62
Figure 3.12: 18097 connector.....	62
Figure 3.13: Data logger setup block diagram.....	63
Figure 3.14: 3M Maxi Driver saw and its attachments.....	64
Figure 3.15: Reciprocating coarse P512 blade.....	65
Figure 3.16: Schematic of the Experiment 1.....	66
Figure 3.17: Illustration of half way transverse cut.....	67
Figure 3.18: Top view of a marked bone.....	68
Figure 3.19: Cutting process in Experiment 1.....	68
Figure 3.20: Top view illustration of sawing. Blade location relative to thermocouples.....	69
Figure 3.21: Sawing with blade held in horizontal position.....	70
Figure 3.22: Sawing with blade held in see-sawing action.....	70
Figure 3.23: Typical temperature graph for tests in which saw blade jammed in bone specimen.....	71
Figure 3.24: Thermocouples position relative to the Sawing Zone in Experiment 2.....	72
Figure 3.25: Schematic of the Experiment 2.....	73
Figure 3.26: Close-up of cutting process in Experiment 2.....	73
Figure 3.27: Blade profile in shadow graph.....	75
Figure 3.28: Blade setup in SEM machine.....	76
Figure 3.29: Transected section of bone and limit of sawing process by 3M and band saw....	77
Figure 3.30: Illustration of CSA of the transected section of bone.....	78

Figure 4.1: Typical temperature measurement graph in Experiment 1 showing 3 zones.....	80
Figure 4.2: Temperature at different location from drilling site.....	80
Figure 4.3: Thermocouples arrangement relative to Sawing Zone in Experiment 1.....	81
Figure 4.4: Three stages of cutting showing blade relative to thermocouples	82
Figure 4.5: Typical temperature measurement graph in Experiment 2	84
Figure 4.6: Comparison of necrosis threshold with average maximum temperatures in 3 zones	85
Figure 4.7: Selection of maximum temperature in zones for extrapolation of saw blade temperature	86
Figure 4.8: Extrapolated values for Sawing Zone	87
Figure 4.9: Illustration of zones exceeding necrosis value more than 60 sec for 20 tests.....	89
Figure 4.10: Comparison of rise time in 3 different zones for 20 tests	90
Figure 4.11: Illustration of rise time versus CSA in 3 zones.....	90
Figure 4.12: Pooled mean value of temperatures at different rates at various distances.....	92
Figure 4.13: Illustration of zones exceeding necrosis value more than 60 sec for 9 tests.....	93
Figure 4.14: Average maximum temperatures for 3 zones at different rates	94
Figure 4.15: Temperature rise as a function of feed rate.....	94
Figure 4.16: Result of one way ANOVA on the effect of cutting rate on record temperature.....	95
Figure 4.17: Typical force graph for cutting rate of 2 mm/min	97
Figure 4.18: Illustration of average force at 3 different cutting rates.....	98
Figure 4.19: Temperature decrease as a result of sticking blade.....	99
Figure 4.20: SEM image of new unused blade in view adjacent to the cutting edge.....	100
Figure 4.21: SEM image of cutting edge of the new unused blade.....	100
Figure 4.22: SEM image of used blade in view adjacent to the cutting edge.....	101
Figure 4.23: SEM image of cutting edge of the used blade	101
Figure 4.24: Cutting edge after 15 trials.....	102

List of Tables

Table 2.1: Bone cells description	15
Table 2.2: Bone remodelling stages	16
Table 2.3: Typical mechanical properties of cortical bone.	23
Table 2.4: Thermal properties definitions	24
Table 2.5: Cortical bone thermal conductivity values according to different researchers.	26
Table 2.6: Maximum temperature recorded while using various saw blades in bovine bone cutting	35
Table 2.7: Geometry of oscillating saw blade	36
Table 2.8: Summary of maximum cortical bone temperatures in studies	46
Table 3.1: Comparison of common types of temperature transducers	50
Table 3.2: Thermocouples types, conductor combinations, characteristics, approximate working temperature, and international color code.....	51
Table 3.3: Specifications for LOCTITE® 454 GEL	55
Table 4.1: Extrapolated average maximum saw temperature in each test in Experiment 1	88
Table 4.2: Various CSA and sawing time for different bone samples in Experiment 1.....	91
Table 4.3: Average maximum temperatures and pooled mean at 3 cutting rates in 4 zones....	92

Chapter 1

Introduction

Chapter 1: Introduction

1.0 Background to Surgical Cutting Process

The cutting of bone is one of the oldest surgical operations in the history of medicine and cutting of bone has been experienced since prehistoric time. Medical amputation was performed with saws made of bone and stone. Trepanation, an operation to take a portion of the skull bone away, may have been performed as far back as 10,000 B.C (Majno, 1975).

The *Hippocratic Corpus*, the starting point of professional medicine, mentions the cases for trepanation as contusion and fissure-fracture, in addition to dents in the skull without fracture. The apparatus used by the Greek physicians was a pointed drill (trypanon), or a crown drill (pridn) which were operated by rolling between the palms or spun by a cord or bow moved crosswise like those used on wood for starting fires.

The practice of using surgical saws dates back to the reign of Tiberius (14 to 37 A.D.) when Celsus illustrated the style of amputating gangrenous limbs. The advance of anesthesia and the wars of the nineteenth century, mostly the American Civil War, increased the use of amputation and the cutting of bone. Amputations were made on any gunshot wound to the leg to fight infection and avoid gangrene. Cutting of the bone was the longest part of the procedure; hence a sharp saw was a precious tool at that time. Hand tools designed for surgical machining of bone have changed in the last 130 years (Wiggins and Malkin, 1978). In recent years, the use of motor-driven burrs, drills, and saws has become more prevalent. Nowadays, clinicians utilise powered saws and drills to decrease the operating time and to present more accurate and precise cuts for arthroplasty insertion and fracture fixation device insertion. The saw

tooth design of today's saws and drills has not changed much over the centuries. Although the cutting speeds of these newer instruments are greater than those of hand-operated ones, the fundamental mechanism of operation of actual cutting tools has not been altered as a result of this evolution.

1.1 Types of Surgical Process

There are several types of surgical cutting process such as sawing, drilling, and reaming which are power cutting. There are other cutting processes which are performed manually including the use of scalpels, chisels, osteotomes, scissors, etc. This thesis will concentrate on the use of power cutting tools particularly sawing and investigate the generation of heat during cutting procedures.

1.2 Aspects of Bone Sawing

In general, bone saws and bone saw blades are used to cut small and large bones in a way that allows the best surgical outcome for the patient. It should be noted that for each specific surgical procedure, different saws and blades have been optimised. Key aspects of the cutting process are the techniques either powered or manual sawing, the saw blade types and heat effect, irrigation and cutting forces impact on temperature.

1.2.1 Sawing Techniques

Surgical sawing may be divided into two categories: power and manual sawing. Power saws available are of electric and pneumatic types. Compressed air powered saws are frequently used for orthopaedic surgery. Power saws such as oscillating and reciprocating saws allow clinicians to make accurate cuts with a lot less effort than with hand saws. The types of power saws most commonly used are:

Reciprocating Saw: This is a quick-cutting instrument for procedures where visibility and reach are a problem (MicroAire Surgical Instruments LLC, Virginia, USA) and it is used for quick cutting, shaping and contouring bone (Hall® Surgical, Linvatec Corporation, USA), for removing the skull cap, making linear cuts, or taking small bone specimens. Figure 1.1 shows a reciprocating saw blade.



Figure 1.1: Reciprocating blade

Oscillating Saw: Oscillating saw movement is defined as an alternating circular movement, defined over an arc of a circle. Figure 1.2 shows the 3M Maxi Driver™ oscillating blade L124.



Figure 1.2: Oscillating saw blade

Sagittal Saw: The sagittal saw hand piece offers good control, power, maneuverability, and visibility for correcting transverse or wedge osteotomies.



Figure 1.3: Schematic of sagittal saw blade

Circular Saw: The blade of a circular saw is similar to that of a handsaw. The basic difference is that the circular saw has a round blade driven by a motor. The circular saw was invented to replace the handsaw.



Figure 1.4: Circular bone saw and blades (www.frets.com/FRETSPages/Luthier/Tools)

Manual sawing involves the use of hand saw and gigli saw as below:

Hand Saw: The hand saw (Figure. 1.5) can be used to saw through the skull, but is much slower than the more commonly used vibrating saw. Hand saws looking very like carpenters' saws are sometimes used for working on large bones.



Figure 1.5: Typical modern hand saw (www.cutleryandmore.com)

Gigli Saw: This is a flexible wire with sharp edges (Figure 1.6), and has the advantage of permitting bone cutting without the need to excise tissue in a large

operating area. The saw is operated using both hands, the flexible blade is oscillated across the target material using sawing action.



Figure 1.6: Gigli saw (<http://www.pbs.org>)

1.2.2 Procedures where Saws are Used

Some of the more common orthopaedic procedures requiring bone saws and reciprocating blade components are: hip and knee replacement, spinal surgery (neck and back), hand including ulnar shortening (Labosky and Waggy, 1996; Firoozbakhsh et al., 2003), wrist, elbow, and shoulder surgery. For different procedures, different saws are utilised as well as various saw blades.

1.3 Heat, Irrigation and Cutting Forces

Issues with power cutting include the heat generation, cutting force (force in direction of cutting) and the use of irrigant. Cutting fluids can enhance the performance of cutting tools by cooling the cutting tool and the workpiece, by lubricating the cutting surfaces of the tool, and by flushing the chips from the work area. Moreover, reduction of frictional rubbing and heat generation and increase in tool life may stem from using coolant.

The reduction of energy and the cutting forces makes it possible to reduce the thermal effect during cutting, and also reduces the amount of effort that has to be made by the surgeon and the tool. The tool wears out less quickly and the surgeon has better control of the instrument, thus ensuring greater manual precision. The shape of the teeth, as with saws, has a direct influence on the amount of heat generated.

1.4 Commentary on what this Project will Focus on

Bone cutting has always been a problem for surgeons. Due to the fact that bone is a hard living material, available techniques for the cutting of bone are still evolving. Many difficulties have been encountered in osteotomy procedures. Problems such as osteonecrosis, frictional heat, clogging, bluntness of tools, and the importance of sharp blades are critical. Orthopaedic bone cutting procedures such as osteotomy and hip arthroplasty involve the cutting of bone with the aid of various cutting instruments including manual and powered bone saws. During surgical procedures the frictional heat generated between the saw blade and bone may cause temperatures to exceed 44°C; the threshold temperature for impaired regeneration of bone (Eriksson et al., 1984), and bone necrosis (cell death) which has a critical impact on bone regeneration and post operative bone healing.

The main aims of this research project are:

1. Development of an experimental technique to measure the temperature in the localised cutting zone during bone sawing;
2. Investigation of the size of the heat affected zones during bone sawing;
3. Investigation of the effect of parameters such as cutting feed rate, and bone cortex thickness on temperature gradient during bone sawing.

Chapter 2

Literature Review

Chapter 2: Literature Review

2.0 Overview

In this chapter the literature regarding bone structure and cutting of bone will be reviewed; the literature review in this study is divided into two particular sections. In the first section the principal definitions related to bone such as what bone is, different types of bone and their structure will be discussed. Next, the mechanical and thermal properties of bone will be outlined. The second section consists of primary cutting procedures like sawing, drilling, and bur cutting and parameters affecting these cutting processes.

2.1 What is Bone?

Bone is a hard, dense tissue that forms the skeleton. In addition to providing shape and structure to the body, bone stores mineral salts and also is involved with cell formation and calcium metabolism. Bones are different in shape and size and they are classified according to four principal types: long bones, short bones, flat bones, and irregular bones.

2.1.1 Long Bones

Long bones are found in the thigh, lower leg, arm, and forearm and include femur, tibia, and fibula (paired), humerus, radius, and ulna (paired). Figure 2.1 shows the typical structure of a human long bone. The central shaft of a long bone is called the diaphysis consisting of a wall of cortical bone and a hollow core called the medullary cavity or marrow cavity containing bone marrow. The ends of the bone are called the epiphyses, and are mostly cancellous bone covered by a relatively thin cortex of

cortical bone. In children, the bones are filled with red marrow (responsible for the formation of blood cells), which is gradually replaced with yellow marrow (fatty tissue) during maturation.

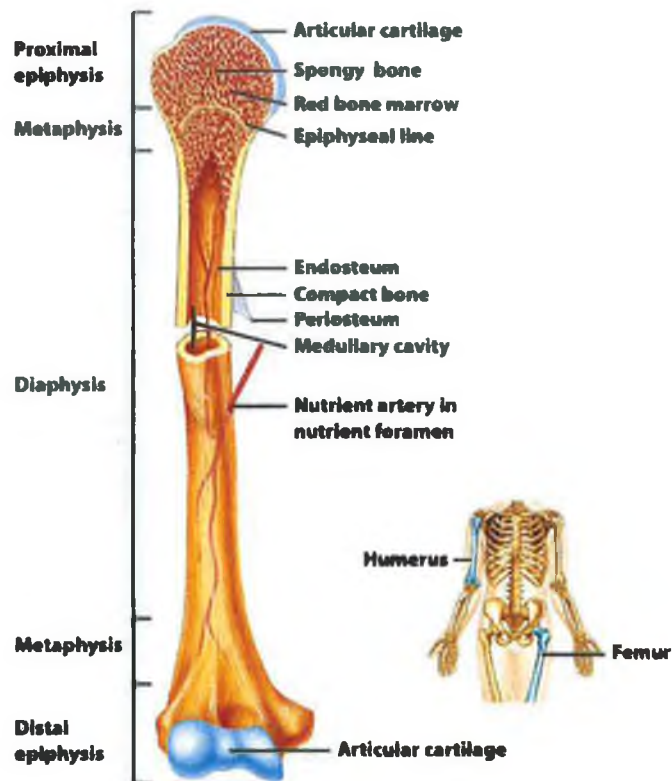


Figure 2.1: Illustration of a typical long bone in humerus (Tortora and Derrickson, 2005)

2.1.2 Short Bones

The structure of short bones is similar to that of long bones, except that they have no medullary cavity. They contain mostly cancellous bone with outer layer of cortical bone. Short bones include the bones of the wrist, ankle, and fingers.

2.1.3 Flat Bones

Flat bones (e.g. the skull and ribs) consist of two layers of cortical bone with a zone of cancellous bone sandwiched between them. Their cross-section is flat and they have marrow, but not a bone marrow cavity.

2.1.4 Irregular Bones

Irregular bones are bones which do not conform to any of the previous forms (e.g. vertebrae) and are variable in size and shape. These are made of cancellous bone covered with a thin layer of cortical bone.

2.2 Structure of Bone Tissue

Figure 2.2 indicates the hierarchical structural organisation of bone at various levels. There are two types of bone tissue in the macrostructure level: compact or cortical bone and trabecular or cancellous bone. These two types of bone vary in density dependant on how tightly the tissue features are packed together. There are other levels as below:

- a. **Microstructure:** Haversian systems and osteons;
- b. **Sub-microstructure:** Lamellae (a planar arrangement of mineralised collagen fibres);
- c. **Nanostructure:** Fibrillar collagen and embedded mineral;
- d. **Sub-nanostructure:** Mineral, collagen and non-collagenous organic proteins.

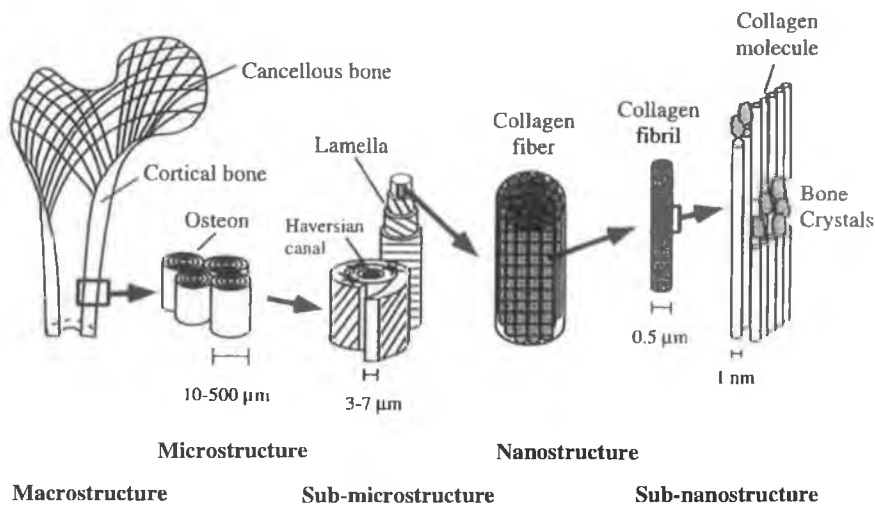


Figure 2.2: Hierarchical structural organisation of bone (Rho et al., 1998)

2.2.1 Cortical Bone

Cortical bone is a dense bone with a porosity ranging between 5% and 10% (Martin et al., 1998). It consists of closely packed secondary osteons also called Haversian systems. The osteon has a central canal called the Haversian canal, which is about $50 \mu\text{m}$ in diameter, and surrounded by about 16 concentric rings (lamellae) of bone matrix. The diameter of an osteon is about $200 \mu\text{m}$ (Martin et al., 1998). Between the rings of the matrix, osteocytes are positioned in sites called lacunae. Osteocytes are connected to each other via a series of small channels called canaliculi, which are used for exchange of nutrients and waste. The Haversian systems are compactly organised in cortical bone resulting in a dense structure. Haversian canals consist of blood vessels that are parallel to the long axis of the bone and these are connected to each other and to the outside of the bone by means of Volkmann's canals. Figure 2.3 shows the structure of cortical bone from the periosteal to the endosteal surfaces. It may be observed that the periosteal surface is composed mostly of concentric layers of bone running around the entire outer surface of the long bone. This is called

lamellar bone. The internal structure is composed of a dense structure of Haversian systems as previously described. Cancellous bone exists on the endosteal surface in the region of the bone epiphysis.

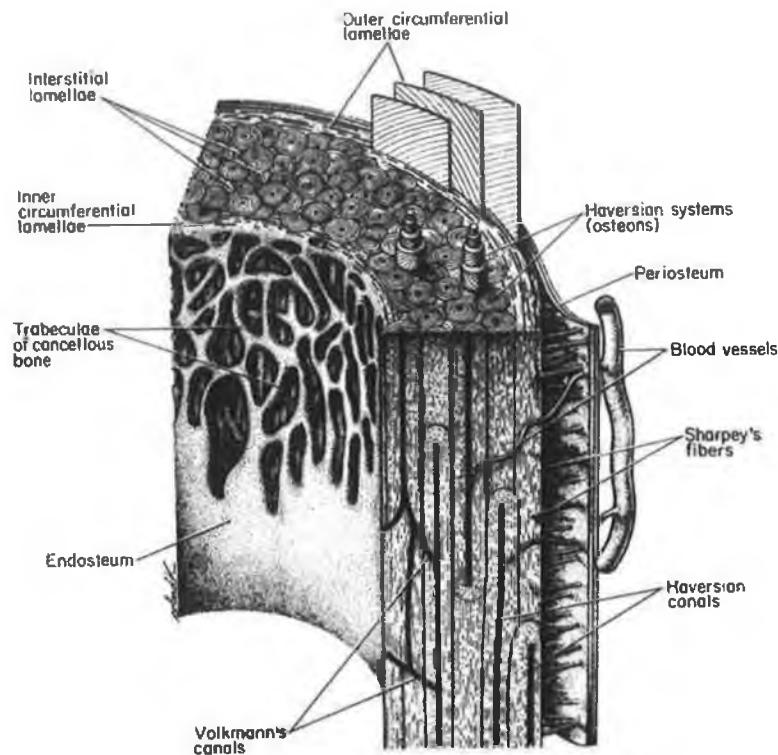


Figure 2.3: Sketch of a typical long bone (After Benninghoff, 1944 reported in Martin et al., 1998)

2.2.2 Cancellous Bone

Cancellous bone is less dense than cortical bone. Its porosity is 75%-95% (Martin et al., 1998). The pores contain red bone marrow and are interconnected between the struts and plates forming the bone structure. The structure of cancellous bone (Figure 2.4) is in the shape of randomly arranged plates which are known as trabeculae. The thickness of each trabeculae is about 200 μm (Martin et al., 1998). Haversian canals and osteons present in cortical bone are not found in cancellous bone.

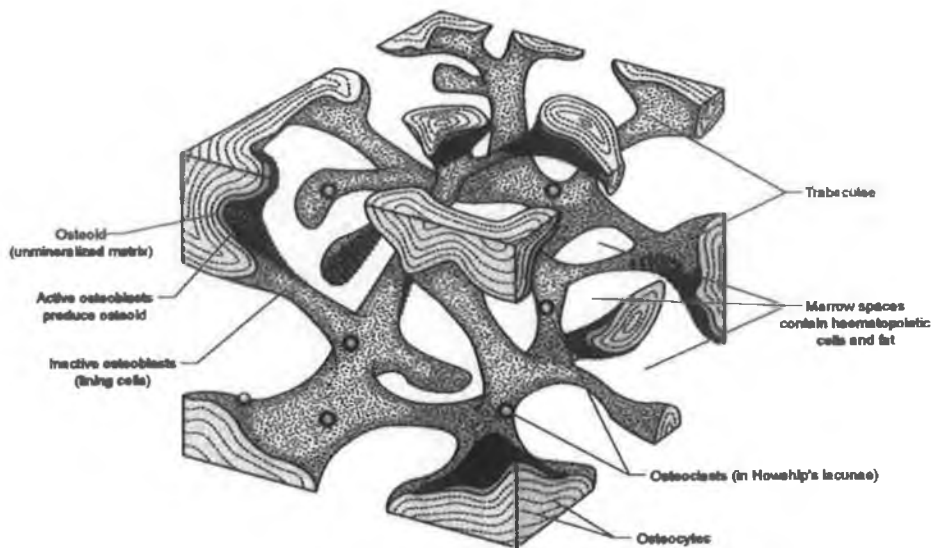


Figure 2.4: Morphology of cancellous bone (Sambrook, 2004)

2.2.3 Lamellar and Woven Bone

Cortical and cancellous bones may contain two kinds of bone tissue, either woven or lamellar. Woven bone is laid down rapidly, more than $4 \mu\text{m}$ a day, during growth or repair which explains its disorganised structure (Currey, 2002). It is so called because its fibres are aligned at random, and as a result has low strength. In contrast lamellar bone as illustrated in Figure 2.5 is slowly formed, has highly organised parallel fibres called lamellae and is much stronger. Woven bone is often replaced by lamellar bone as growth continues.



Figure 2.5: Lamellar bone structure
(<http://www.engin.umich.edu/.../bonestructure.htm>)

2.2.4 Primary and Secondary Bone

Cortical bone may be further characterised as primary or secondary bone. Primary bone is put down *de novo* on an existing bone surface; for instance; the periosteal surface, during growth. It may include circumferential lamellar bone and plexiform bone. Plexiform, or fibrolamellar cortical bone has a structure like a “brick wall” (Martin et al., 1998). It is primarily found in large, fast-growing animals like cows (Currey, 2002).

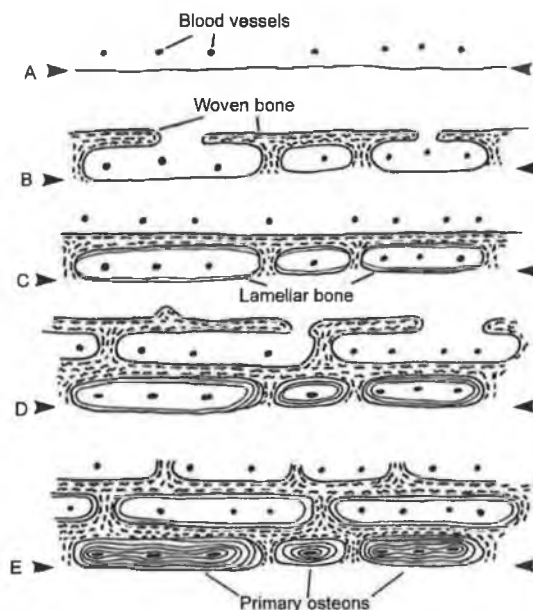


Figure 2.6: The formation of plexiform bone (Currey, 2002)

Figure 2.6 shows the growth of plexiform bone and illustrates how bone is laid down around vascular channels forming woven bone, then lamellar bone and finally primary osteons. Figure 2.7 is the illustration of the plexiform bone.



Figure 2.7: Plexiform bone
 (<http://www.engin.umich.edu/.../bonestructure.htm>)

Secondary bone stems from replacement of existing bone by new lamellar bone. It results from a process known as remodelling. This bone consists of cylindrical structures known as secondary osteons or Haversian systems which were described earlier. The boundary between the osteon and the surrounding bone is called the cement line. In adult humans, most cortical bone is made up of secondary bone, which may consist of entire osteons and the remains of older osteons that have been partially resorbed (interstitial bone, shown in Figure 2.8).

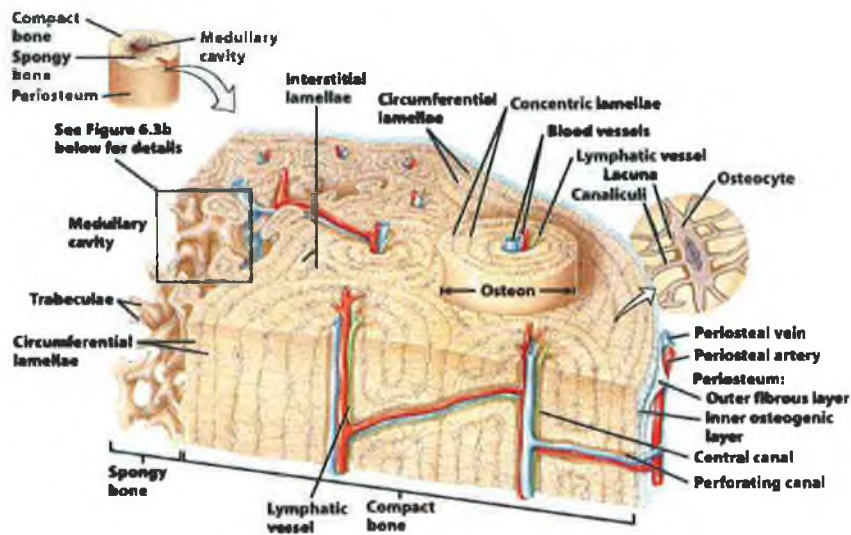


Figure 2.8: Illustration of Haversian systems and interstitial lamellae (Tortora and Derrickson, 2005)

2.2.5 Bone Cells

There are four types of bone cells including osteoblasts, osteoclasts, osteocytes, and bone lining cells as described below in Table 2.1.

Cell	Description
Osteoclasts	Bone resorbing cells located on bone surfaces in what are called Howship's lacuna. They are large cells which demineralise the adjacent bone with acids by dissolving its collagen (Martin et al., 1998).
Osteoblasts	Bone forming cells which are responsible for the formation of bone. They are located near to the bone surface and responsible for manufacture of osteoid, which is primarily composed of collagen, noncollagenous proteins, proteoglycans, and water.
Osteocytes	Originate from osteoblasts. They are former osteoblasts that become trapped and surrounded by bone matrix which they themselves produce. The space which they occupy is known as a lacuna.
Lining cells	Retired osteoblasts which escaped being trapped and buried in newly formed bone. They rest on the bone surface when formation stops.

Table 2.1: Bone cells description

Osteoblasts and osteoclasts work together in the bone structure like a team and they are dependent on each other. These teams of bone cells are known as BMUs (Basic Multicellular Units).

2.2.6 Modelling and Remodelling of Bone

Modelling is the continuous process by which bone mass increases to change the shape, size, and structure of the bone. This occurs during bone growth by resorption and formation of bone at different sites and rates.

Remodelling is a cyclical progress by which bone maintains a steady state through resorption and formation of a small amount of bone at the same site. Remodelling eliminates a portion of older bone and replaces it with newly formed bone.

Microscopic damage and fatigue fracture are repaired by remodelling process. Martin et al. (1998) have hypothesised that remodelling ‘fine tunes’ the skeleton mechanically to increase its mechanical efficiency. There are five stages in bone remodelling as outlined in Table 2.2.

Stage	Description
1. Activation	Recruitment of osteoclasts to a bone surface and signal coupling of osteoblasts
2. Resorption	Resorption of bone by osteoclasts and the Howship’s lacuna is created at this stage
3. Reversal	Osteoclasts stop resorbing and osteoblasts start refilling the defect region
4. Formation	Laying down of bone by osteoblasts and lacuna is filled with osteoid
5. Quiescence	Resting of the bone surface; bone lining cells rest on the surface of the new piece of bone

Table 2.2: Bone remodelling stages

Figure 2.9 illustrates the remodelling sequence in cortical bone and cutting cone. Osteoclasts resorb tunnels along the longitudinal axis of the bone. Following a reversal phase, osteoblasts begin depositing concentric layers of new bone matrix to gradually fill the tunnel while the central canal of the secondary osteon is lined by resting osteoblasts. The typical remodelling process in cancellous bone is also shown in Figure 2.10.

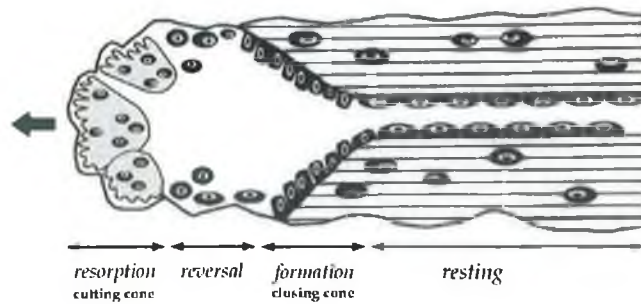


Figure 2.9: Remodelling sequence in cortical bone showing the cutting cone (Arnett, 2005)

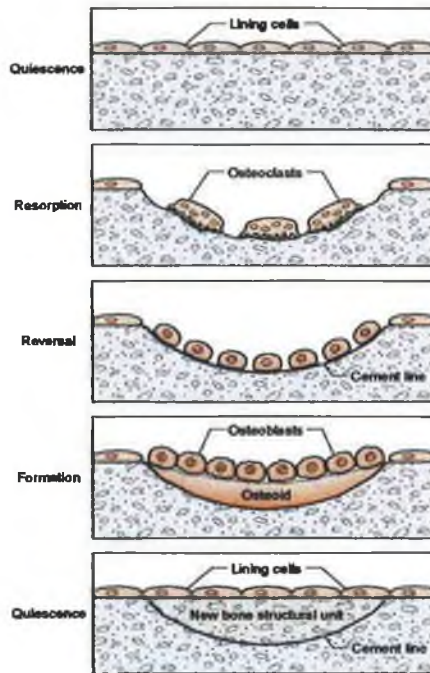


Figure 2.10: Typical remodelling process in cancellous bone (Sambrook, 2004)

2.3 Properties of Bone

Bone is hierarchical, has a varying macrostructure, is anisotropic and so has different characteristics in different dimensions when loaded in different ways. Many studies have been carried out regarding mechanical and thermal properties of bone.

2.3.1 Stress and Strain

Geometry and the properties of a loaded material are important when considering mechanical properties of a structure. In this regard, stress and strain are fundamental to this concept.

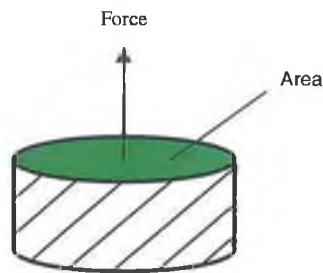


Figure 2.11: Conventional definition of stress

Stress is related to the load applied to a material and the size of the cross sectional area under load as shown in Figure 2.11 by the formula:

$$\sigma = F/A,$$

where F is the load and A represents the cross-sectional area through which the force is applied. Stress is usually measured in pascals (Pa) or N/m^2 .

Strain is the fractional change in dimension of a loaded material. It has no units and it is reported as relative to deformation (a strain of 0.01=1% deformation) (Turner and Burr, 1993). It is represented by the symbol ϵ .

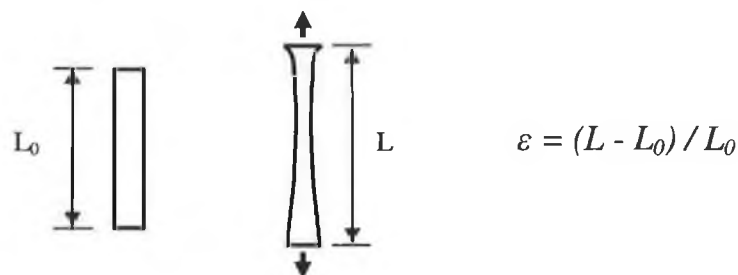


Figure 2.12: Normal strain

L is the length of the object after deformation and L_0 is the original length.

Figure 2.13 shows a typical load-deformation (stress-strain) curve for bone which consists of an elastic and plastic region. When load increases in the elastic region, the deformation increases linearly. Permanent deformation begins to occur at the yield point where bone starts to deform plastically. Therefore, this region beyond the yield point is called plastic region. If the load applied increases, failure or fracture takes place at the failure point (Turner and Burr, 1993; Martin et al., 1998; Currey, 2002).

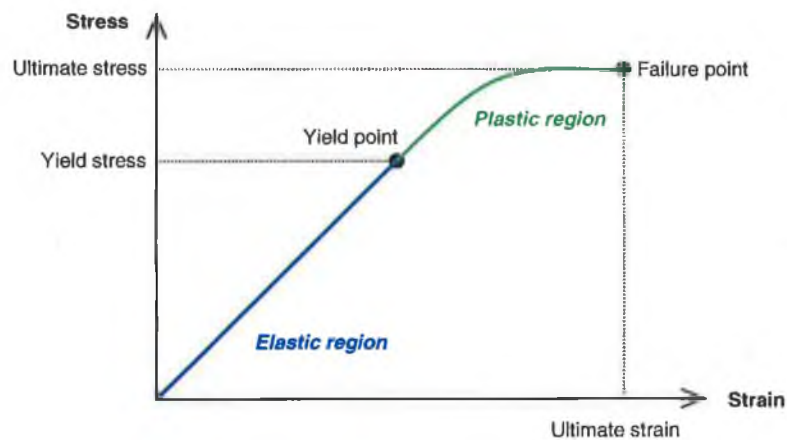


Figure 2.13: Stress-strain curve of bone

The slope of stress-strain curve within the elastic region is known as Elastic Modulus or Young's Modulus which is a measure of natural stiffness or rigidity of the material for normal loading (tension or compression) (Martin et al., 1998). When a structure is loaded in tension, it gets longer in the load direction but it gets narrower in the transverse directions. The ratio of the transverse strain to the longitudinal strain is called Poisson's ratio. Different loading scenarios produce different stress types in a structure described as compressive, tensile, shear, torsion, and bending stress (Turner and Burr, 1993). Figure 2.14 illustrates the different stresses relative to the load condition.

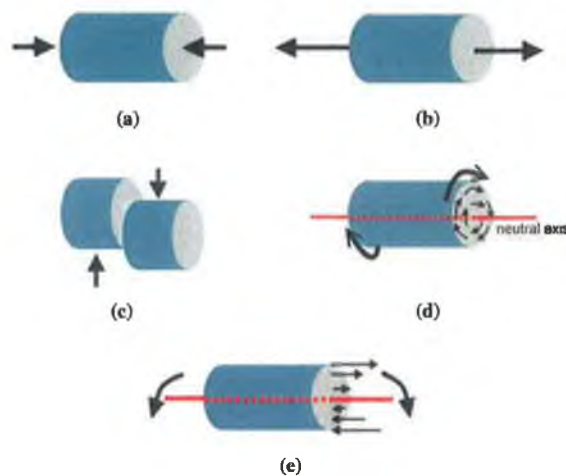


Figure 2.14: Different types of stress
 (a) Compression, (b) Tension, (c) Shear, (d) Torsion, (e) Bending

2.3.2 What is Heat?

Heat is a form of energy that is transferred by a difference in temperature. It usually moves from the warmer substance to the cooler substance until they usually reach the same temperature. There are three different ways which heat can be transferred: conduction, convection, and radiation. In this thesis, the focus is on the conduction which is the transfer of heat from one substance to another through direct contact between them. Heat can be produced as the result of friction between the cutting tool and the bone. Heat can be transferred through the bone by conduction and this might be harmful for bone tissue. The time rate of heat flow Q through a perfectly insulated block, as shown in the Figure 2.15 is proportional to the gradient of temperature difference (Figure 2.16).

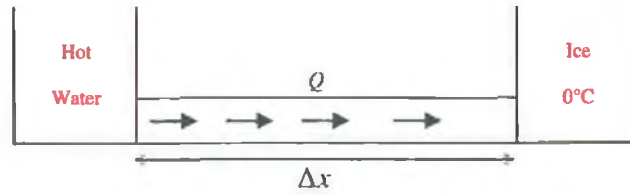


Figure 2.15: A perfectly insulated block

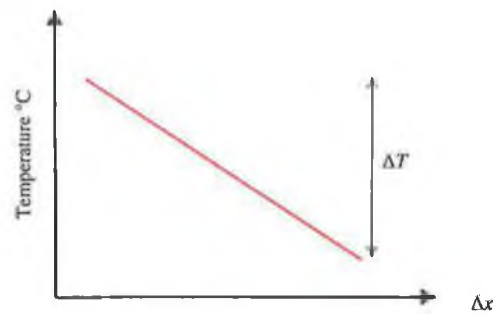


Figure 2.16: Proportional relation of heat transfer with insulation

The heat conduction formula is as below:

$$Q = KA \frac{\Delta T}{\Delta x}$$

K is thermal conductivity, A is the area, Δx is thickness of the body of matter through which the heat is passing, and ΔT is the temperature difference through which the heat is being transferred.

If no insulation is used (Figure 2.17), heat loss will occur and the corresponding graph will be exponential (Figure 2.18).

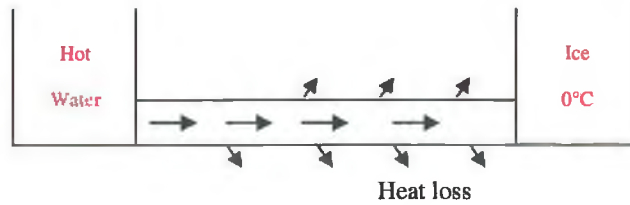


Figure 2.17: A block without insulation

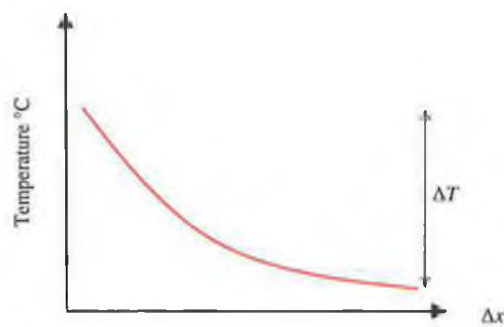


Figure 2.18: Exponential relation of heat transfer with no insulation

It seems that in most bone cutting procedures using reciprocating or oscillating saw, there is heat loss to the surrounding environment as no insulation would be used during normal operative procedures, so in this series of experiments conducted in this research, which will be explained in Chapter 3, it is assumed that the result may be best fitted with an exponential curve for all experiments.

2.3.3 Mechanical Properties of Cortical Bone

Table 2.3 show the typical mechanical properties of cortical bone in human and bovine cited in Martin et al. (1998). Bone is considered as an anisotropic material due to the fact that it has different properties in different directions.

Property	Human	Bovine
Elastic Modulus, (GPa)		
Longitudinal	17.4	20.4
Transverse	9.6	11.7
Bending	14.8 ^a	19.9 ^b
Poisson's ratio	0.39	0.36
Tensile yield stress, (MPa)		
Longitudinal	115	141
Transverse	-	-
Tensile ultimate stress, (MPa)		
Longitudinal	133	156
Transverse	51	50
Tensile ultimate strain		
Longitudinal	0.0293	0.0072
Transverse	0.0324	0.0067
Compressive yield stress, (MPa)		
Longitudinal	182	196
Transverse	121	150
Compressive ultimate stress, (MPa)		
Longitudinal	195	237
Transverse	133	178
Compressive ultimate strain		
Longitudinal	0.0220	0.0253
Transverse	0.0462	0.0517
Shear modulus, (GPa)	3.51	4.14
Shear yield stress, (MPa)	54	57
Shear ultimate stress, (MPa)	69	73
Shear ultimate strain	0.33	0.39
Bending ultimate stress, (MPa)	208.6 ^a	223.8 ^b
Bending ultimate strain	-	0.0178 ^b

Table 2.3: Typical mechanical properties of cortical bone in human (tibia and femur) and bovine (femur). Data listed from Cowin (1989), pp. 102, 103, 111-113, except as indicated (adapted from Martin et al., 1998).

^a From Currey and Butler (1975); adult femur, three-point bending.

^b From Martin and Boardman (1993); tibia, three-point bending.

2.3.4 Thermal Properties of Bone

Thermal properties of bone tissue have been studied by some researchers (Lundskog, 1972; Balasubramaniam and Bowman, 1977; Zelenov, 1985; Biyikli et al., 1986; Ranu, 1987; Moses et al., 1995; Davidson and James, 2000) and the values published illustrate a degree of variability. Aside from the wide variation in the quantitative results obtained from these studies, test methods and procedures have also varied significantly. It has been shown that the structure of bone either cortical or cancellous, including the bone matrix, fat and water contents, and vascular system have a significant role in the properties of bone (Biyikli et al., 1986). The most important thermal characteristic of a material are summarised in Table 2.4.

Thermal properties terms	Scientific definition
Specific heat “C” (J/kgK)	is the measure of the heat energy required to raise the temperature of a specific quantity of a substance by 1 K.
Thermal conductivity “k” (W/mK)	is the intensive property of a material that indicates its ability to conduct heat.

Table 2.4: Thermal properties definitions

Lundskog (1972) implanted a heated rod into rabbit tibia and observed that the isotherms near the rod were circular, and thus concluded that cortical bone is thermally isotropic. This conclusion is similar to that of Davidson and James (2000). On the other hand, Zelenov (1985) investigated the thermophysical properties of human cadaveric femoral cortical bone and found higher conductivity and diffusivity in the longitudinal direction than in the transverse direction as shown in Table 2.5.

Abouzgia and James (1997) reached the conclusion that bovine cortical bone was thermally anisotropic as they found different temperature gradients in different directions while drilling through bone, consistent with Zelenov's results. They observed an average temperature drop of 20°C in the longitudinal direction and about 8°C over the same distance in the circumferential direction.

Biyikli et al. (1986) who were the only investigators who utilised insulation in their experimental test measured thermal properties of human femur and heat flow. They found thermal conductivity of 0.3W/mK for fresh human cortical bone while Davidson and James (2000), who used similar methods, measured the thermal conductivity of bovine cortical bone (using insulation) around 0.56 ± 0.039 W/mK which is almost double Biyikli et al.'s result. As Biyikli et al. (1986) did not mention anything regarding use of any thermal conductive paste to eliminate air gaps between the bone sample and other parts of the system, this may be the reason for different thermal conductivity value in these two studies as the presence of an air gap acting like a thermal insulator will have the effect of reducing effective heat transfer to the measurement thermocouple and thereby resulting in lower apparent thermal conductivity.

Table 2.5 illustrates the different thermal conductivity values of cortical bone which have been measured by various researchers.

Researcher	Bone samples	Conductivity (W/mK)
Chato (1965)	Fresh, human	0.38
Kirkland (1967)	Bovine and caprine	0.888-3.08
Vachon et al. (1967)	Dry ox	0.601
	Fresh ox	2.27
Lundskog (1972)	Dry, human	3.56
	Human (longitudinal)	12.8
Zelenov (1985)	Human (radial)	9.7
	Human (circumferential)	9.9
Biyikli et al. (1986)	Fresh, human	0.3
	Dry, human	0.2
Moses et al. (1995)	Saturated, equine	0.80
	Dry, equine	0.70
Davidson and James (2000)	Fresh, bovine (longitudinal)	0.58
	Fresh, bovine (radial)	0.54
	Fresh, bovine (circumferential)	0.53

Table 2.5: Cortical bone thermal conductivity values according to different researchers.

2.4 Thermal Injury in Bone During Cutting of Bone

Thermal damage in bone may stem from drilling or sawing during orthopaedic operations arising from interfacial friction between the cutting tool and bone material.

The effect of thermal injury on tissue, including bone, has previously been investigated. Heat production varies with the cutting speed, force, and loading of the cutting tool and heat has harmful effects on existing bone tissue (Thompson, 1958; Pallan, 1960; Matthews and Hirsch, 1972; Larsen and Ryd, 1989) which may result in infection and reduced mechanical strength of bone (Christie, 1981). Irreversible

changes to the mechanical properties of bone were observed when the bone was heated to 50°C (Bonfield and Li, 1968).

After orthopaedic surgery, frictional heat generated between the saw blade and bone may result in delayed post operative healing (Pallan, 1960). Drilling into cortical bone was carried out by Collins (1953) who said bone was “burned to death” and that no evidence of repair process could be seen postoperatively after five weeks. Effect of temperature on bone became more clearly defined by Rouiller and Majno (1953) (Article in German, reported in Horner 1961). They exposed rabbit bones to various degrees of heat for different periods of time. With an exposure to 55°C for 1 minute, necrosis of osteocytes was observed within 24 hours.

Severe histologic reactions such as hyperemia, degeneration of osteocytes, changes in bone stainability, tears, and fragmentation of the bone around the drill hole edges were found in bone specimens during drilling of bone (Thompson, 1958). The areas of thermal necrosis around bur holes were identified by the presence of osteocytes around holes (Moss, 1964). Less osteocytes characterised the maximum bone damage while more osteocytes around the periphery of a bur hole showed minimal bone damage.

Matthews and Hirsch (1972) believed the critical temperature for thermal bone injury is around 56°C the temperature at which alkaline phosphatase is denatured. In a rabbit experimental model, Lundskog (1972) observed some histochemical evidence of bone death adjacent to an implanted rod that was heated to 50°C for 30 seconds.

Regarding thermal damage in bone, some other researchers (Eriksson et al., 1982) experimented on thermal injury to bone by heating using a thermal chamber. A temperature of 53°C was reported to cause an irreversible bone injury. In 1983,

Eriksson and Albrektsson studied the hard tissue changes after heating in the range of 47°C to 50°C. Some effects such as stopping of blood flow occurred in some cases. Two to five days after heating, most fat cells became darker which was the early sign of fat cell injury. Consequently, their work indicated that 47°C for 1 minute is the threshold level for bone survival and temperature of more than 47°C caused increase in bone resorption and fat-cell degeneration. Temperatures lower than 47°C did not seem to influence the bone tissue at the microscopic level. Eriksson and Albrektsson (1984) defined the threshold temperature for impaired regeneration of bone in the range of 44°C to 47°C when measured at a distance of 0.5mm from the implant at an exposure time of 1 min.

2.5 Bone Osteotomy

Techniques available for cutting bone have been reviewed by previous authors (Giraud et al., 1991; Baumgart et al., 1998), and they have concluded that irrespective of the type of instrument used the effectiveness of the cutting process is affected by the degree of sharpness of the instrument, and the use of coolant when using powered instruments to avoid bone cell necrosis, and the site location and tissue protection. A surgical procedure requiring the clinician to cut bone known as an osteotomy may occur for various reasons such as:

- a. bone fracture requiring fixation;
- b. bone augmentation, excision, grafting and realignment to enhance mobility or joint functionality;
- c. bone reconstruction for plastic surgery purposes;
- d. insertion of bone implants for joint replacement or bone repair.

Cutting of bone may be performed in three different directions dependant on the osteon direction as Figure 2.19 illustrates three different sawing modes relative to the predominant osteon direction.



Figure 2.19: Illustration of the cutting modes relative to predominant osteon direction
(Plaskos et al., 2003)

2.6 Studies on Bone Cutting

The cutting process involves a cutting instrument (chisel, saw, drill, bur), the target material (cortical or cancellous bone or both), and a system that causes the instrument to cut the material, this is normally a force either applied directly or indirectly. The primary source of research in cutting system analysis has been metal cutting and numerous landmark studies have been completed which define the process where a cutting tool has been used to cut the target material. Force models have been developed in these studies that provide a starting point for modelling of the bone cutting process (Merchant, 1945a; 1945b; Khambay and Walmsley, 2000). Emphasis will be placed on the temperature changes and thermal effects during cutting of bone in this literature review. The primary cutting procedures used are:

- Sawing using either reciprocating or oscillating saw;
- Drilling;
- Bur cutting.

In most experiments, bovine bone was used as the specimen material to be cut because of its availability in sufficient quantities, useful size, widely publicised properties, and its structural resemblance to human bone (Jowsey, 1966). The effects of different cutting procedures and different effects of speed, force, load, and irrigation will be discussed.

2.7 Bone Sawing

In the orthogonal bone cutting process, a single edge cutting tool as shown in Figure 2.20 moves in a straight line with a velocity of v parallel to the surface of the workpiece. The cutting edge is aligned at right angles to the direction of the cutting motion. The mechanics of the cutting process can be resolved by considering the cutting action as a two dimensional process. The bone saw blade instrument can vary in size, shape, and geometry, and is normally designed to meet the requirements of the cutting process though improvisation may occur. The cutting component of the instrument is normally manifested in a toothed blade.

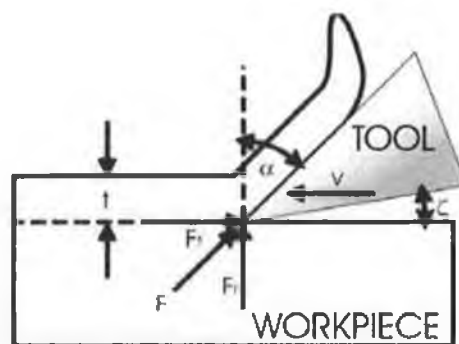


Figure 2.20: Orthogonal cutting illustration (Plaskos et al., 2003)

Reciprocating and oscillating saws are used widely in joint arthroplasty to reduce the surgery time and allow accurate bone cuts and shaping for conformance to the implant design.

2.7.1 Effects of Cutting Forces on Temperature

Krause et al (1982), using a reciprocating saw, performed a set of clinical trials to measure the force and temperature response on the saw blades during total knee and hip arthroplasty. A thermocouple was securely fastened onto the saw blade to record the saw temperature. They reported temperature without application of any irrigation exceeding 200°C (Figure 2.21). The vertical force applied by surgeon fluctuated between 4.5 and 7.5 N.

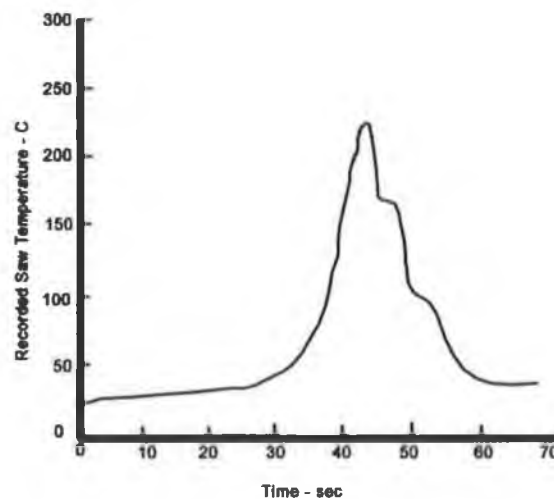


Figure 2.21: Temperature recorded on saw (Krause et al., 1982)

In another study by Wachter and Stoll (1991), osteotomy was performed by hand using an oscillating saw. The applied forces (either continuous or intermittent) were directly recorded. They placed a thermocouple at the base of saw and temperatures greater than 100°C were recorded on the saw blade and in the bone while cutting with a continuously applied load (approximately 4 N), regardless of irrigation and up to 140°C were observed using intermittent load (up to 10 N).

2.7.2 Effect of Cutting Speed on Temperature

In the case of sawing, either reciprocating or oscillating saw, no information was evident in the literature about cutting speed effect on temperature.

2.7.3 Effects of Irrigation on Temperature

Tetsch (1974) conducted a series of experiments in the lower jaw of cats using an oscillating saw and recorded a temperature up to 300°C without using coolant. Temperatures of 150°C and 75°C were observed on the saw tooth and in the bone adjacent to the cut, respectively when no irrigating fluid was used (Krause, 1977). Krause et al. (1982) demonstrated that the use of 60 mL/min of saline lessened the temperature from 170°C (without irrigation) to the value of 38°C in *in vitro* cutting tests.

Toksvig-Larsen et al. (1990; 1991) developed an oscillating saw blade (Figure 2.22) made up of two individual blades with an intermediate channel and sealed on the blade edges to direct cooling fluid to the saw teeth. The cooling agent was successfully led to the saw teeth and the saw chips were cleared away from the kerf and the temperatures achieved were below the critical temperature for bone necrosis (44°C to 47°C). They also commented that irrigation using saline delivered by a syringe reduced the maximum temperature. However cooling by this method was very inefficient since the assistant, using the syringe, had to direct the coolant consistently along the blade surface to the teeth.

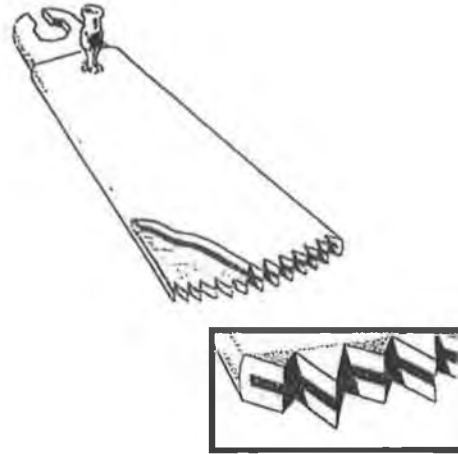


Figure 2.22: Illustration of double saw blade (Toksvig-Larsen et al., 1991)

Wachter and Stoll (1991) found out that cutting of bone using an intermittent load (up to 20 N) combined with the use of coolant was more successful in controlling temperature and that bone chips could be removed easily by this method. A mean temperature of 45°C was observed at the saw blade and temperatures did not exceed 61°C. Irrigation combined with continuously applied load was ineffective because saline solution could not reach the bottom of saw cut and the temperature increased to 130°C. Thus, intermittent bone osteotomy with use of irrigation was recommended by these researchers.

2.7.4 Effect of Saw Design on Temperature

Results from sawing experiments show that the design of the cutting teeth on the saw blade have an impact on the amount of heat generated and resulting temperature in bone sawing (Krause et al., 1982). Figure 2.23 shows different temperature response of two different saw blades in their study. It can be seen that the temperature recorded for the 1384-039 saw blade with more efficient design is less than that of 1384-19.

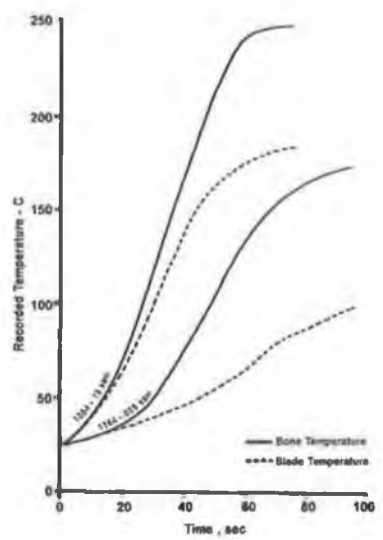


Figure 2.23: Different temperature response in 2 different saw blades (Krause et al., 1982)

However, Toksvig-Larsen et al. (1992) compared different saw blades (Figure 2.24) with different design and they showed that the sawing geometry did not lower the temperature significantly below the critical level. Table 2.6 shows their results regarding cutting of bovine bone using different saw blades.

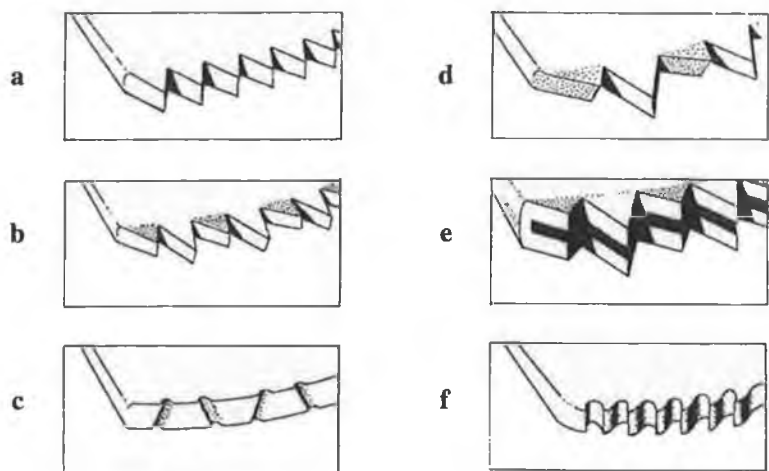


Figure 2.24: Different saw blade design. (a) 3M P512 reciprocating, (b) 3M L122 oscillating, (c) 3M L122 modification "half" teeth, (d) 3M L122 Sandvik modification chamfer angel of 30°, (e) Double saw blade, (f) Hall saw blade

Blade	No. tests	Average temp (°C)	Temp range (°C)
3M oscillating L122	61	101 ± 36	34-184
½ teeth	17	196 ± 61	88-290
0 teeth	10	188 ± 110	78-450
Sandvik 10°	29	93 ± 37	41-194
Sandvik 30°	18	116 ± 48	53-187
Hall	12	153 ± 38	100-200
3M reciprocating P512	19	103 ± 37	40-200
Double saw blade	19	91 ± 19	49-112
Bone (20°C) 3M L122	34	108 ± 23	72-171

Table 2.6: Maximum temperature recorded while using various saw blades in bovine bone cutting

2.7.5 Wear of Saw Blades

Regardless of the widespread usage of saw blades and power cutting tools in surgery, there has only been a few researchers that have investigated saw blade performance in experimental models (Krause et al., 1982; Wevers et al., 1987; Toksvig-Larsen et al., 1990; 1992; Ark et al., 1997a; 1997b; 1997c). For any orthopaedic operation, the durability of the blade has been a crucial concern for any surgeon (Ark et al., 1997b). Furthermore, blunt cutting tools may require the application of extra force (Allan et al., 2005), which in turn may contribute to excessive frictional heat. Saw blade wear has been attributed to two different factors. Firstly, repeated use of blades was assumed to dull the blade and secondly, it has been postulated that inadvertent contact of the blade with a metal jig or cutting guide while conducting the surgery may be the main cause of blunting of the saw blade. Wevers et al. (1987) found that half of the saw blades taken from the operating room were severely damaged. They noted that frequent use of saw blades could decrease the cutting efficiency. They also found the force required to cut cortical bone using a blunt saw (32.08 N) was nearly five times greater than that encountered with new blades (6.75 N). This is in accordance with

Matthews and Hirsch (1972), who investigated drilling in human cortical femoral bone in vitro and found worn drills to cause much greater temperature changes than new drills.

2.7.6 Oscillating Saw Blade Geometry

After reviewing the literature, information could be only found regarding geometry of oscillating saw blade but not about reciprocating saw blade. The oscillating saw blade can be distinguished by its width, thickness, length, and sawing radius. The cutting teeth at the end of the blade can be defined by pitch, tooth offset. Ark et al. (1997a) defined the key factors of the oscillating saw blade shown in Table 2.7.

Term	Description
Blade width	the distance across the blade body
Blade thickness	the distance between the opposing surfaces of the blade body
Blade length	the distance from the hub to the ends of the teeth of the blade
Sawing radius	the distance from the centre of the mounting hub to the tip of a tooth on the cutting edge shown in Figure 2.25
The pitch	teeth per inch
Tooth offset	the dimension from the extreme corner of one tooth to the extreme corner of an opposed tooth (Figure 2.26)

Table 2.7: Geometry of oscillating saw blade

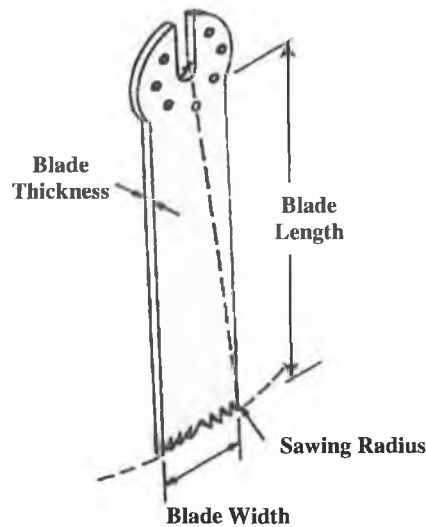


Figure 2.25: Oscillating saw blade dimensions (Ark et al., 1997a)

When the blade teeth are offset, they are typically oriented such that each successive tooth is alternated to opposing sides to produce a balanced cutting action. The offset causes the blade to cut a path that is wider than the thickness of the blade, hence creating a gap or passage to allow the escape of bone debris from the cutting edge.

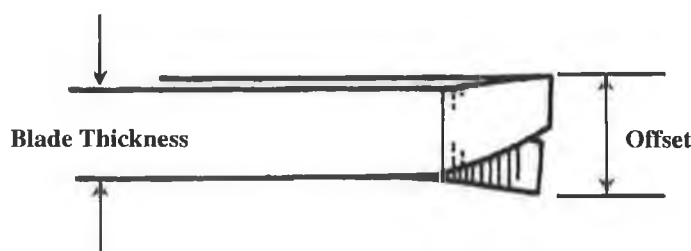


Figure 2.26: Measurement of tooth offset (Ark et al., 1997a)

Blade teeth can be categorised as having symmetric or asymmetric tooth designs:

- The symmetric tooth arrangement has symmetry about an axis perpendicular to the cutting direction (Figure 2.27a).
- The asymmetric tooth lacks an axis of symmetry perpendicular to the cutting direction (Figure 2.27b).

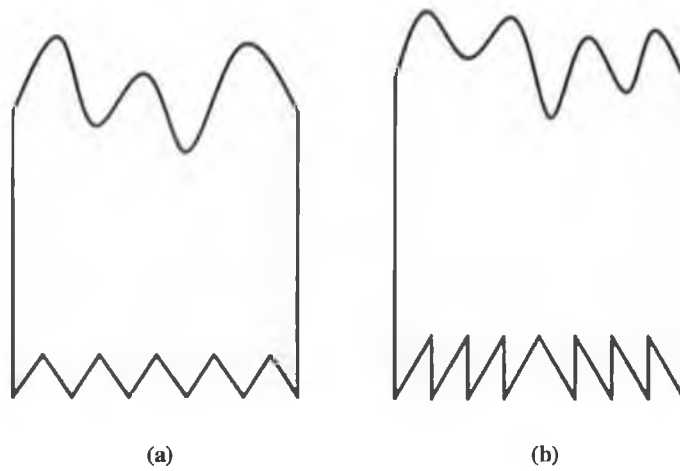


Figure 2.27: Oscillating saw tooth arrangement (a) symmetric, (b) asymmetric
(Adapted from Ark et al., 1997a)

2.7.7 Geometry of Oscillating Saw Teeth

Blade teeth possess a triangular wedge shape formed by opposing surfaces and two side faces. The tooth removes material by initiating a series of fractures as it moves along the surface of the bone. The bone chips that are removed by the cutting process flow up the leading tooth face. The apex of the tooth serves as primary cutting edge and the other tooth edges are considered secondary cutting edge.

The shape of the tooth is defined by the tooth height and wedge angle. Figure 2.28 shows the tooth height which is the distance from the apex of the tooth to the base of the triangular-shaped tooth and the wedge angle which is the angle between the secondary cutting edges on the surface of the triangular tooth.

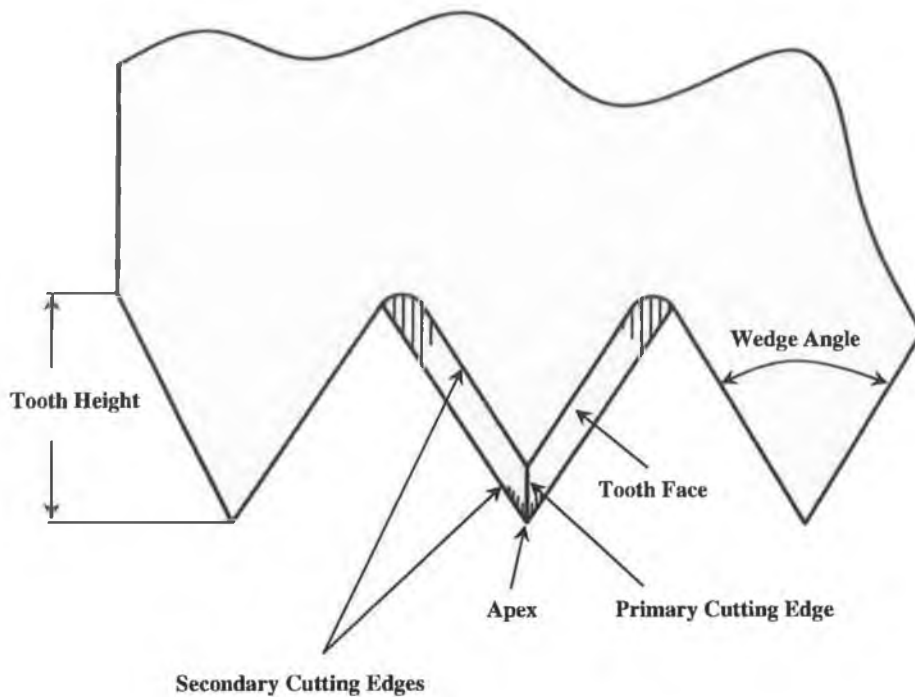


Figure 2.28: Dimension of oscillating saw teeth (Adapted from Ark et al., 1997a)

A significant concern in determining the cutting efficiency in sawing is the rake angle which is defined by the sawing radius, the line from the centre of the tooth hub to the tip of the tooth, and the leading tooth face. Figure 2.29 shows the different rake angles.

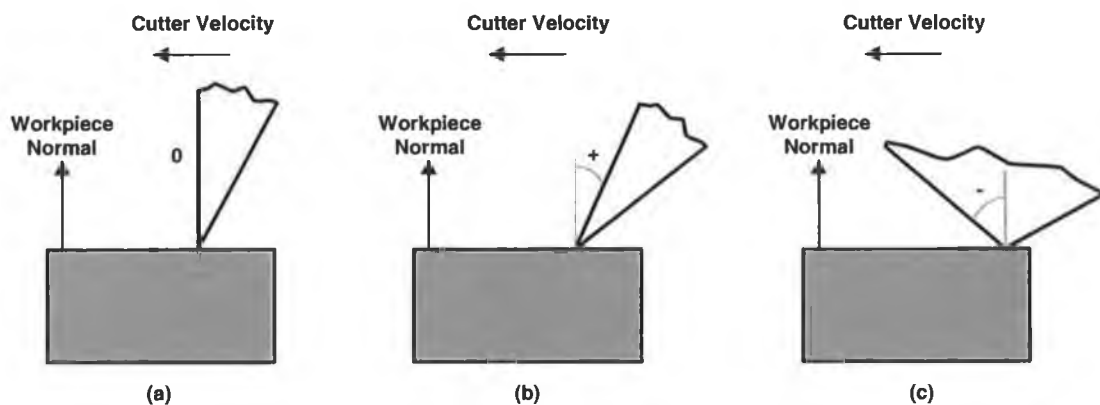


Figure 2.29: Illustration of different rake angles. (a) Neutral, (b) Positive, (c) Negative

2.8 Drilling of Bone

Drilling in bone has significant clinical applications particularly as a preliminary step in the insertion of pins or screws during repair of fractures or installation of prosthetic devices. Generation of heat is one of the major problems encountered when drilling. Several factors have been reported to influence temperature rise during drilling procedures such as drilling depth (Wiggins and Malkin, 1976), drill flute geometry (Jacobs et al., 1974; Wiggins and Malkin, 1976), sharpness of the cutting tool (Matthews and Hirsch, 1972), variation in cortical thickness (Eriksson et al., 1984), drilling speed (Costich et al., 1964), pressure applied to the drill (Matthews and Hirsch, 1972), irrigation (Lavelle and Wedgwood, 1980; Eriksson et al., 1984) and the bone density (Yacker and Klein, 1996). Figure 2.30 illustrates Bachus et al. (2000) study in which different temperature as a function of time was recorded in 3 different locations from the drill site.

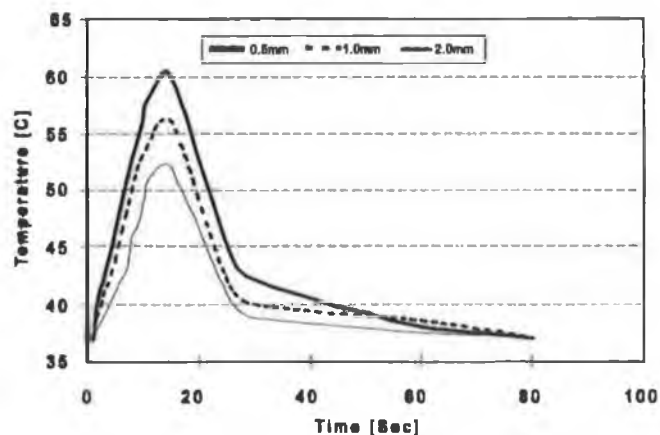


Figure 2.30: Temperature at different location from drilling site (Bachus et al., 2000)

Matthews and Hirsch (1972) demonstrated that the very high local increase of temperature present in drilling can destroy cell viability in the area surrounding a hole. They studied the temperature obtained when drilling bone, in order to determine

the optimum drilling conditions for cortical bone using a standard drill. The experiment involved measuring the increase in temperature and the duration of that increase in the cortical wall of a human femur, at a specific distance from the drilling zone, for various rotation velocities and pressure applied to the drill. The effects of using a drill guide, of manual and forced irrigation, of drilling a pilot hole and of impact drilling were also studied. The results showed that neither the drill guide nor impact drilling produce any additional increase in temperature. The force applied to the tool was a more critical factor than drill rotation speed as far as temperature was concerned.

It can be observed that the variation in cortical thickness between species leads to having different temperature elevation during cutting of bone, i.e., temperature of 40°C in rabbit with mean cortical thickness of 1.5mm, 56°C in dogs with mean cortical thickness of 3.5mm, and 89°C in human with mean cortical thickness of 6.5mm were recorded while drilling in the femoral cortex at a distance of 0.5mm from the periphery of the drill hole (Jacob et al., 1976; Eriksson et al., 1984).

2.8.1 Effects of Drilling Force on Temperature

Although there is a widespread agreement that a sharp, coolant irrigated cutting instrument effectively limits excessive drilling temperatures, there still is disagreement as to how drilling forces affect the cortical temperatures and their duration of application. Studies have found that maximum cortical bone temperatures are directly related to drilling force. In a study that tested light drilling forces, cortical temperatures increased as forces increased from 1.5 to 4 N (Abouzia and James, 1997). They later discovered that as forces continue to rise from 4 N to 9 N, cortical temperatures decreased. However, several researchers such as Matthews and Hirsch

(1972), Abouzgia and Symington (1996), Abouzgia and James (1997) and Brisman (1996) have reported that cortical bone temperatures are inversely related to drilling force. They all observed a significant decrease in maximum cortical temperatures as the result of force increase.

Matthews and Hirsch (1972) tested forces ranging from 20 N to 118 N and found that by increasing the force, bone temperatures and their duration above 50°C decreased, in agreement with Bachus et al. (2000). Although the exact reason for this temperature decrease is vague, a higher force may reduce the time required to penetrate the cortex of the bone.

2.8.2 Effects of Drilling Speed on Temperature

Thompson (1958) studied low drilling speeds, temperature increases, and tissue damage. He drilled extrasketal pins into canine mandibles and examined bone reaction to different drill speeds. He also measured temperatures adjacent to the drilling site using thermocouples at the distance of 2.5mm and 5mm from the drill point. Temperature at 125 rpm was 39°C rising to over 65.5°C for speeds of 1,000 and 2,000 rpm at 2.5mm from the drilling site. Thus, a drilling speed of 500 rpm was recommended by him to minimise histologic response and thermal damage in bone, also in agreement with Pallan (1960).

Abouzgia and James (1997) found that the maximum temperature rise decreased with speed, for free running speeds from 27,000 rpm to 97,000 rpm. Except for the study by Matthews and Hirsch (1972), there seems to be general agreement that temperature rise increases with drill speed up to approximately 10,000 rpm.

2.8.3 Effects of Irrigation on Temperature

Clogging of drill flutes is identified as a serious problem which causes increase torque and energy as the drill bit penetrates deeper into bone. Therefore, it is necessary that the bone chips be removed from the cutting zone while the drill bit continues to penetrate. One method which could be used to reduce the impact of clogging is surgical irrigation (Wiggins and Malkin, 1976).

Low rotation rate, using saline solution, and gradually intermittent drilling to help the saline reach the depth were suggested to defeat the temperature elevation while drilling (Tetsch, 1974).

2.9 Bur Cutting

The majority of investigation on high speed rotary cutting burrs has been performed in the dental and oral surgery areas with respect to physiologic and histologic response of bone cutting with rotary tools. The reaction of bone following the use of burrs at conventional and ultra-high velocities, with and without application of physiologic solution as a coolant was investigated (McFall et al., 1961; Moss, 1964; Hall, 1965; Jacobs and Ray, 1972). In such studies the main focus was on thermal injury to bone leading to necrosis (cell death).

2.9.1 Effects of Bur Cutting Forces on Temperature

No information was evident in the literature regarding the effect of cutting force on temperature during bur cutting.

2.9.2 Effects of Bur Cutting Speed on Temperature

Hall (1959), Costich et al. (1964), Moss (1964), and Boyne (1966) considered ultra-high speeds of 200,000 rpm to 300,000 rpm for cutting of bone using rotary burs with

application of coolant and found less damage to the bone and more bony repair than those observed at lower speeds, with sufficient coolant. Therefore, it can be assumed that it is more beneficial to cut the bone with higher speed using coolant.

Krause et al. (1982) examined the thermal effects and cutting forces of spherical burrs working at 20,000 and 100,000 rpm for different feed rate (ranging between 1.8mm/sec and 6.35mm/sec) and depth of cuts. It was observed that the maximum temperature was decreased by increasing the feed rate. It was felt that the increase in feed rate had a greater effect on the temperature response than the rotational speed, so that cutting with a 100,000 rpm tool was satisfactory if a fast feed rate was used.

2.9.3 Effects of Irrigation on Temperature

It is an accepted surgical principle that a cooling agent is vital during bone surgery by means of rotary instruments (Moss, 1964; Costich et al., 1964; Lurie et al., 1984) but sometimes with cooling agent the temperature adjacent to burs may often reach 60°C and above (Lavelle and Wedgwood, 1980). Round bur and semi-elliptical bur, each containing a central channel to facilitate internal irrigation, were used to examine the effects of internal irrigation on frictional heat generated when cutting bone (Lavelle and Wedgwood, 1980). They measured the temperature when using burs with internal, and external irrigation, and without irrigation. They reported that high heat developed in all cases without irrigation and the minimal heat developed with internal irrigation.

2.10 Effect of Depth of Cut on Temperature

The importance of the cutting depth for heat generation has been pointed out in some experiments (Tetsch, 1974; Krause, 1977; Krause et al., 1982).

Increase in cortical temperatures was found as the depth of cut increased during an investigation for bur cutting (Krause et al., 1982). While drilling through bone, greater temperature increase was observed at the 8mm depth versus the 4mm depth and the efficacy of irrigation in decreasing the frictional heat was evident at shallow depth (4mm) (Cordioli and Majzoub, 1997), in accordance with Hillery and Shuaib (1999).

Table 2.8 is the summary of maximum cortical temperatures in studies.

Study	Maximum temperature (° C)	Distance from drill periphery (mm)	Bone type	Type of study	Cooling	Free running speed (rpm)	Force or feed rate
Thompson	> 65	2.5	Dog mandible	in vivo	No	125 to 2000	Not indicated
Pallan	65	2	Dog mandible	in vivo	No	125 to 2000	Not indicated
Mathews and Hirsch	140 < 50	0.5	Human Femur	in vitro	No Yes	345, 885, 2900	20, 59, 118 N
Jacobs and Ray	38	2	Rat radius	in vivo	Yes	2500	Not indicated
Tetsch	300 76	1	Cat mandible	in vivo	No Yes	Sawing 20,000	Not indicated
Lavelle and Wedgwood	89 74 50	0.5	Human femur	in vitro	No Ext. irrigation Int. irrigation	350	≈ 59 N
Krause et al.	55 130	near periphery	Bovine femur	in vitro	No	20,000; 100,000 sawing	1.8-6.35 mm/s
Eriksson et al.	41 57 96	0.5	Rabbit femur Dog femur Human femur	in vivo	Yes	20,000	Not indicated

Table 2.8: Summary of maximum cortical bone temperatures in studies

Chapter 3

Materials and Methods

Chapter 3: Materials and Methods

3.0 Selection of Components

In this section the experimental components which were utilised in this project will be discussed such as the temperature measurement device, data logging system, and also sensor bonding adhesive. A typical method for setting up an experiment for temperature measurement is illustrated below in Figure 3.1. Temperatures in bone during cutting are measured using thermocouples. A thermocouple is connected via an A/D converter to a data logger which is connected to a PC with which temperature measurements can be stored and then analysed by means of proprietary software.

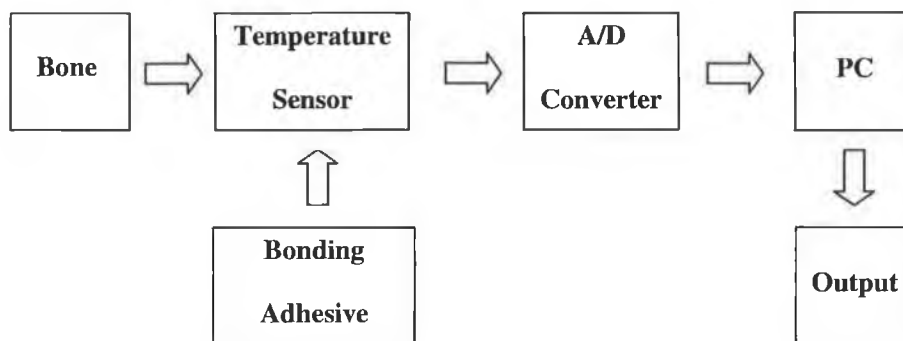


Figure 3.1: Schematic layout of typical heat measurement experiment

When inserting the sensor in bone or on the surface, adhesive is used to ensure a good contact and a bond to ensure that no gap between the sensors exists that could influence the result. Thus, a special bonding adhesive was chosen for this purpose.

3.1 Selection of the Appropriate Temperature Transducer

Researchers have used thermocouples (Matthews and Hirsch, 1972; Lavelle and Wedgwood, 1980; Krause et al., 1982; Toksvig-Larsen et al., 1990; Wachter and Stoll, 1991; Cordioli and Majzoub, 1997; Hillery and Shuaib, 1999; Bachus et al.,

2000; Sharawy et al., 2002; Firoozbakhsh et al., 2003), thermistors; a sensor that measures temperature via a variable resistance value; (Jacobs and Ray, 1972; Tetsch, 1974), RTD's; a resistance temperature device which is a sensor used for measuring temperature where resistance varies as temperature changes; and infrared thermograph; which determines the temperature of objects remotely by infrared radiation; (Lundskog ,1972; Watanabe et al., 1992; Shin and Yoon 2006). Thermocouples were utilised in this project because they are more rugged than other types of transducers and offer a much broader temperature range. Furthermore, they do not need a power source, and their low cost makes them attractive choice for numerous experimental acquisitions. Table 3.1 shows the advantages and disadvantages of using all temperature transducers.

3.1.1 The Principle of Operation of Thermocouples

Thermocouples are temperature measurement sensors which are used in industrial control applications because of their low price and their accessibility in variety of ranges. They are made of two electrical conductors with dissimilar metal alloys. When these dissimilar metals are placed in contact, a voltage drop occurs across the interface. This voltage is a function of temperature. This voltage can then be read by means of an A/D converter or any voltmeter. The electrical conductors are usually built into a cable and isolated in a heat resistance sheath. PVC covered thermocouples were used in this project. The two conductors are joined by welding or soldering and sometimes are twisted together at one end of the thermocouple cable which is known as the hot junction. This junction is connected to the source of heat (i.e. bone) to be measured. The opposite end is called the cold junction or reference junction which is connected to a measurement system such as a data logger. By insertion of the hot

junctions in multiple thermocouple holes in the bone, it is therefore possible to measure heat in a number of adjacent regions.

3.1.2 Thermocouples Types

A variety of thermocouples are available, suitable for different measuring applications in industrial, scientific, food temperature, and medical research fields as well as various operating environments and conditions.

The type **K** is known as a general purpose thermocouple. It is low cost and it is available in a wide variety of probes. They are accessible in the -180°C to $+1300^{\circ}\text{C}$ range. It has been utilised by some researchers in measurement of bone temperature (Matthews and Hirsch, 1972; Bragger et al., 1995; Abouzgia and Symington, 1996; Abouzgia and James, 1997; Khanna, 1999). There are other types such as type **T**, **J**, **N**, **E**, **R**, **S**, and **B**; their properties are described in Table 3.2.

3.1.3 Thermocouple Selection for Measuring Heat in Bone

To find and utilise a proper thermocouple type for the heat sensing function of this research, physical conditions, duration of exposure, sensor lifetime, and accuracy had to be taken into account. Through discussion and information gathering with specialist companies regarding thermocouple such as Omega and TC Direct, it was found that the type **T** thermocouples was most appropriate for this project. It has also been used by Krause et al. (1982), Biyikli et al. (1986), Toksvig-Larsen et al (1992), Wachter and Stoll (1991), Ark et al. (1997), Reingewirtz et al. (1997), and Firoozbakhsh et al. (2003).

	RTD	Thermistor	IC sensor	Thermocouple
Measurement type	Absolute		Relative	
Advantages	<ul style="list-style-type: none"> ▪ Most stable ▪ Most accurate ▪ More linear than thermocouples 	<ul style="list-style-type: none"> ▪ High sensitivity ▪ Fast ▪ Two-wire measurement 	<ul style="list-style-type: none"> ▪ Most linear ▪ highest output ▪ Inexpensive 	<ul style="list-style-type: none"> ▪ Self powered ▪ Rugged ▪ Inexpensive ▪ Wide variety of physical forms ▪ Wide temperature range
Disadvantages	<ul style="list-style-type: none"> ▪ Expensive ▪ Slow ▪ Current source required ▪ Small resistance change ▪ 4 wire measurement ▪ Self-heating 	<ul style="list-style-type: none"> ▪ Nonlinear ▪ Limited temperature range ▪ Fragile ▪ Current source required ▪ Self-heating 	<ul style="list-style-type: none"> ▪ Limited to 250°C ▪ Power supply required ▪ Slow ▪ Self-heating ▪ Limited configurations ▪ Large mass 	<ul style="list-style-type: none"> ▪ Nonlinear ▪ Low voltage ▪ Reference required ▪ Least stable ▪ Least sensitive

Table 3.1: Comparison of common types of temperature transducers (www.agilent.com)









Type	Conductor Material	Temperature range °C (continuous)	Temperature range °C (short term)	IEC Color code	Notes
K	Nickel-Chromium (-) (Chromel)	0 to +1100	-180 to +1300		Most suited to oxidizing atmospheres, it has a wide temperature range and is the most commonly used.
	Nickel-Aluminum (+) (Alumel)				
T	Copper (+)	-185 to +300	-250 to +400		Excellent for low temperature and cryogenic applications. Good when moisture may be present.
	Copper-Nickel (-) (Constantan)				
J	Iron (+)	0 to +700	-180 to +800		Commonly used in the plastics moulding industry. Used in reducing atmospheres as an unprotected thermocouple sensor. NB. Iron oxidises (rusts) at low and at high temperatures.
	Copper-Nickel (-) (Constantan)				
N	Nickel-Chromium-Silicon (+) (Nicrosil)	0 to +1100	-270 to +1300		Very stable output at high temperatures it can be used up to 1300°C. Good oxidation resistance. Type N stands up to temperature cycling extremely well.
	Nickel-Silicon-Magnesium (-) (Nisil)				
E	Nickel-Chromium (+) (Chromel)	0 to +800	-40 to +900		Has the highest thermal EMF output change per °C. Suitable for use in a vacuum or mildly oxidizing atmosphere as an unprotected thermocouple sensor.
	Copper-Nickel (-) (Constantan)				
R	Platinum-13% Rhodium(+)	0 to +1600	-50 to +1700		Used for very high temperature applications. Usually in ceramic sheath.
	Platinum (-)				
S	Platinum-10% Rhodium(+)	0 to 1600	-50 to +1750		Type S has similar characteristics to Type R as shown directly above.
	Platinum (-)				
B	Platinum-30% Rhodium(+)	+200 to +1700	0 to +1820		Type B has similar characteristics to Type R and S but is not so popular. Generally used in glass industry.
	Platinum-6% Rhodium (-)				

Table 3.2: Thermocouples types, conductor combinations, characteristics, approximate working temperature, and international color code

3.1.4 Thermocouple Type T

Type T is a Copper-Constantan thermocouple. As can be seen in Figure 3.2, type T thermocouples have a positive Copper wire and a negative Constantan wire.

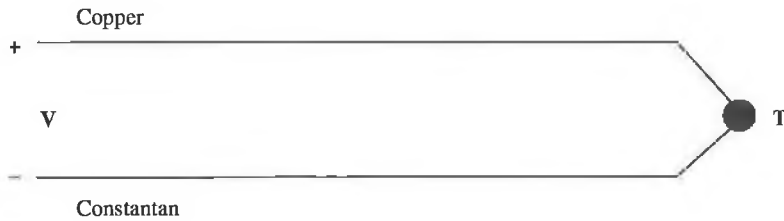


Figure 3.2: Thermocouple type T. The voltage V across the Copper and Constantan wires is a function of the temperature T at the junction

Their operating range is between $-250\text{ }^{\circ}\text{C}$ and $+400\text{ }^{\circ}\text{C}$ and they are commonly used for moist or sub-zero temperature monitoring applications because of:

- superior corrosion resistance, and
- greater homogeneity of the component wires that reduce errors due to temperature gradients

As indicated in Table 3.2, these thermocouples are good when moisture is present. In this study due to the fact that bone surface is damp and temperature within the measuring range of the thermocouple were expected, this type was used.



Figure 3.3: Illustration of thermocouple type T international color code

3.2 Introduction to Data Loggers

A data logger is any device which can be utilised for storing data and may consist of many data acquisition devices such as plug-in boards or serial communication systems which use a PC as a real time data recording system.

3.2.1 Data Logger SQ2020

This data logger was selected for use as an A/D converter for temperature measurement. The SQ2020 Type1F8 (Grant Instrument Ltd, Cambridge, UK) has 24 inputs, 16 of which can be configured to sample a variety of analogue inputs such as voltage, current, or resistance and thermocouples, the remaining 8 being dedicated to digital, high voltage as well as a reference temperature sensor internal to the logger. The thermocouples connected to the bone were used as analogue inputs for the data logger. The 16 analogue inputs are connected to blocks A through to D, so only block A, B, C, and D were used in this project and block E for digital and block F for high voltage were not utilised. Configurations of block are as shown in Figure 3.4. The SQ2020 has a screw terminal connector to connect to the thermocouples. This terminal may be disconnected from the logger to allow hot swappable connection of sensors.

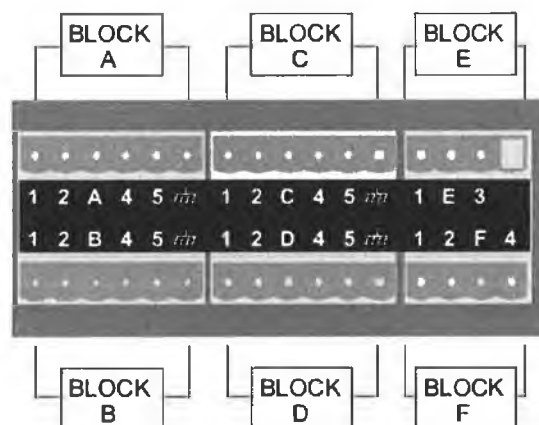


Figure 3.4: Rear view of PHOENIX connectors

Accuracy of this logger is +/- (0.05% of reading + 0.025% of span) and the maximum sampling rate is 20 samples per second and linearity is 0.015%.

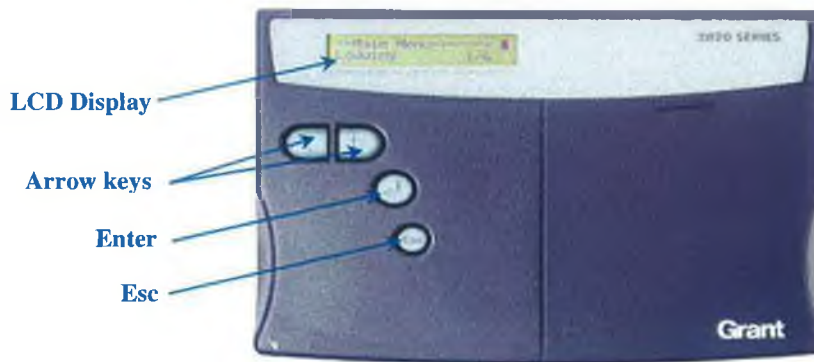


Figure 3.5: SQ2020 data logger

3.2.2 SquirrelView Software

The SquirrelView Assistant (Figure 3.6) is the control interface for all functionality within SquirrelView used to log temperature.

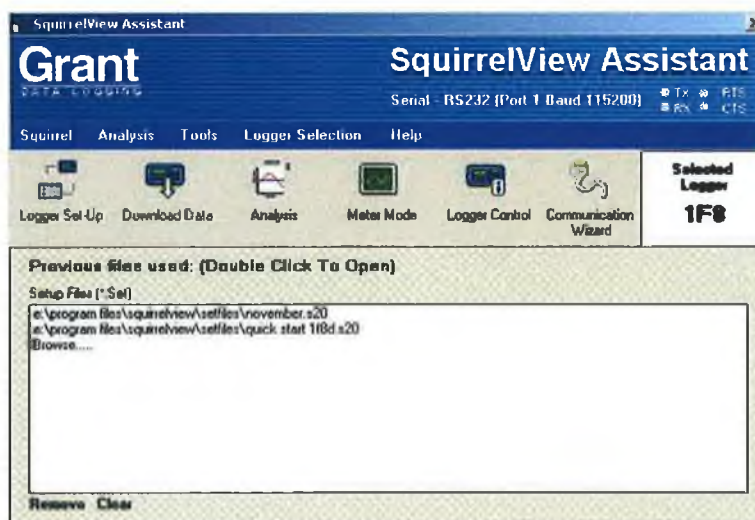


Figure 3.6: SquirrelView Assistant window

To setup the SQ2020, channels which are going to be used must be setup by using the SquirrelView Assistant window and details of the Sensor Type for each required channel can be selected. As was mentioned earlier, differential type T thermocouple and the range of -200°C to 400°C (available range in Logger) was selected.

3.3 Selection and Use of Thermocouple Bonding Adhesive

When inserting thermocouple into a drill hole, there should be a good contact between the thermocouple and bone specimen, moreover, there should not be any gap in which air could influence the test results. Thus, to limit any error in all measurement processes, thermocouples were glued in position into the holes.

A cyanoacrylate adhesive (LOCTITE[®] 454 GEL) which is extremely rapid curing adhesive, a derivative of Instant Adhesive, Super Glue, or Crazy Glue was used. It can be used for bonding metals, composite material, wood, cork and etc.

The operative specifications for this glue are shown below in Table 3.3.

Specifications	
Operating Temperature	up to 80°C
Fixture Time (on steel)	5-20sec
Viscosity mPa.s	Gel
Especially for	Porous Substrates

Table 3.3: Specifications for LOCTITE[®] 454 GEL

3.4 Experimental Methods

The purpose of this section is to clarify all procedures which were used in the experimental work of this project as outlined below:

1. Preparation of bone specimen;
2. Insertion of thermocouples into the bone;
3. Sawing procedure;
4. Saw blade inspection.

Two series of experiment were carried out in this project.

3.5 Experiment 1

In this experiment, whole mid diaphysis of bovine tibia was cut by hand using a reciprocating saw.

3.5.1 Preparation of Bone Specimens

Bovine bone was chosen as the material to be used because of availability in sufficient quantities, useful size, widely publicised properties, and its structural resemblance to human bone. Whole bone specimens from bovine hind quarters were obtained from a local abattoir. The bones were then transferred to the laboratory within 4 hours where the distal and proximal ends were removed using a circular saw. Bone samples were marked and tagged, so that it would be possible to distinguish different bone sources at later stages if required. The bones were transferred to the bone freezer and stored at $-20\text{ }^{\circ}\text{C}$ until use. Thus it was possible to prevent bone dehydration which is known to affect properties of bone (Lundskog, 1972).

Prior to experimental testing, it was necessary to prepare test sites on bone specimens by removing excess soft tissue and insertion of thermocouples in the area adjacent to the cutting zone. Experiments were conducted on portions of mid diaphysis of bovine tibia. The frozen tibias were removed from the freezer and allowed to thaw for two hours under a damp cloth to prevent dehydration. After thawing, the surface of each specimen was cleaned of any fats and tissues with a sharp knife. The bone marrow was also taken out from all samples similar to Matthews and Hirsch (1972) study.

3.5.2 Bone Clamping Fixture

After cleaning the surface and removing the bone marrow, the specimen was held in a clamping fixture. The fixture is shown below in Figure 3.7.

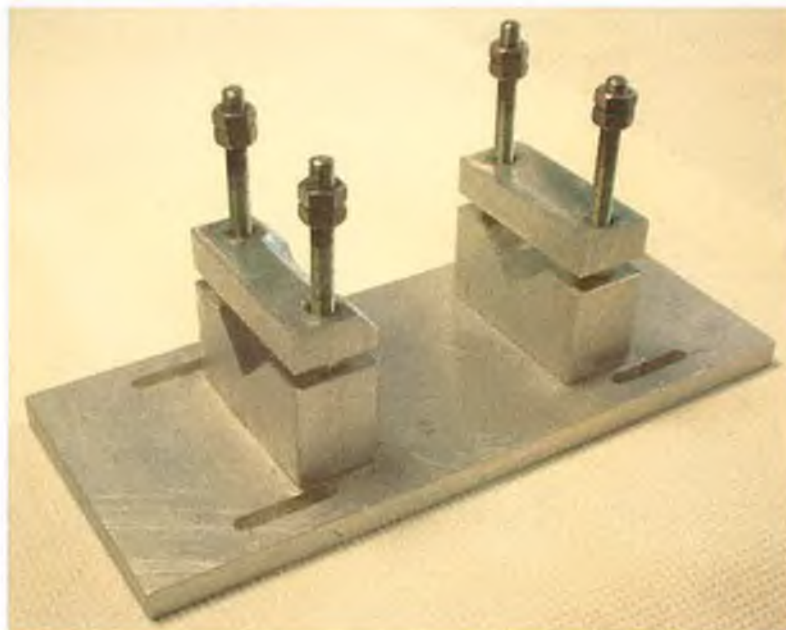


Figure 3.7: Bone clamping fixture

This fixture was used to prevent movement of the bone during preparation of the thermocouple site and also during experimental sawing process.

3.5.3 Preparation of Thermocouple Holes

While holding the specimen on the fixture, a drill template was placed on the flat side of the tibia. This template was used to assist in accurate location of the thermocouple holes. In this way it was possible to reduce sources of temperature error by inconsistent positioning of thermocouples on subsequent test samples. The design of this special template can be seen in Figure 3.8. These holes are 1.4mm in diameter and are positioned on a 3mm grid.

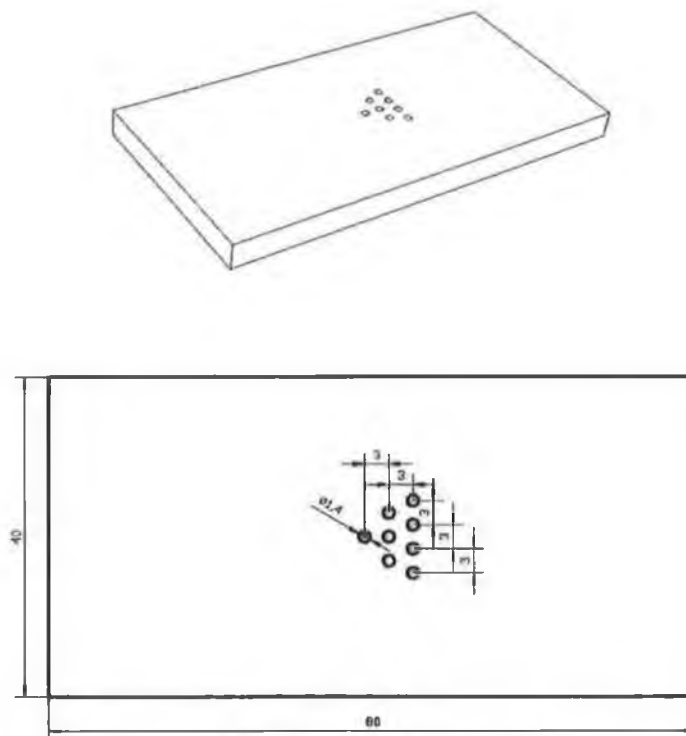


Figure 3.8: Drill template and its dimensions

This aluminum template was secured by a toggle action clamp acting on the flat and round surface of the bone sample.

3.5.4 Drilling the Holes

A drill size was selected that would facilitate insertion of the thermocouple wires into the bone while also providing scope for fixation of the thermocouple using bonding adhesive. After initial trials, it was found that a diameter 1.3mm drill bit would be most suitable.

First, the hole positions were marked by the drill bit to a depth of 1mm or 1.5mm via the drill template. Then the template and the toggle action clamp were removed off the sample to simplify drilling conditions. Finally each hole was drilled to a depth of 5mm into the specimen (Figure 3.9).

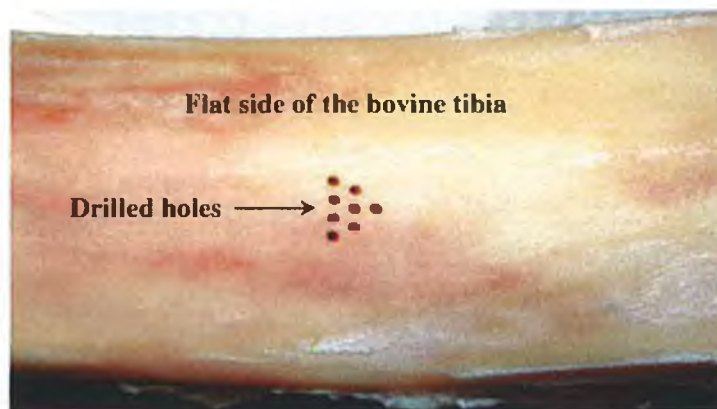


Figure 3.9: Drilled holes

3.5.5 Time Required for Drilling each Hole

The approximate time for each cavity preparation was in the range of 17 sec to 30 sec, is dependent on use of water irrigation while drilling which helps to minimise bone damage.

3.5.6 Problems During Drilling

Holes were drilled in the bone by application of intermittent force to facilitate bone chip removal from drilled holes. It was observed that when a continuous drilling action was used, clogging occurred more often than with an intermittent drilling action. It should be noted that some of these drilling procedures were done without presence of any coolant or irrigant and some drilling were done with water irrigation to observe the difference in drilling efficiency. As it has been reported in the literature worn drills cause greater maximum temperature elevation and also greater durations of temperature elevation (Matthews and Hirsch, 1972), new drills were used at the first visual indication of wear or after approximately 40 holes had been drilled. After finishing hole preparation, the sample was released from the bone fixture and it was immersed into the saline for ten minutes to prevent dehydration and then placed under a damp cloth. If it was not intended to use the specimen immediately, it was otherwise returned to the bone freezer.

3.5.7 Thermocouples' Zones Relative to the Cutting Zone

The thermocouples were organised in three different zones relative to the cutting zone. Thermocouples T1, T2, T3, and T4 were chosen to be in the first zone relating to the sawing line. T5, T6, and T7 were selected to be in the second zone and lastly T8 for the third zone. A triangle shape was chosen for hole position. The first reason was the limit for the number of thermocouples (eight differential thermocouples) which could be used by data logger. The area close to the sawing line (Zone 1) was important during this project to observe the effect of temperature gradient, so by taking into account the limitation on number of thermocouples, four thermocouples were placed in the first zone. To determine temperature distribution through the bone

in different directions, three holes were made in the second zone. One thermocouple was placed in the third zone. Figure 3.10 shows the arrangement of the holes relative to the Sawing Zone.

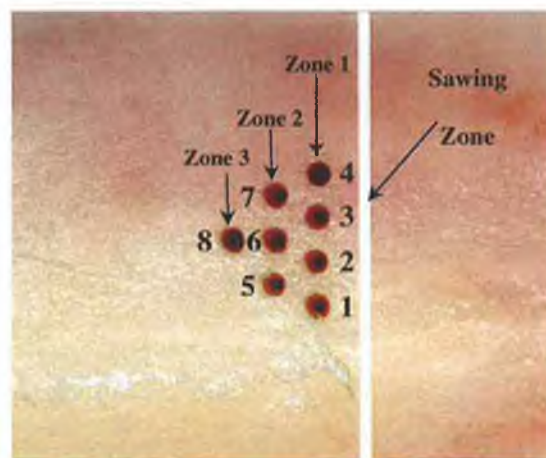


Figure 3.10: Thermocouples position relative to the sawing line in Experiment 1

3.6 Thermocouple Preparation

As was mentioned previously, type T thermocouple was selected to be used in the whole series of tests because they are tolerant to moisture on the bone surface. Thermocouple cables were cut off in the proper length of approximately 550mm. The PVC covers at both ends were taken out by means of a wire stripper. Afterwards, the two metal conductors were twisted together at one end which was described earlier as the hot junction and this end was glued with LOCTITE 454 GEL into the previously drilled holes into the bone (Figure 3.11).

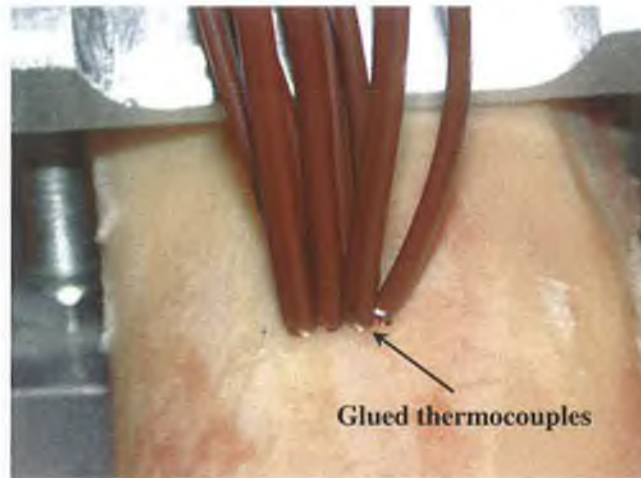


Figure 3.11: Thermocouples type T glued and inserted into the drilled holes

The opposite thermocouple ends at the cold junction were placed and screwed into special 6 way connectors (18097 connectors, Grant Instruments Ltd, Cambridge, UK). Four connectors were used in each test and with each connector providing connections for two thermocouples, eight thermocouples were connected to the measurement system, which was the universal portable data logger SQ2020.

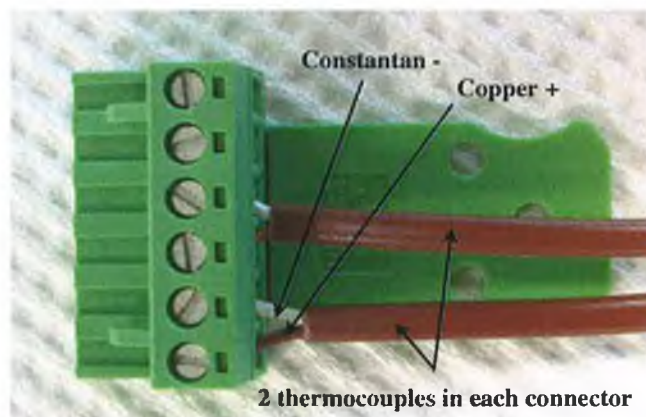


Figure 3.12: 18097 connector

3.7 Data Logger Set-up

After positioning of all thermocouples in the bone sample and in the connectors, the processes described in Figure 3.13 were performed for setting up the data logger.

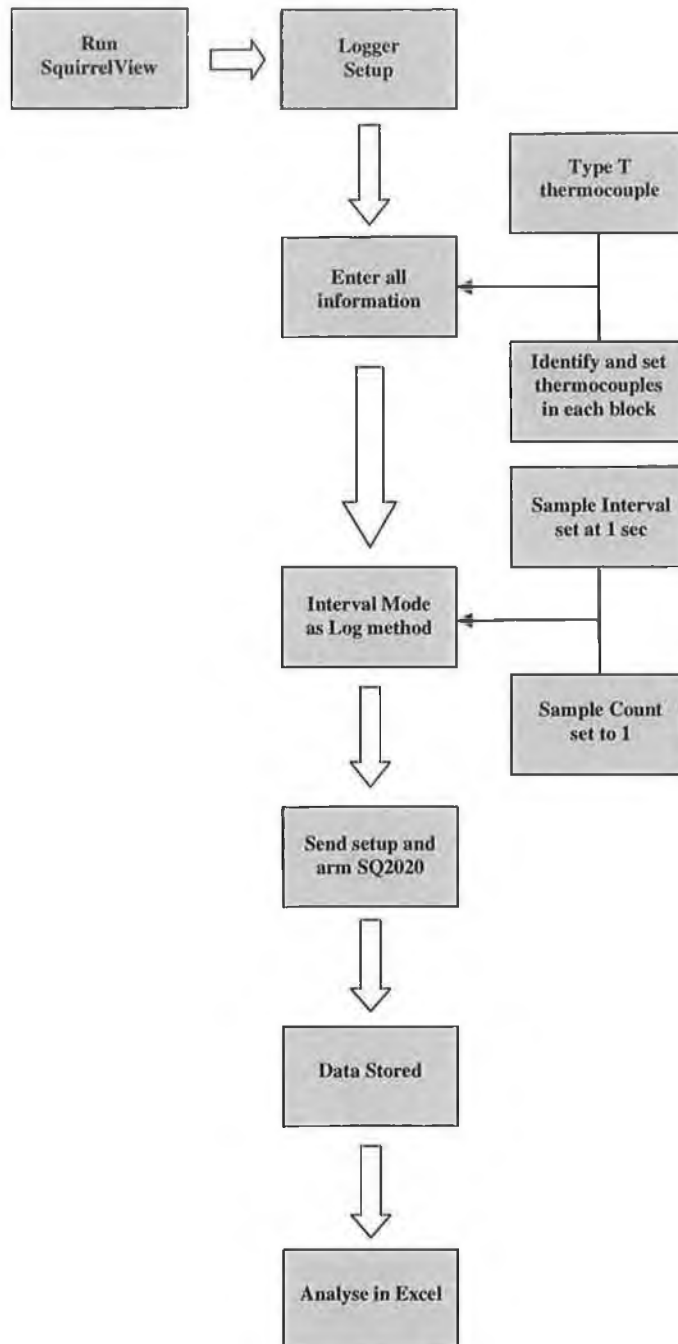


Figure 3.13: Data logger setup block diagram

After running the SquirrelView software, information such as sensor type was entered. Sample Interval of 1 sec and Sample count of 1 was set, so the reading would be stored every 1 sec. Then, the setup was sent to the logger and it was armed (activated). All data was stored and then exported to Excel for further analysis.

3.8 Bone Saw

Sawing procedures were carried out with an air-powered 3M Maxi Driver[®] Reciprocating Saw connected to the main air power system in the laboratory. This device works at approximately 3,800 rpm and at 7 bar pressure (Toksvig-Larsen et al, 1992). All sawing procedures in Experiment 1 were performed by hand.

There are a number of attachments which could be connected to the saw such as oscillating saw, Jacobs chuck, reamer which are kept in a sterilising case. These attachments are shown below in Figure 3.14.

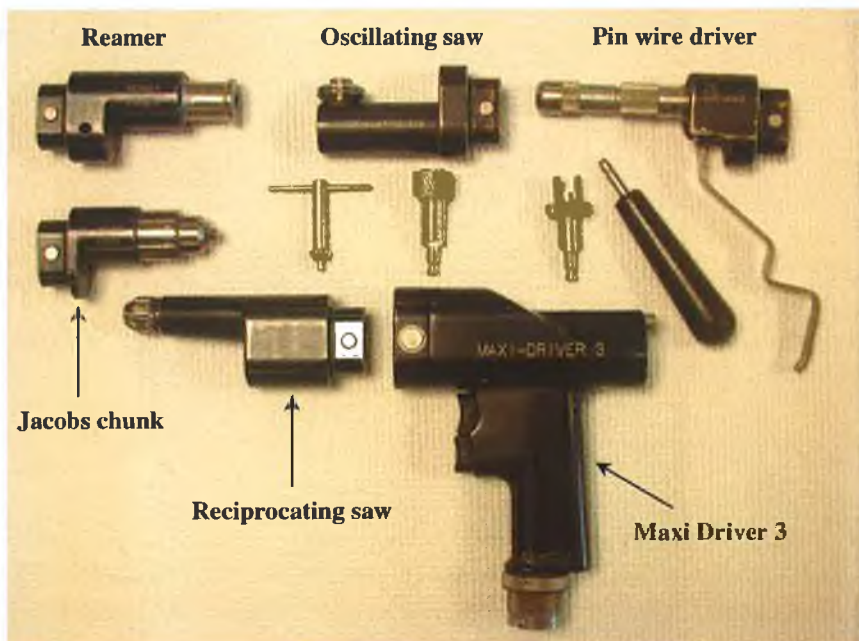


Figure 3.14: 3M Maxi Driver saw and its attachments

3.8.1 Saw Blade

A number of reciprocating, coarse blades, P512 (Hall® Surgical, Linvatec Corporation, Florida, USA) were used in all series of tests. The dimensions of the blade are: 8.9mm × 79.8mm × 0.89mm and the cut thickness is 1.40mm.

The advantage of using the P512 is that tooth offset produces a cut wider than the thickness of the blade, providing an escape route for the bone chips from the cutting area. Each blade was individually numbered with an engraver to be distinguished from others, during post experiment evaluation of wear.

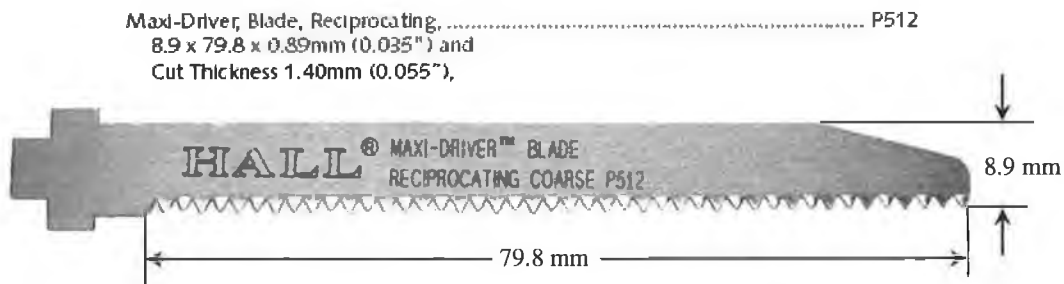


Figure 3.15: Reciprocating coarse P512 blade

3.9 Experimental Procedure

The previously prepared bone specimen was taken out of the freezer and this frozen specimen was immersed into water at room temperature for 1.5 to 2 hours for thawing. Next, the fully thawed bone (18 °C to 20 °C) was removed from the water. The hot junctions of eight prepared thermocouples were bonded and inserted into hole locations and cold junctions which were previously connected into the 18097 connectors, were attached to the data logger. Then, the sample was placed and clamped into the bone fixture. The bone fixture was also held onto the work bench using a toggle action clamp (Figure 3.16).

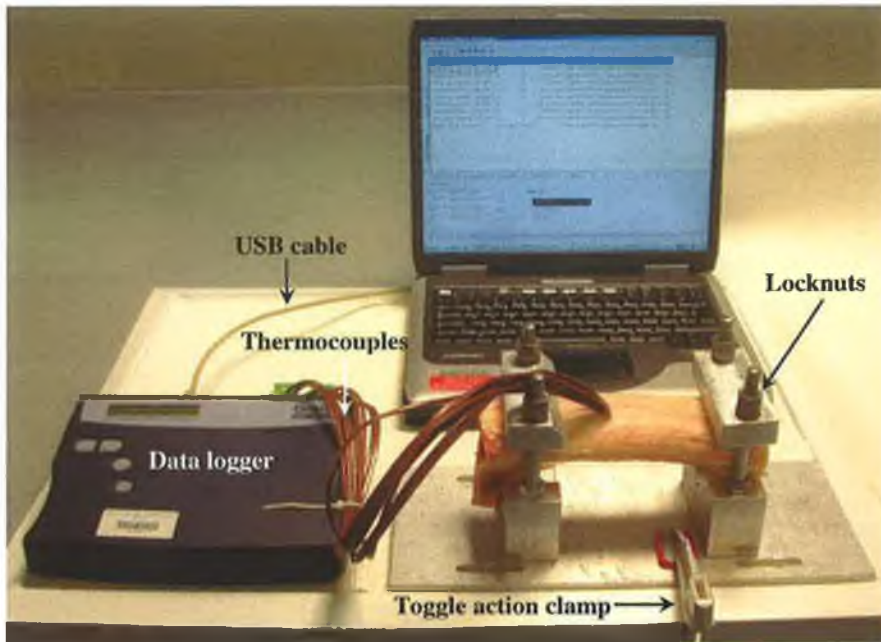


Figure 3.16: Schematic of the Experiment 1

By means of a sharp knife, a line on the bone sample in a distance of 3mm from the line of first zone was marked to place the blade for the first contact with bone and to have the exact line of cutting. The P512 blade was placed into the reciprocating saw and air hose was connected to laboratory main air system. By sending the previously setup information for data logger which was explained earlier to the logger, data logger was armed and sawing was started simultaneously.

Transverse cutting across the tibia was conducted. The sawing procedure and saw blade position on the bone will be explained in section 3.10. When the saw blade cut more than half way through the bone section (Figure 3.17), sawing was stopped and temperature measurement was continued until the temperatures were returned almost to the room temperature.

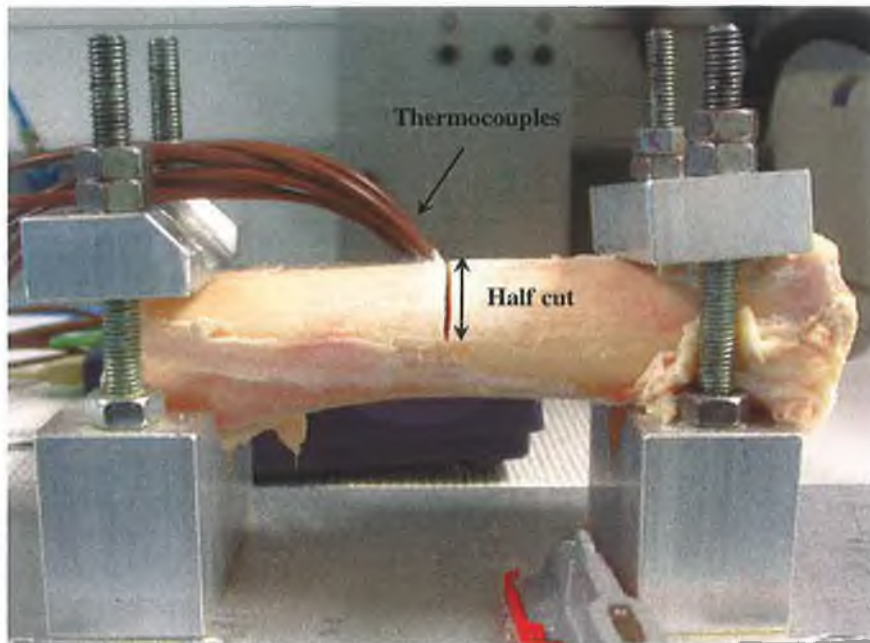


Figure 3.17: Illustration of half way transverse cut. Front view

After completion of cutting, the logger was disarmed and data file was downloaded and imported to SquirrelView software for Analysis. All data was exported to Excel. The blade was permitted to cool adequately to room temperature after each test. Thermocouples were disconnected from the sample by a wire cutter and sample was released from the bone fixture. To distinguish the samples from each other, the test number and the blade number were marked on the bone specimen with a permanent marker (Figure 3.18). Eventually, the sample was put in freezer for further investigation regarding the CSA of the cutting zone and the rate of the bone removal. Twenty samples were cut in Experiment 1.

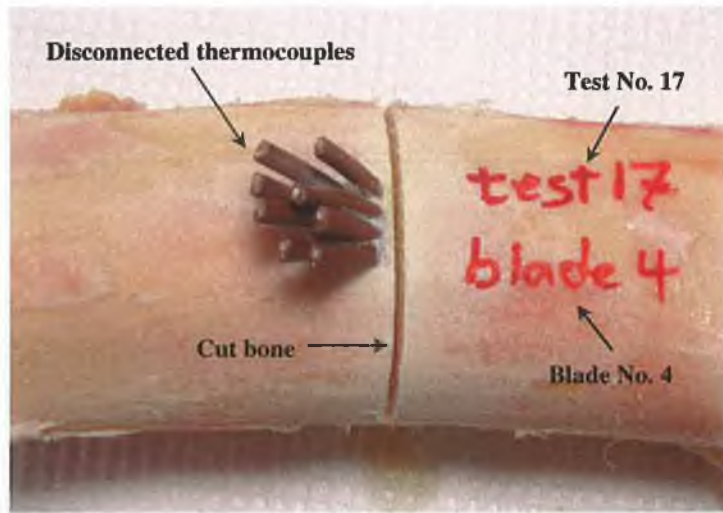


Figure 3.18: Top view of a marked bone

3.10 Sawing Procedure in Experiment 1

The typical sawing process in Experiment 1 was as shown in Figure 3.19. The blade was maintained in a horizontal orientation.

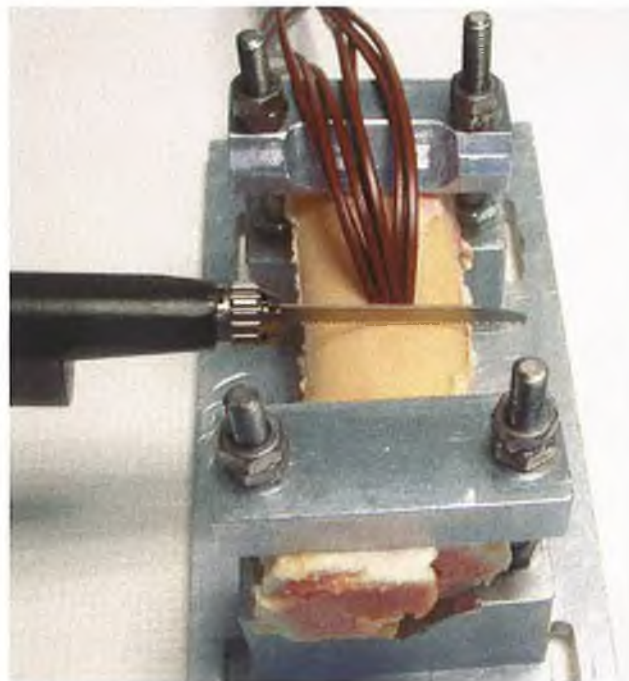


Figure 3.19: Cutting process in Experiment 1

Figure 3.20 illustrates the sawing process from the top view and position of the blade is 3mm from the first zone of thermocouples.

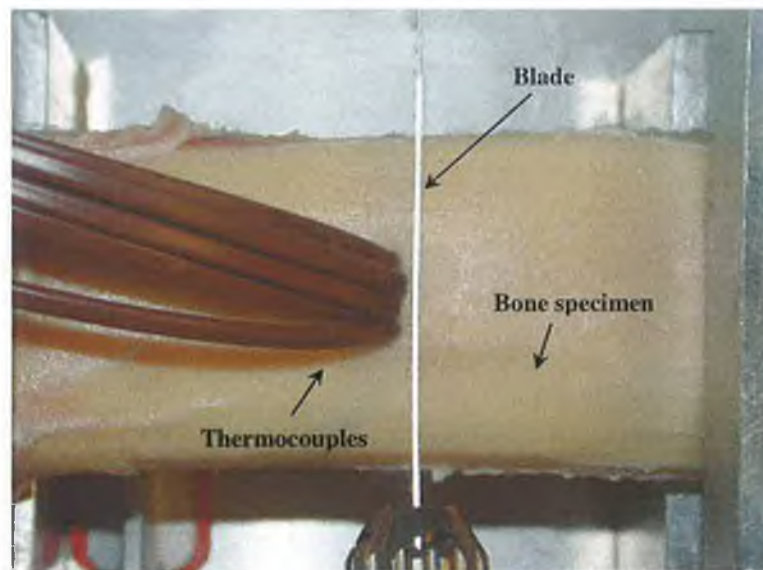


Figure 3.20: Top view illustration of sawing. Blade location relative to thermocouples

As it can be seen in Figure 3.21, the blade and bone have maximum contact in this position making initial sawing difficult. Therefore, the cutting action was adapted to a see-sawing action (Figure 3.22) to reduce the initial area of contact and hence improved the cutting efficiency of the blade. When the bone surface was cut almost 1.5mm then the saw blade could be positioned in a horizontal direction (Figure 3.21). It was observed that the more contact area between the blade and the bone, the greater the difficulty in completion the cutting process without intermittent sticking.

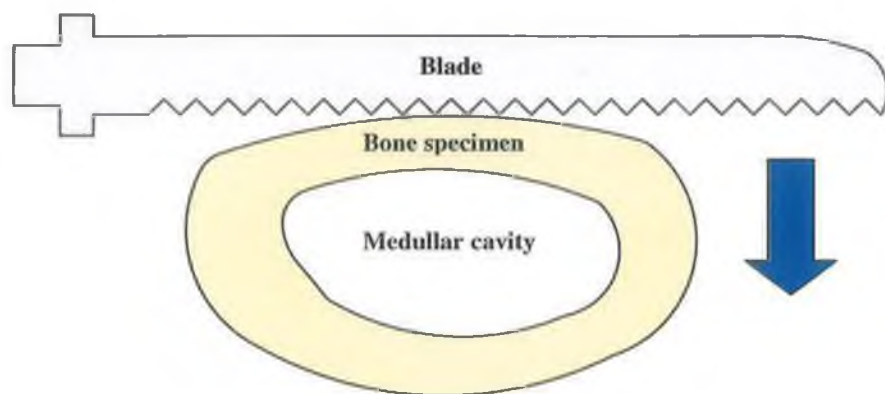


Figure 3.21: Sawing with blade held in horizontal position. Feed is in vertical direction

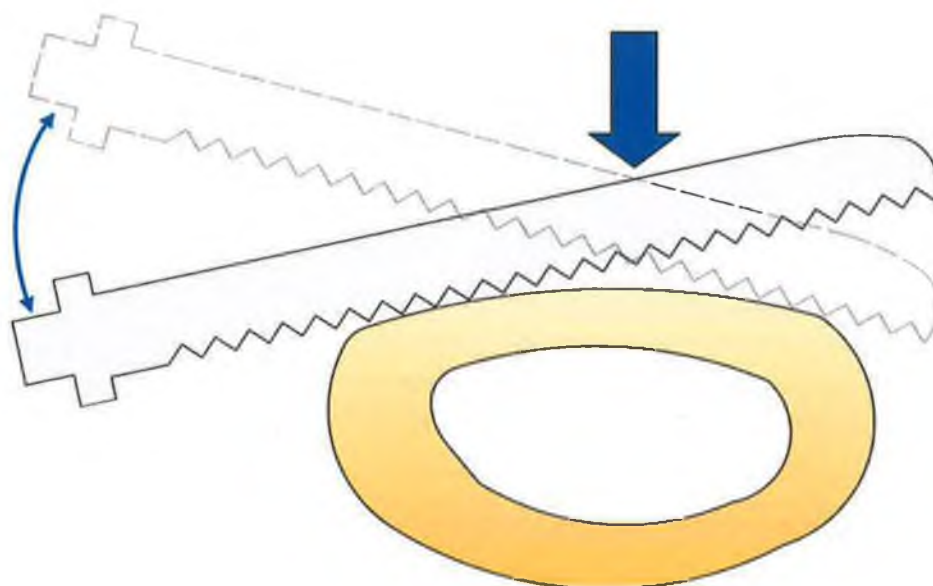


Figure 3.22: Sawing with blade held in see-sawing action. Feed is in vertical direction

3.10.1 Problems During Sawing Procedure

During sawing, some problems were encountered. The main problem was related to the reciprocating saw head which jammed several times. This may be related to the age and condition of the 3M Maxi Driver borrowed from the Orthopaedic

Department, Sligo General Hospital. Figure 3.23 shows the graph which stems from jamming the saw during a test.

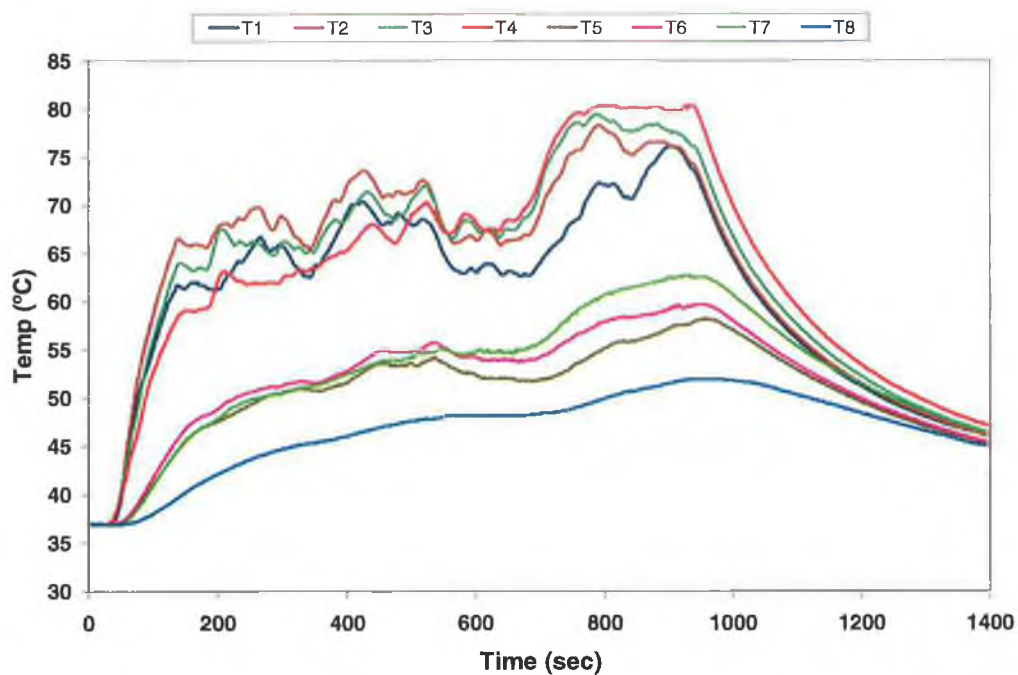


Figure 3.23: Typical temperature graph for tests in which saw blade jammed in bone specimen

The influence of heat on the saw generated during sawing may have stemmed from the continuous use of bone saw and possible expansion in the saw components such as bearings and shafts may have stopped blade movements. Thus, it was decided that some parts of reciprocating saw such as all bearings and the bronze bush should be replaced. After these replacements, a series of test were carried out to check saw's performance and it worked correctly.

3.11 Experiment 2

3.11.1 Bone Specimen Preparation

Using the same source for bone as already explained in section 3.5.1 and the same condition, a second series of tests (Experiment 2), with smaller size of bone specimen

were conducted in beams of bone of approximately 90mm × 15mm × 7.5mm. All bone specimens were carefully cut using a low speed band saw to similar size. In these series of tests, the previous bone clamping fixture was modified to retain the smaller specimen.

For temperature measurements, three thermocouples were inserted and glued into the specimens at the distance of 3mm from each other and first thermocouple was 3mm from the Sawing Zone. Figure 3.24 illustrates the thermocouples position relative to the Sawing Zone in Experiment 2.

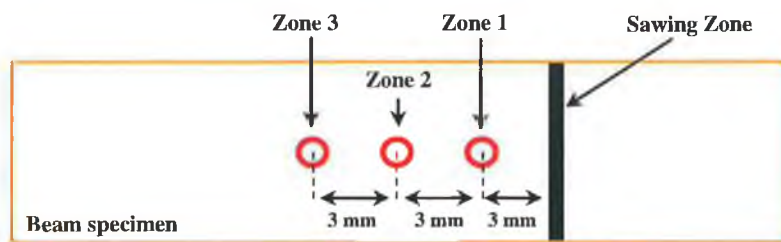


Figure 3.24: Thermocouples position relative to the Sawing Zone in Experiment 2

To have controlled tests, not only were the standard size samples used, but also control on the rate of cutting was made and rate of force in relation to different cutting speed was monitored to observe the effects of cutting rate on resulting force and wear of saw blade as well as the temperature rise while cutting bone. The modified bone fixture was mounted on a Kistler dynamometer (Type 9257BA) to measure the load while applying the saw onto the bone during sawing. The dynamometer was placed and screwed onto a Hounsfield machine (Hounsfield 100 HK S-series). The saw was mounted vertically on the top of the Hounsfield machine via a special fixture. The blade was fed down to the sample at three different rates of 1, 2, and 3mm/min. The setup of the Experiment 2 is indicated in Figure 3.25.



Figure 3.25: Schematic of the Experiment 2

Prior to the bone cutting test, high density foam specimens (saw bones) were cut to determine approximate cutting rates for effective cutting. Afterwards, the speeds were set in the Hounsfield machine. The close-up picture of cutting process in Experiment 2 is shown in Figure 3.26.

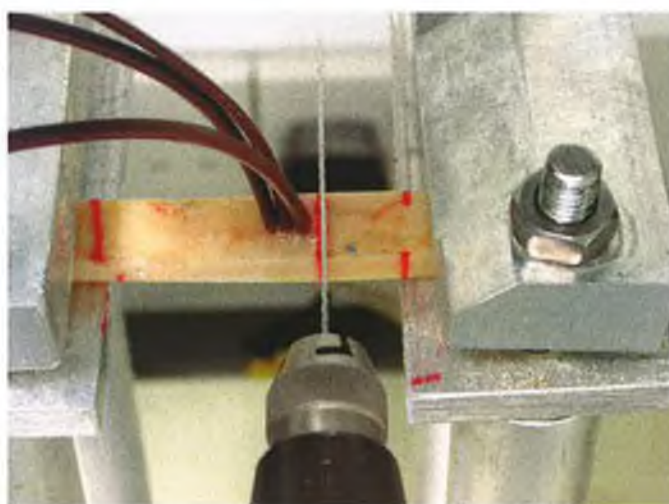


Figure 3.26: Close-up of cutting process in Experiment 2

For the data logger set up, three thermocouples were set under the same condition as previously explained for Experiment 1. Nine specimens were cut using this controlled experimental study, with three specimens each used for various feed rates of 1, 2, and 3mm/min.

3.12 Saw Blade Inspection

According to manufacturer guidelines saw blades should be used once but in reality they are frequently used more than once in orthopaedic operations. A series of tests were done to investigate the maximum durability of each blade and it was found on examination that each blade showed excessive wear after being used five times. This deficiency manifested as blunting could be observed by the researcher (during Experiment 1) whenever the sawing procedure became difficult as more pressure was needed on the saw. On the first indication of bluntness, the blade was inspected with a shadow graph machine to see the teeth if they were damaged but for further observation in order to identify blunting of the teeth, loss of teeth, scouring of surfaces, and loss of sets, investigation was carried out using SEM to observe the difference in the teeth profiles.

3.12.1 Blade Inspection by Shadow Graph

The blade was first inspected by a shadow graph Mitutoyo (Model: PJ 300). The profile of the blade was projected and it was possible to see some damaged teeth on each used blade compared to the new unused blade. The comparison of the new blade and five times used blade are shown in Figure 3.27a and Figure 3.27b, respectively. Sharp tooth and damaged tooth are apparent in these figures.

It should be notified that no clamping was necessary to hold the blade on the shadow graph bed.

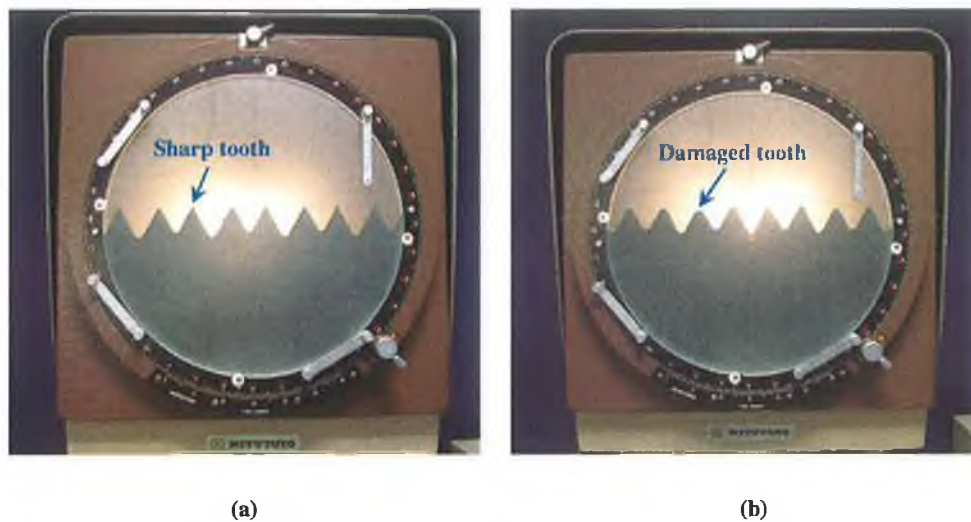


Figure 3.27: Blade profile in shadow graph (a) new, (b) damaged

3.12.2 Using SEM for Examination of the Blades

For this investigation, the bone chips and dust were cleaned from the surface and teeth of each blade as these could be mistaken as being damaged parts of the blade during the scanning process. This cleaning was done by means of a 3510 Branson Ultrasonic cleaning bath. Blades were put into water with cleaning solution; Buehler Ultramet sonic cleaning solution; and they were left for at least one hour to clear the debris off the teeth and the surface of the blades.

3.12.3 Test Set up for SEM

Blades were placed into Scanning Electron Microscope (Type: Topcon SM 600) and they were retained by means of a centering vice as shown in Figure 3.28. Two positions were chosen to take images of each blade, one from the cutting edge and another from the view adjacent to the cutting edge. In each case, two similar sections

of blade teeth were marked with an engraver. These two sections were scanned separately. First images were taken from a new unused blade and the second images were taken from the same blade after use in tests. The different characteristics of a blade before use and after five times usage were examined.

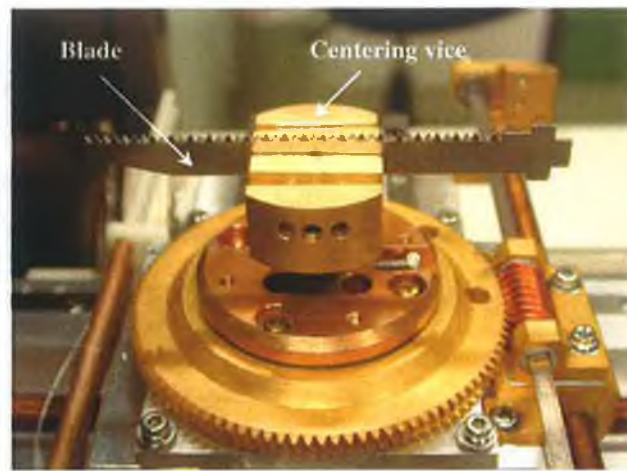


Figure 3.28: Blade setup in SEM machine

3.13 Preparation of Experimental Data for Result Analysis

Specimens' size and their cortical thickness were different but the CSA of each sample was calculated to observe the different effect on sawing time, volume of bone removal, and finally the rate of bone removal.

3.13.1 Bone Removal Volume

The volume of bone removed during all sawing was verified by measurements of transected end of bone samples and offset of the blade (described in Chapter 2) which achieved the cut.

The cross-sectional area (CSA) of cortical bone was calculated by means of ImageJ software. First of all, the images were taken with a digital camera from both

transected sections of the specimen. One ruler was placed in the same level with the transected bone to have a measurement scale for image calibration of images in ImageJ software. As can be seen in Figure 3.29, the section lines show the limit of sawing process by means of 3M Maxi Driver Reciprocating saw. The rest of the bone was cut with a band saw. Images were uploaded to ImageJ software and the cross-sectional areas which were cut by 3M Maxi Driver for both ends were calculated. The periphery of the cut sample was digitised to form an enclosed area (Figure 3.30). Using the previously defined image calibration, the digitised area of the cut surface was calculated. The average CSA from opposing cut surfaces was calculated, using the area measurement function in ImageJ.

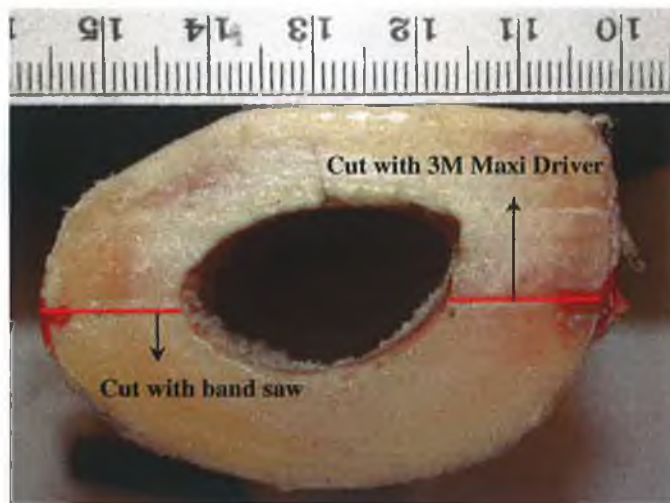


Figure 3.29: Transected section of bone and limit of sawing process by 3M and band saw

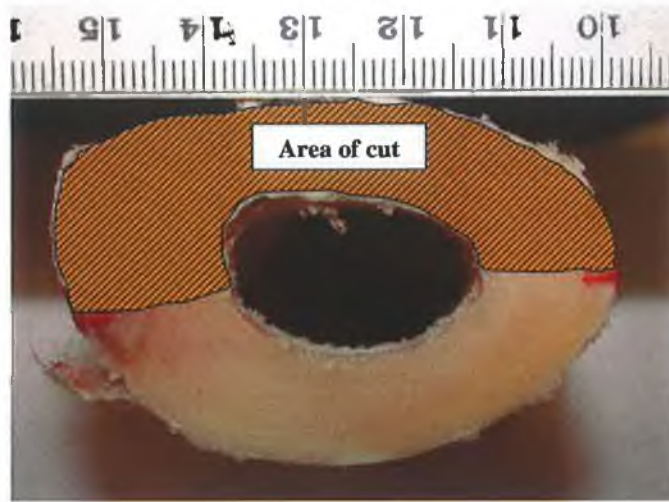


Figure 3.30: Illustration of CSA of the transected section of bone

Finally, the volume of removed bone was determined by multiplying the CSA of the cut bone surface by the blade offset.

$$\text{Volume}_{\text{removed bone}} = \text{CSA}_{\text{cut bone surface}} \times \text{Blade offset}$$

3.13.2 Rate of Bone Removal

The average rate of bone removal was calculated from the volume of removed bone divided by the sawing time recorded during experiments for each specimen.

$$\text{Average rate of bone removal} = \text{Volume}_{\text{removed bone}} / \text{Sawing time}$$

Chapter 4

Results and Discussions

Chapter 4: Results and Discussions

4.1 Overview

This study has been concerned primarily with an investigation into the temperature associated with frictional rubbing during cutting of bone which can result in necrosis. The overall objective of the study was to focus on the magnitude of temperature in the cutting zone and the size of the overheated zone relative to the cutting position with the investigation of the effect of various other parameters such as bone CSA, rate of cutting and cutting forces on the size of the affected zone.

Two series of experiments were performed as explained in Chapter 3. In the first series (Experiment 1), the sawing procedure was performed by hand using the 3M Maxi Driver reciprocating saw and the bone specimens used were the entire mid diaphysis of tibia. In the second series (Experiment 2), beams of bone of approximately 90mm × 15mm × 7.5mm were used. The bone fixture was mounted on a Kistler dynamometer, on a Hounsfield machine to measure the load while moving the saw into the bone during sawing at constant rates. The saw was mounted on the top of the Hounsfield machine via a special fixture. The blade was fed down to the sample at three different rates of 1, 2, and 3mm/min. Temperature measurements were made by T-type thermocouples and recorded by data logger.

4.2 Typical Temperature Measurement Graph

The baseline temperature for these experiments was room temperature on the day of all trials and this was typically 21°C. Normal body temperature is 37°C which is 16°C above the baseline temperature for these experiments. Therefore, this difference was

added to all temperature measurements in accordance with previously established procedures for this type of experimental process (Krause et al., 1982).

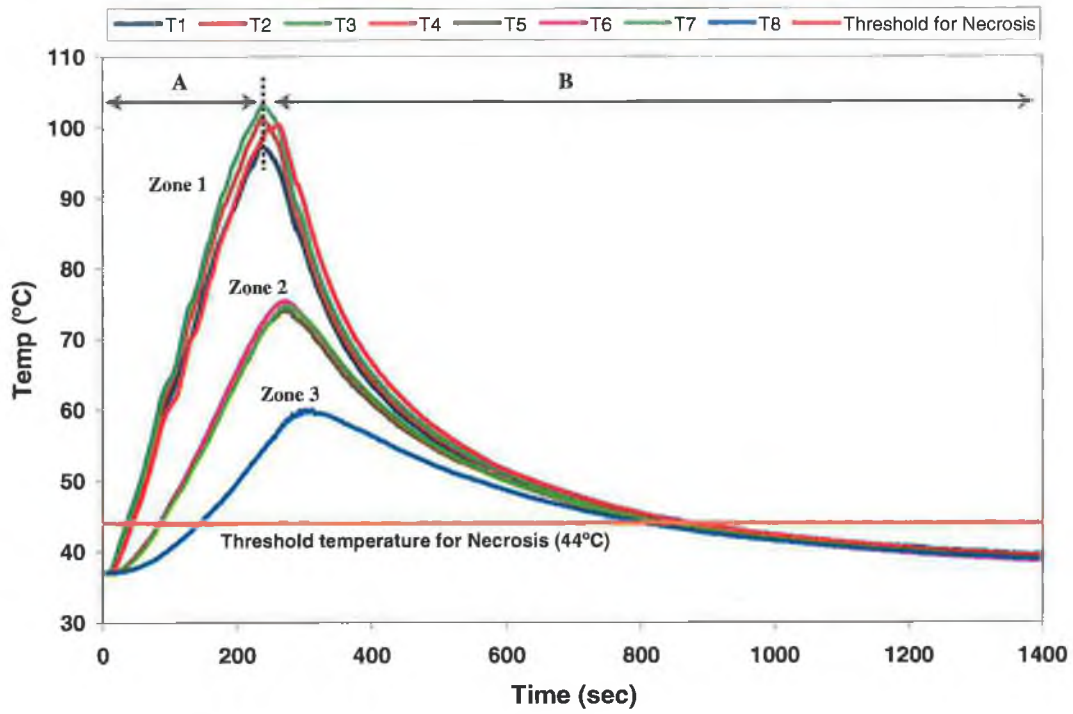


Figure 4.1: Typical temperature measurement graph in Experiment 1 showing 3 zones

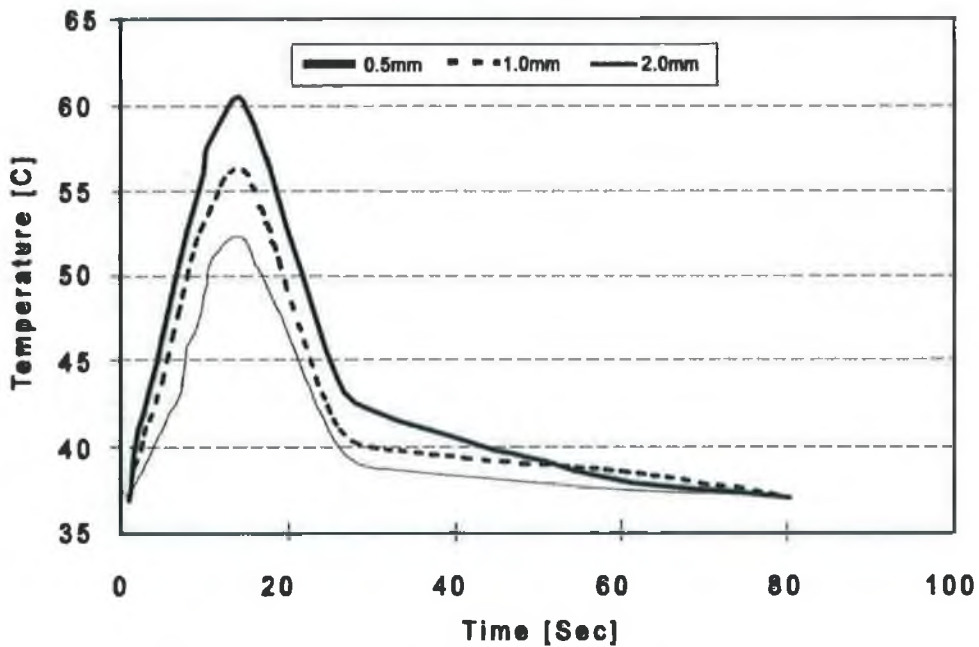


Figure 4.2: Temperature at different location from drilling site (Bachus et al., 2000)

Figure 4.1 illustrates a typical graph of temperature measurement versus time for all 8 thermocouples in Experiment 1. It may be observed from Figure 4.1 that there are three distinct clusters of data each corresponding to the measurement zones in which thermocouples were placed as described in Chapter 3 and shown again in Figure 4.3 (T1, T2, T3, and T4 in Zone 1; T5, T6, and T7 in Zone 2; T8 in Zone 3).

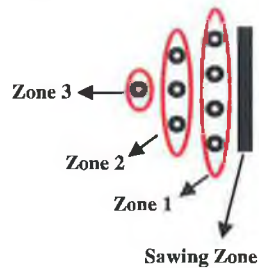


Figure 4.3: Thermocouples arrangement relative to Sawing Zone in Experiment 1

This result is similar to that of Bachus et al. (2000) showing different temperature in different location from the drill site as shown in Figure 4.2. In both of these graphs it may be observed that there is a linear increase in the temperature until it reaches a peak value with a decline in the temperature after removal of the cutting tool from the bone. Although the time taken for cutting is less for studies carried out by Bachus et al. (2000) the characteristics of the time temperature response are very similar.

As expected, the cortical bone temperatures recorded by thermocouples positioned in Zone 1, 3mm away from the Sawing Zone were always higher than those recorded by thermocouples located either in Zone 2 or Zone 3, 6mm and 9mm from the Sawing Zone, respectively. In addition, Zone 1 is closest to the region where bone necrosis, due to the excessive heat generation is most likely to occur. As such, this zone is of primary importance to clinicians and researchers investigating the effect of thermal necrosis.

From the literature it was observed that the threshold temperature for necrosis is in the range of 44°C and 47°C (Eriksson et al., 1984). For this experiment, it was decided to consider the minimum value of necrosis, 44°C as shown in Figure 4.1. In Figure 4.1, Zone 1 displayed a rapid linear increase in temperature over time period of 240 sec to the point which sawing was stopped (peak point) in the region of A. The region A includes Stage 1 and Stage 2 of cutting as shown in Figure 4.4. Stage 1 is the first contact of the blade and the bone resulting in temperature increase (starting point of Figure 4.1). Temperature increase continues due to the progress of the cutting blade into the specimen in Stage 2 until the blade totally passes the thermocouples location (Stage 3 in Figure 4.4). At Stage 3, a transverse cut half way through the bone was obtained as described in Chapter 3 and sawing was stopped. It may also be observed that the see-sawing action used to commence the cutting process has negligible effect on the profile of the Time/Temperature curves as shown in Figure 4.1.

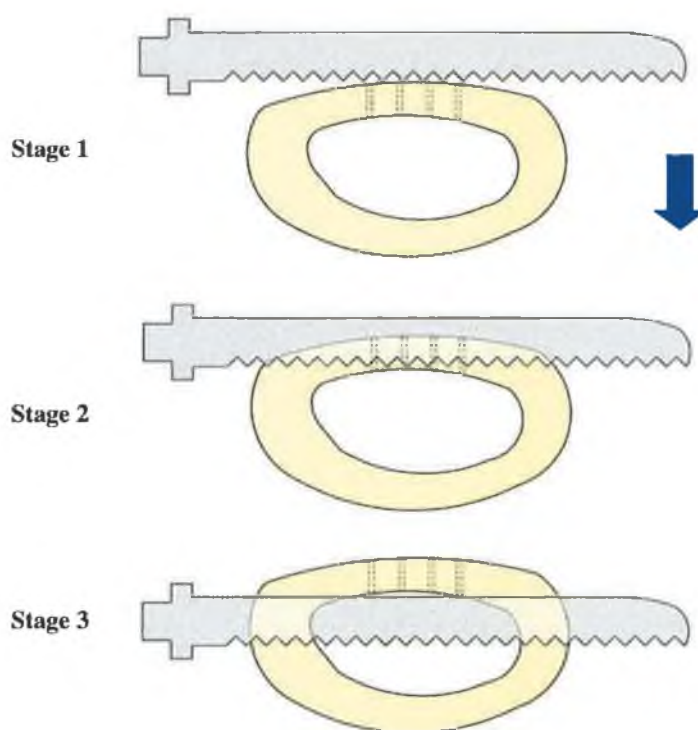


Figure 4.4: Three stages of cutting showing blade relative to thermocouples

The gradual nonlinear decrease of temperature over the time period of 1160 sec can be observed in region B to the point at which baseline temperature was reached. This decrease looks exponential as expected due to heat loss to environment during cooling. In the literature, it was noted that if no insulation in the matter of heat transfer is used, there would be heat loss to the surrounding environment and the graph will be exponential.

The same trend was observed for Zone 2 and Zone 3 with lower maximum temperature response and with a time lag at maximum points as it expected because of time taken for heat to travel through the bone from zone to zone. There is a time lag of 40 sec between Zone 1 and Zone 2, and 20 sec between Zone 2 and Zone 3.

In Zone 2, there is a sharp linear increase in temperature over 210 sec and subsequently decreasing over 1120 sec. In Zone 3, the increase occurs over 170 sec with temperature decreasing slowly over 1100 sec. From Figure 4.1, all 3 zones exceeded the limit for threshold temperature for necrosis and this was observed to occur in all trials in Experiment 1.

Experiment 1 was carried out on 20 bone samples. Analysis was carried out on the resulting data to find the cross-sectional area (CSA) of the bone cut, volume of the bone removal, and finally the approximate bone removal rate, so that the effect of these parameters on temperature could be evaluated.

In Experiment 2, three thermocouples were used to record the temperature data from the beam of bone. The typical temperature measurement graph for this experiment is indicated in Figure 4.5 showing similar trends to those of Experiment 1 but slightly lower temperatures were observed most likely due to the smaller CSA of the bone cut and shorter blade-bone contact time which could be result in less contact friction

which generates localised heating. Linear increase in temperature over 230 sec was observed in Zone 1. When the specimen was cut, gradual exponential decline can be seen over the time period of 800 sec until the baseline temperature was reached. In Zone 2 and Zone 3, the trend was similar to that of Zone 1 with lower temperature. The linear increase after 120 sec for Zone 2 and after 160 sec for Zone 3 is displayed. Finally, temperature decreased over 760 sec and 730 sec for Zone 2 and Zone 3, respectively.

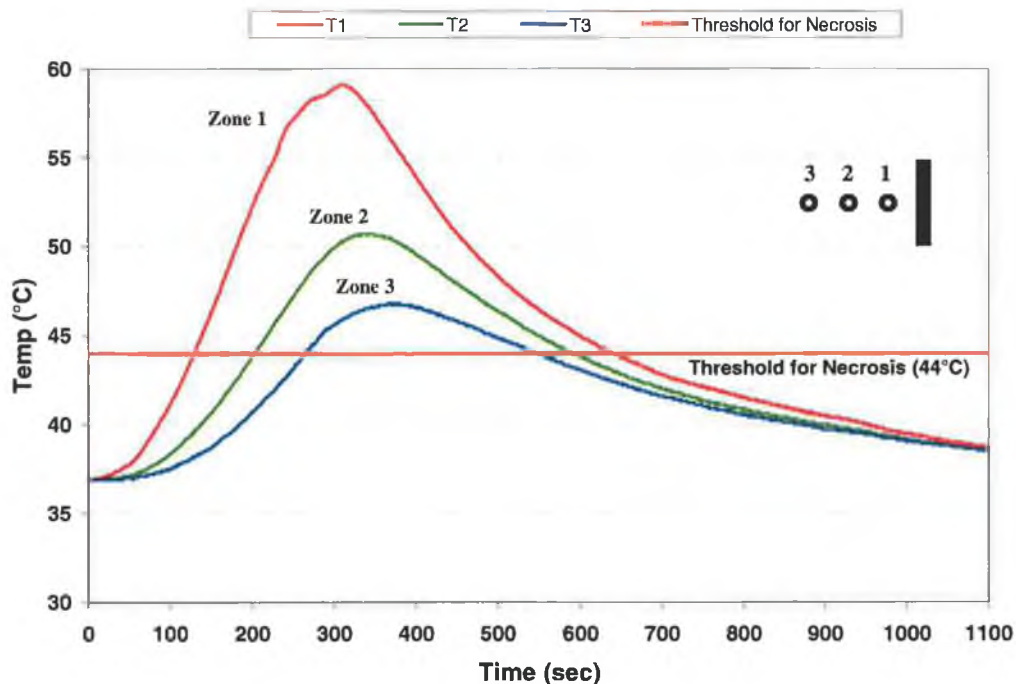


Figure 4.5: Typical temperature measurement graph in Experiment 2

4.3 Experiment 1 Results

4.3.1 Average Maximum Temperatures in each Zone

Figure 4.6 shows the average maximum temperatures for 20 tests in three different zones at 3, 6, and 9mm away from the Sawing Zone. The data was pooled and average maximum temperatures in each zone were calculated.

As can be seen in Figure 4.6, there is some scatter in each zone which may be expected with experimental measurements in bone. This scatter could also be due to uncontrolled rate of cutting, different CSA of bone and different thermal properties of bone, and was the key reason a controlled series of experiments (Experiment 2) was conducted.

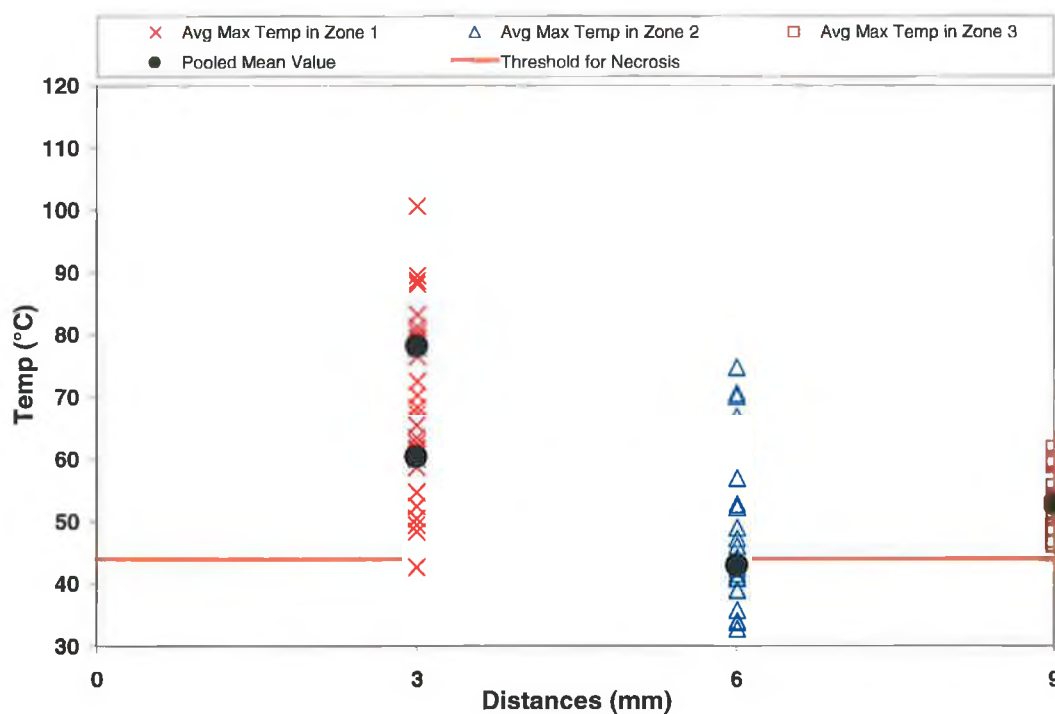


Figure 4.6: Comparison of necrosis threshold with average maximum temperatures in 3 zones

It can be observed from the graph that temperatures in all 3 zones exceeded the threshold temperature for necrosis. Average maximum temperatures of $78 \pm 9^\circ\text{C}$, $60 \pm 6^\circ\text{C}$, and $52 \pm 5^\circ\text{C}$ were observed in Zone 1, Zone 2, and Zone 3, respectively.

Using the temperature values in each zone, it is possible to extrapolate the temperature value at any time interval during experiment such as 100, 200, and 300 sec. In contrast to the previous studies conducted by Krause (1977), Krause et al. (1982), and Wachter and Stoll (1991), in this study, no thermocouple was placed on the saw blade to measure the actual temperature on the saw blade. However, it was

possible to extrapolate the temperature at sawing position (Sawing Zone) by having the three values for 3 existing zones in Experiment 1 as shown in Figure 4.7.

To assess maximum saw blade temperature, maximum temperature (peak points) in all 3 zones was chosen as shown in Figure 4.7. These three values for all trials are plotted against distances as illustrated in Figure 4.8 and assuming a heat loss to the surrounding environment, the saw blade temperature is extrapolated by fitting an exponential curve through the data points.

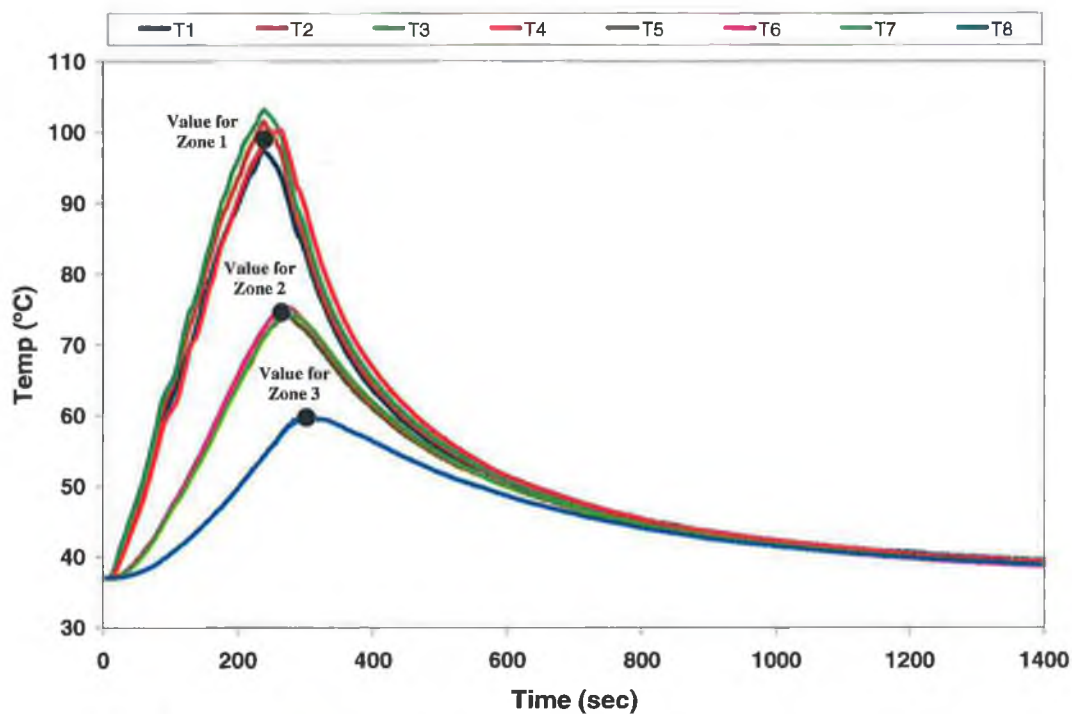


Figure 4.7: Selection of maximum temperature in zones for extrapolation of saw blade temperature

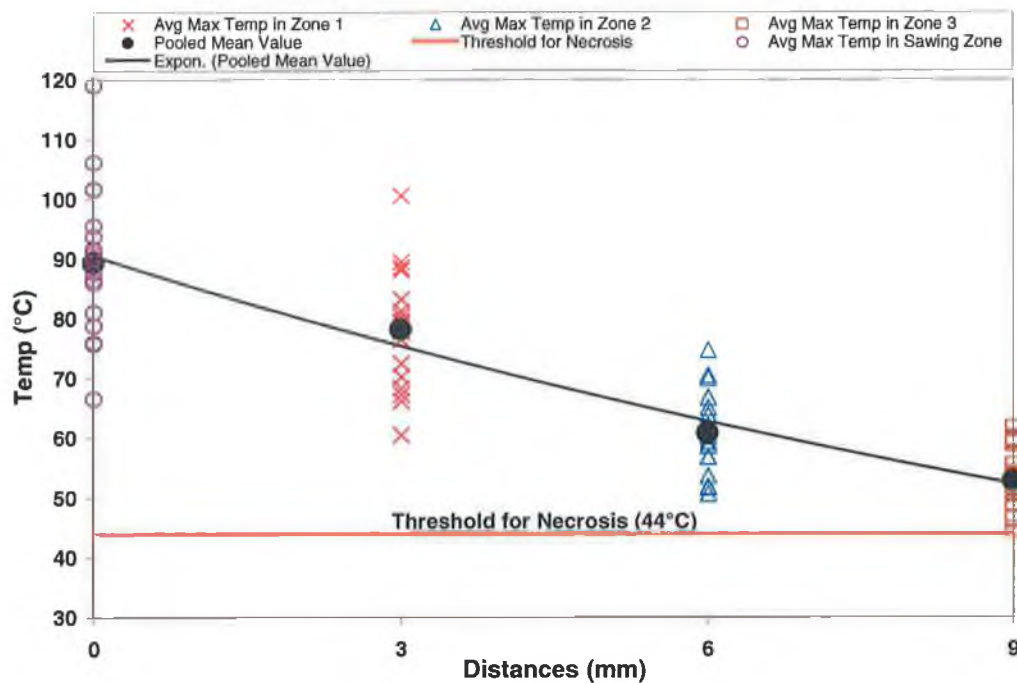


Figure 4.8: Extrapolated values for Sawing Zone

The extrapolated temperatures at the Sawing Zone are indicated in Table 4.1. The extrapolated pooled mean value for the saw blade temperature for all tests was $89 \pm 12^\circ\text{C}$.

Krause (1977) and Krause et al. (1982) reported temperature exceeding 150°C and 200°C on the saw blade, respectively, while temperature greater than 100°C was recorded by Wachter and Stoll (1991). In this research, temperature over 100°C was observed at Sawing Zone in four test trials in Experiment 1. Different experimental conditions in our experiment compare to Krause (1977), Krause et al. (1982) and Wachter and Stoll (1991) such as employing different cutting saw blades, variations in specimen thickness and inherent variations in structural, mechanical, thermal properties of bone might be the reason for variations in temperature response, therefore, it is difficult to draw general conclusions.

Test No.	Average maximum saw temperature (°C)
1	76
2	66
3	92
4	90
5	106
6	76
7	91
8	94
9	76
10	95
11	81
12	86
13	102
14	91
15	87
16	88
17	102
18	119
19	79
20	90
Mean± SD	89±12

Table 4.1: Extrapolated average maximum saw temperature in each test in Experiment 1

4.3.2 Total Time that Temperatures Exceeded 44°C

Chapter 2 highlighted that if the temperature elevation during cutting of bone exceeds 44°C for longer than 1 min (60 sec), bone repair is impaired (Eriksson et al., 1984). Therefore, in the Experiment 1, for each zone the total time that the temperature in that zone exceeded 44°C was monitored and recorded. For this, in each zone one thermocouple was chosen and the total period for which temperature exceeded the necrosis threshold was measured. If this value is more than 60 sec, it may be assumed that the bone in this zone could undergo necrosis. Figure 4.9 shows a graph of results analysis and indicates that in all except one test, all zones exceeded the time temperature threshold for necrosis.

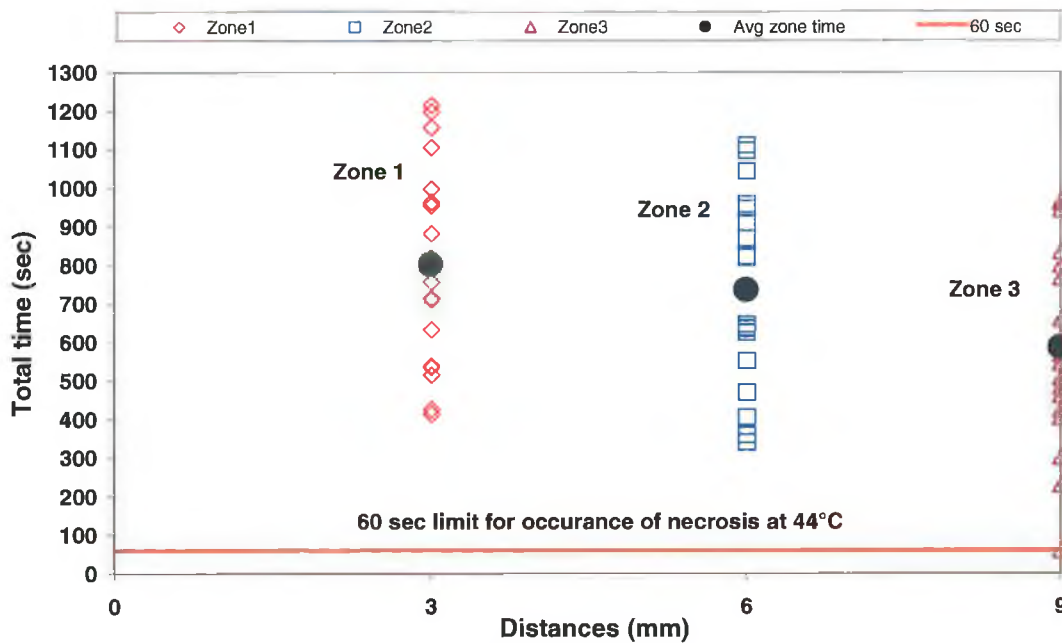


Figure 4.9: Illustration of zones exceeding necrosis value more than 60 sec for 20 tests

4.3.3 Rate of Temperature Increase

To establish the variation in rate of temperature increase in each zone the rise time for all three zones for 20 tests was calculated. To investigate this, two points were chosen in the linear portion of the typical temperature measurement graph for each zone and the rise times ($\Delta T/\Delta t = ^\circ\text{C}/\text{sec}$) were calculated. The result of this calculation is indicated in Figure 4.10. The rate of temperature increase is affected by the temperature difference between two points (one hot, one cold), the thermal conductivity of the material and the CSA of the material, and time over which temperature transfer occurs. In the case of this experiment, it is assumed that the only variable is the CSA of the specimen and results for temperature increase were plotted against CSA of cut specimen (Figure 4.11). A neutral relationship can be observed in all 3 zones as illustrated in Figure 4.11, so it may be concluded that different CSA values will not have a significant impact on the temperature increase.

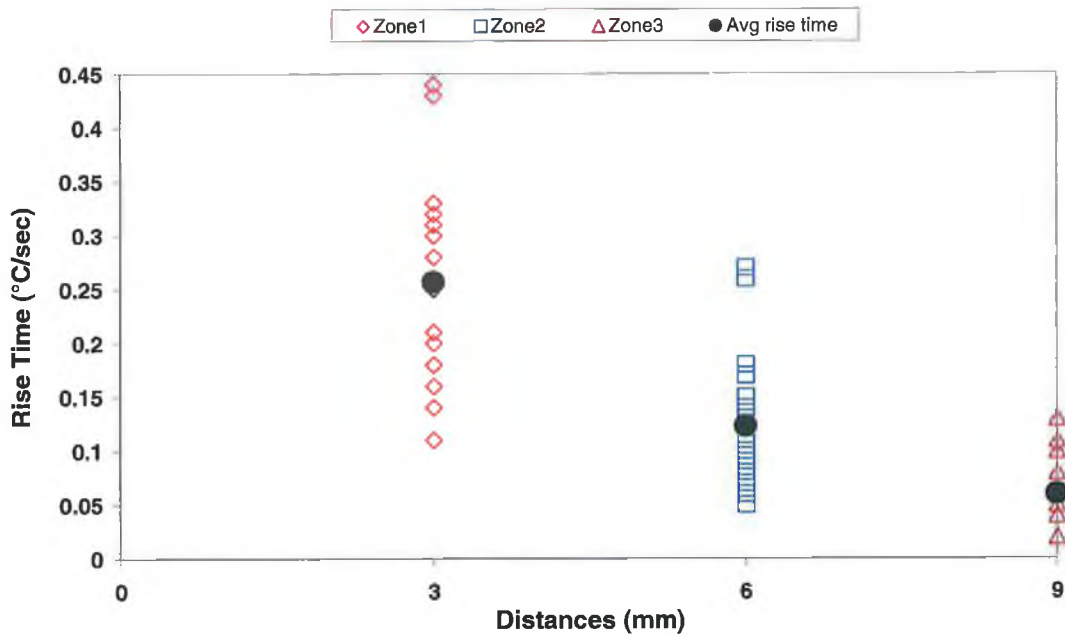


Figure 4.10: Comparison of rise time in 3 different zones for 20 tests

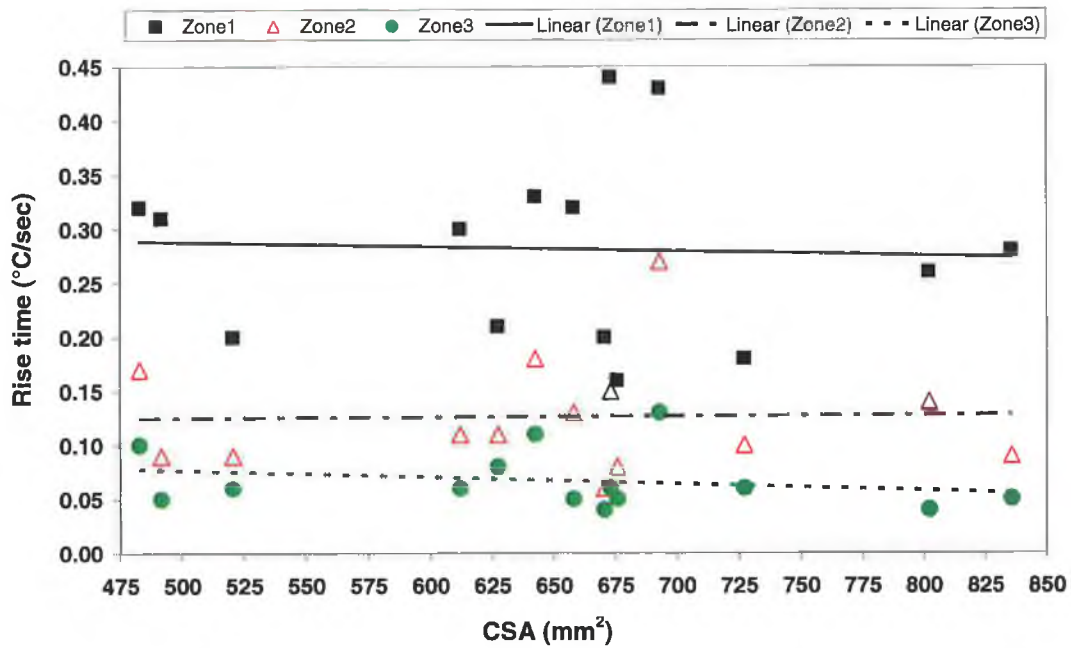


Figure 4.11: Illustration of rise time versus CSA in 3 zones

For CSA values, there were only 15 measured values out of 20 samples because the first 5 samples were lost due to storage problems, so the work was carried out just for

15 samples. The CSA values for these specimens and the time which took for sawing are shown in Table 4.2.

Test No.	CSA (mm ²)	Sawing time (sec)
6	802	600
7	658	600
8	670	480
9	727	420
10	836	480
11	673	360
12	612	480
13	676	600
14	491	480
15	520	300
16	627	360
17	482	420
18	642	300
19	561	240
20	693	240

Table 4.2: Various CSA and sawing time for different bone samples in Experiment 1

4.4 Experiment 2 Results

4.4.1 Average Maximum Temperatures in each Zone

Average maximum temperature in each zone for Experiment 2 for different cutting rates may be seen in Table 4.3. The same assumption was made for this experiment regarding exponential transfer of heat through the specimen, so values at the Sawing Zone were extrapolated in a similar manner. The pooled mean value of temperature at different rates of cutting for different zones is also illustrated in Table 4.3 and the graphical relation is shown in Figure 4.12. These values are lower in comparison to the values in Experiment 1 (78°C, 60°C, and 52°C). The recorded range is smaller, and this is most likely due to the greater control in terms of cutting rates, and specimen sizes.

Average maximum temperature (°C)					
Test No.	Cutting rate	Zone 1	Zone 2	Zone 3	Sawing Zone
1	1 (mm/min)	78	67	63	85
2		73	60	48	86
3		70	58	50	78
Pooled mean±SD		74±4	61±5	54±8	83±4
4	2 (mm/min)	56	50	45	62
5		59	51	47	64
6		56	47	43	62
Pooled mean±SD		57±2	49±2	45±2	63±2
7	3 (mm/min)	68	52	46	78
8		52	45	41	57
9		62	50	45	70
Pooled mean±SD		61±8	49±4	44±3	68±11

Table 4.3: Average maximum temperatures and pooled mean at 3 cutting rates in 4 zones

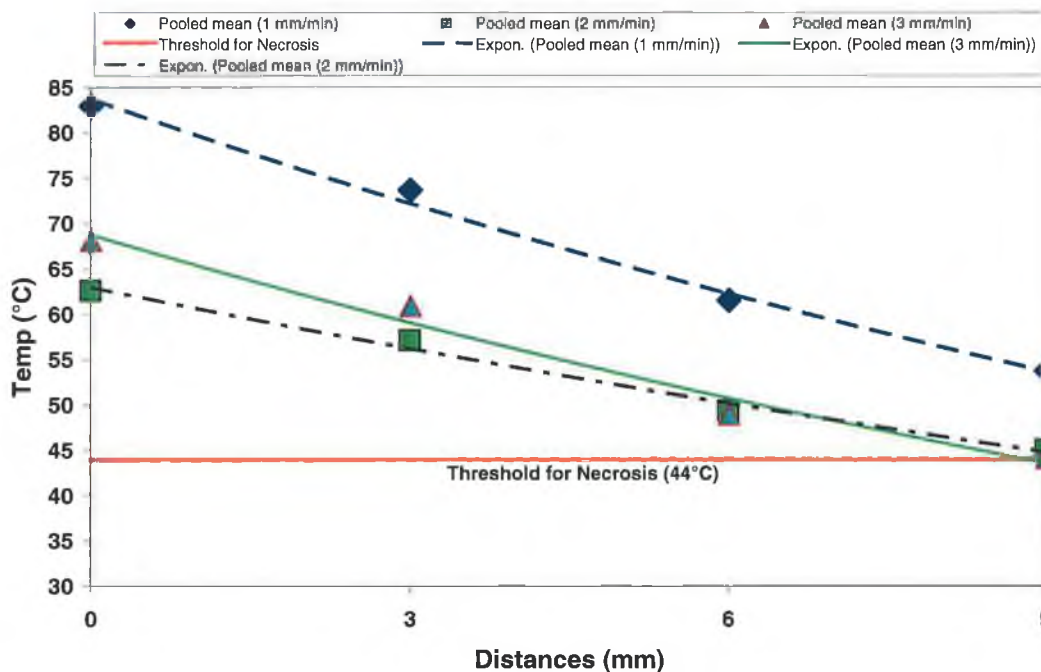


Figure 4.12: Pooled mean value of temperatures at different rates at various distances

Although specimen CSA was smaller for these specimens than used in Experiment 1, all zones exceeded the threshold temperature for necrosis. Higher temperature was measured for the rate of 1mm/min in all zones in comparison to other cutting rates while a similar temperature response can be seen in the rate of 2 and 3mm/min.

4.4.2 Total Time that Temperatures Exceeded 44°C

The same process to evaluate the period of time that temperature exceeds the threshold for necrosis as explained earlier in section 4.3.2 was carried out for Experiment 2 and shown in Figure 4.13. As in Experiment 1 the temperature in all three zones exceeded the temperature threshold for necrosis and therefore, it is likely that cell necrosis could occur in all zones. The total time that temperature in each zone exceeds this threshold is less in Experiment 2 most likely due to shorter cutting time which will affect bone-blade contact time. Reduction of this bone-blade contact would likely reduce frictional heat generated in the cutting zone.

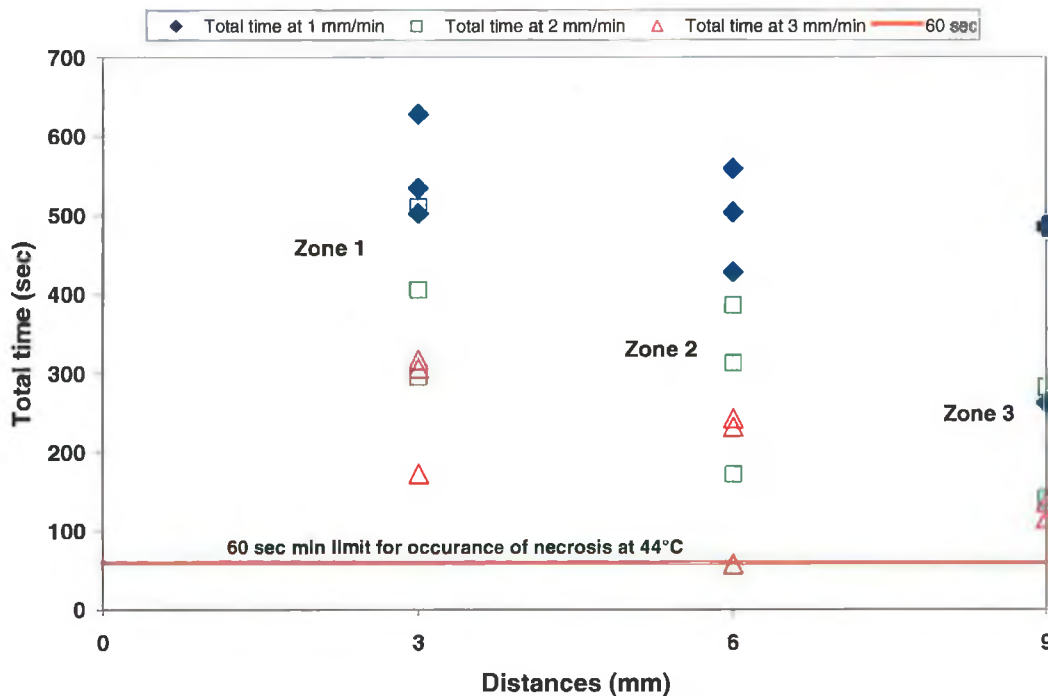


Figure 4.13: Illustration of zones exceeding necrosis value more than 60 sec for 9 tests

4.4.3 Effect of Cutting Rates on Temperature Response

Figure 4.14 shows the average maximum temperatures which were observed in 3 zones for experiments conducted at various rates which is quite similar to that of

Krause (1977) who illustrated temperature versus different feed rates as a function of depth of cut for bone bur (Figure 4.15).

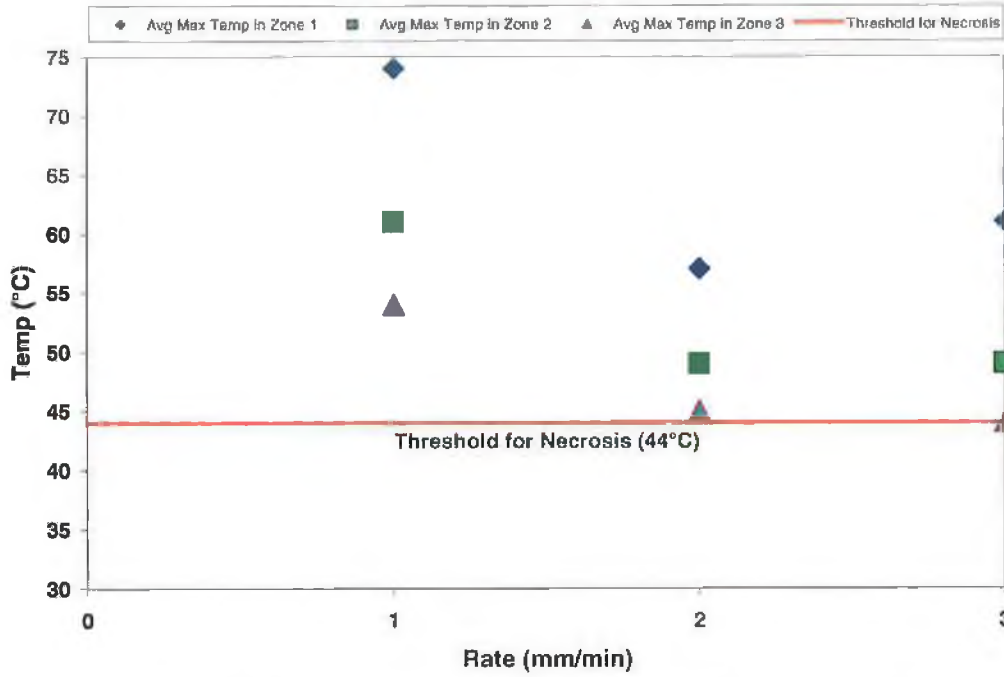


Figure 4.14: Average maximum temperatures for 3 zones at different rates

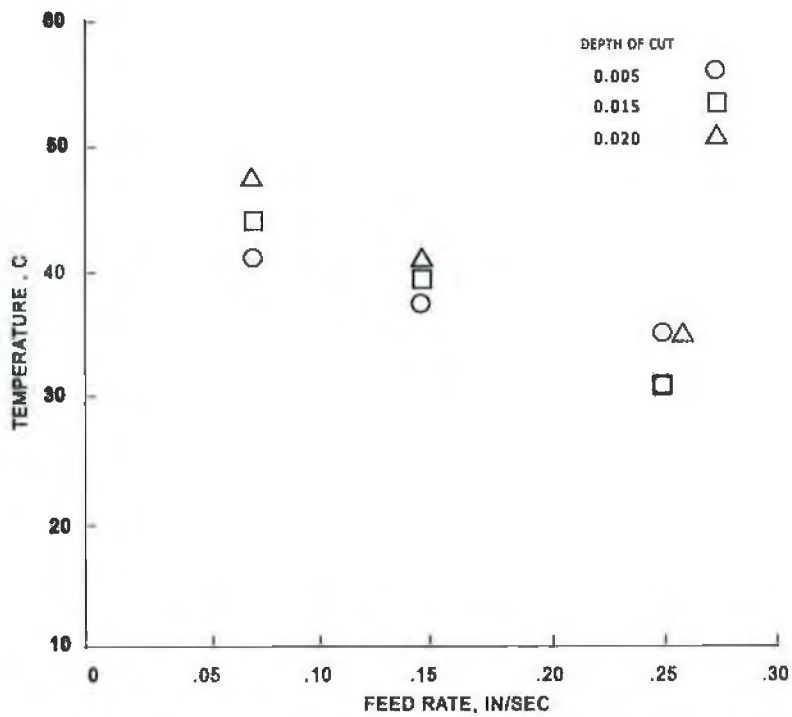


Figure 4.15: Temperature rise as a function of feed rate (Krause, 1977)

From this analysis it may be observed that the p-value (P) calculated is 0.006 ($p < 0.05$) which supports the hypothesis that the cutting rate affects the magnitude of the temperature generated in the cutting process.

In this study, it was shown with higher cutting rates, there is a shorter blade bone contact time resulting in less heat generated and also shorter time for temperature to return to baseline temperature. This is in accordance to Sharawy et al. (2002) who drilled porcine jawbone. Therefore, it seems likely that is advantageous to use higher rates for cutting than 3mm/min in dense bone, because it should reduce the time of sawing and generate less heat.

4.4.4 Force Measurement

Figure 4.17 indicates the typical force measurement at the cutting rate of 2mm/min. In region A, the blade makes contact with the bone. The blade then cuts through the specimen making a full contact with the bone and the force response is shown in region B. The fluctuation of force in this region might be due to occurrence of fracture and bone chipping or blade vibration during this time period. Finally, in region C the bone was totally cut through and cutting force drops back to zero.

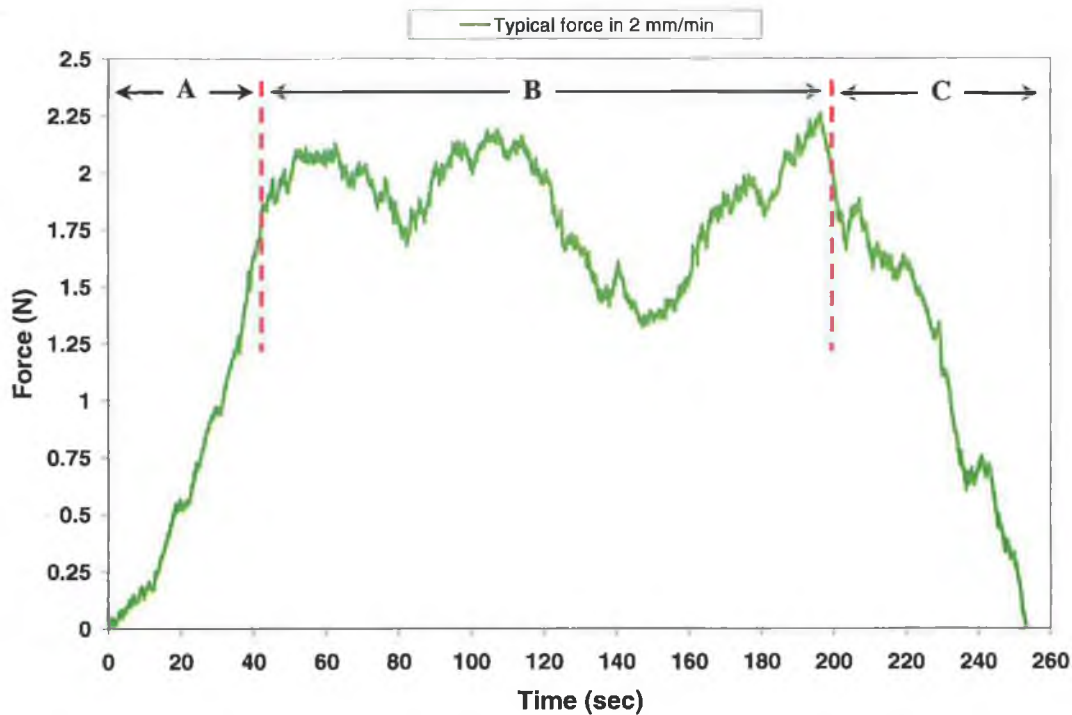


Figure 4.17: Typical force graph for cutting rate of 2 mm/min

4.4.5 Comparison of Different Forces at Different Cutting Rates

The average forces in the duration of cutting for each cutting rate were calculated and they were then plotted against the cutting rates. Figure 4.18 shows that the highest force was observed at the least cutting rate of 1mm/min. There is a sharp decline in the force value as the cutting rate was increased. When increasing the cutting rate from 2mm/min to 3mm/min, slight increase in the force value was detected, however, it is not possible to conclude from this data alone if this trend would continue for further increase in cutting rates.

Krause et al. (1982) measured the force applied by a surgeon during sawing of bone, using a reciprocating saw; and found a vertical force of 4.5 N to 7 N. The result of our study showed this vertical force value can be variable even with constant cutting rates, while the cutting rate also varies with feed rate with the force value varying between 1N and 10N.

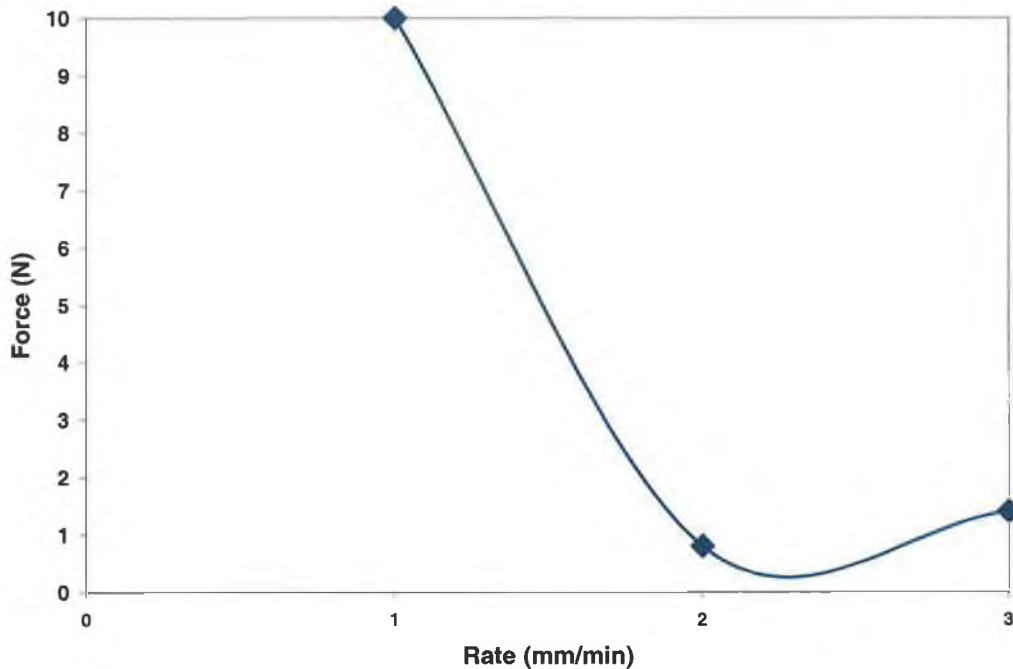


Figure 4.18: Illustration of average force at 3 different cutting rates

It should be noted that more consistent load was observed at rate of 2mm/min in Experiment 2; however, there are insufficient results from this study to prove conclusively that this would be the optimum cutting rate for bone. Other factors that would have to be considered are the potential variations in mechanical properties of the bone used in experiments, the effects of variations in cutting blade design and the use of external variants such as coolant.

It is also suggested that the clinicians interrupt the cutting process at least every 5 sec for at least 10 sec. The interruption will dramatically reduce the time the cortical bone temperature is elevated. This is most important in the most dense bone types (Sharawy et al., 2002; Wachter and Stoll, 1991). As was shown in our experiment when the cutting blade was jammed in the bone specimen and had to be released, there was a decrease in temperature (Figure 4.19).

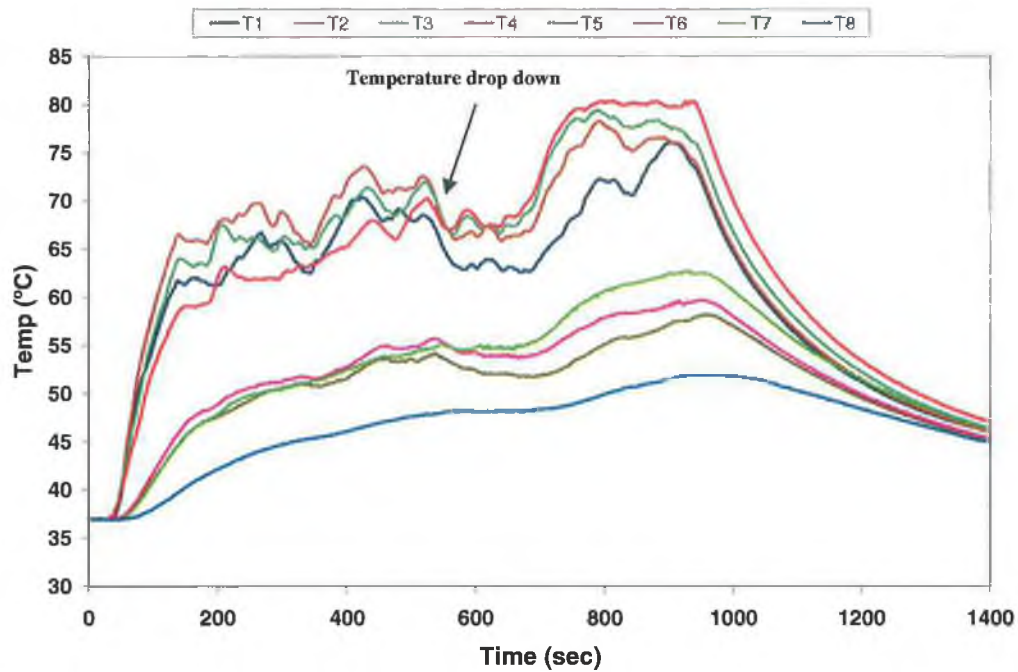


Figure 4.19: Temperature decrease as a result of sticking blade

4.5 Blade SEM Observation Results

In Chapter 3, the process for observation of the damaged blade using Scanning Electron Microscope was explained. The side and the cutting edge of a new unused blade tooth before the cutting action may be seen in Figure 4.20 and Figure 4.21, respectively. The sharp edges are clear in these images. There are some black spots on the tooth which is probably related to the manufacturing process and tooth surface is not that polished in these SEM images which can not be seen by naked eyes. After subsequent cutting trials up to five cutting trials, another series of SEM images were taken from the same tooth which are indicated in Figure 4.22 and Figure 4.23. The blunt edges are distinguishable and it was observed that the rate of wear is more pronounced on the cutting tooth between fourth and fifth trial.

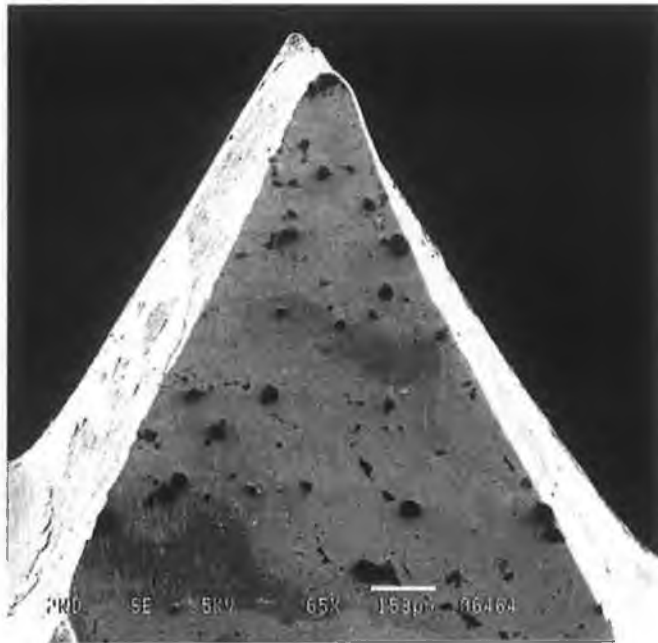


Figure 4.20: SEM image of new unused blade in view adjacent to the cutting edge

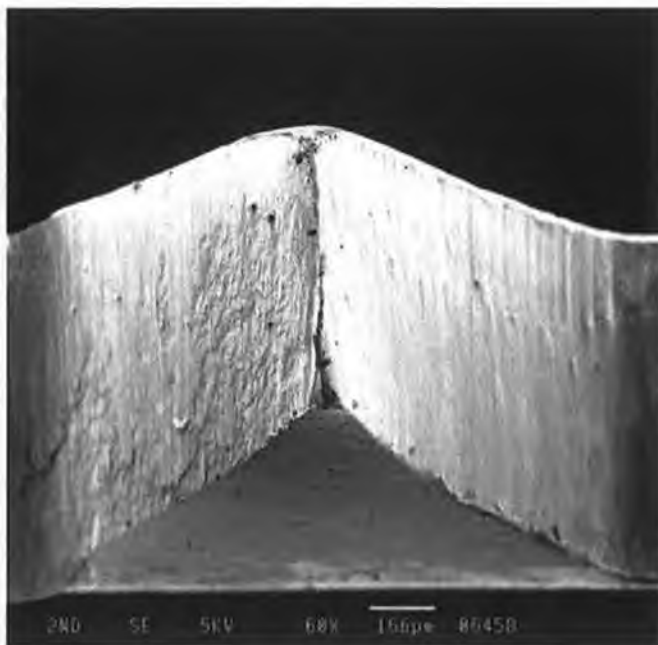


Figure 4.21: SEM image of cutting edge of the new unused blade

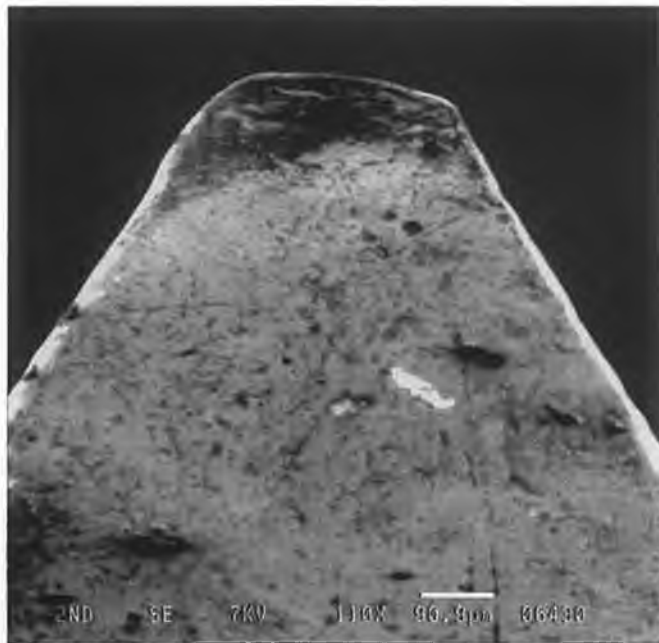


Figure 4.22: SEM image of used blade in view adjacent to the cutting edge



Figure 4.23: SEM image of cutting edge of the used blade

It can be seen that the cutting edge in Figure 4.24 is totally damaged and worn after 15 trials.

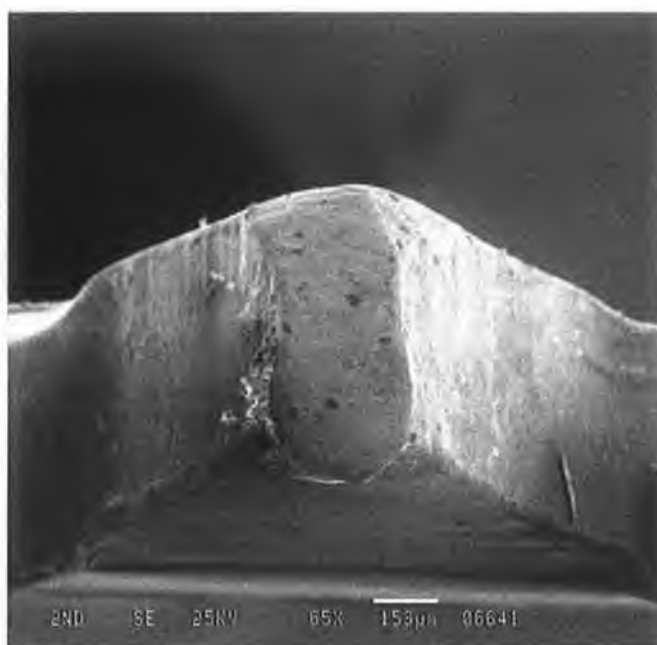


Figure 4.24: Cutting edge after 15 trials

Blade sharpness is one of the most significant factors in its cutting efficiency which should be considered in any orthopaedic surgery as much greater temperature elevation were recorded when a worn drill was used (Matthews and Hirsch, 1972). In our study, the wear of saw blade after 5 and 15 trials illustrated the damage on the cutting tooth. It is suggested that the cutting blade be examined by shadow graph or SEM and it should be replaced after each use in accordance with Allan et al. (2005) who studied the effect of drill wear on temperature and concluded that drills must be discarded after single use. In reality, most hospitals do not discard saw blades and drills bits after one use simply from an economic point of view.

4.6 Threshold for Necrosis

Regarding the temperature threshold for necrosis, it has been highlighted that either in Experiment 1 (Figure 4.7) or Experiment 2 (Figure 4.12), all zones as well as Sawing Zone exceeded the temperature limit of 44°C for necrosis, so did the duration of total

time above 44°C in both experiments. In the case of the size of the overheated zone relative to the cutting position, the study conducted by Bachus et al., (2000) showed that necrosis happens at distance of 2mm from drilling sites however there was no further results presented showing the extent of necrosis over the larger bone sample. However, this study showed thermal necrosis extends outwards from the cutting zone to a distance of at least 9mm either side of the cutting blade for the temperatures recorded. The obvious side affect of these increases in cutting temperatures and heat in this zone is impaired bone regeneration previously established by other researchers (Eriksson et al., 1984), infection and reduced mechanical strength of bone (Christie, 1981), and delayed post operative healing (Pallan, 1960).

Due to the low thermal conductivity of bone, heat generated during cutting is not dissipated quickly but remains around the cutting site. It is reasonable to assume therefore based on the results from Experiment 1 and Experiment 2 that the creation of even higher temperatures than recorded during these experiments could lead to extension of the cutting zone beyond the 9mm distance measured with this experimental arrangement thus leading to local necrosis, delaying bone repair.

Chapter 5

Conclusions and Future Work

Chapter 5: Conclusions and Future Work

Two experiments were carried out which have shown the extent of the temperature gradient in three zones through the bone in all trials. The data from these experiments was found to be in good agreement with published literature. It was not possible to compare other results from this experimental work such as cutting feed rate effects during bone sawing due to lack of information in the literature.

The main conclusions from this research work may be summarised as follows:

1. A technique for measurement of temperature in the localised cutting zone while sawing of bone has been developed.
2. There will be a region of bone at least 9mm either side of the cutting blade with impaired bone regeneration as temperatures in this region exceeded the threshold temperature for necrosis in all experiments. It has previously been established that this will lead to an increase in bone healing time and could cause reduced bone strength in this region.
3. The results of this research shows that there is an exponential relationship between the temperature measured in the three cutting zones assuming a potential heat loss which may be due to environmental or material factors.
4. The cutting rate of 2mm/min has been identified as the optimum rate for cutting of bone using a reciprocating saw as minimum cutting temperatures was observed for this rate. Furthermore, it may be observed that the minimum cutting forces were also measured at the same cutting rate.
5. Increasing the cutting rate from 1mm/min to 2mm/min led to a decrease in the temperature and cutting force, as well as the total duration for which the bone

was subjected to a temperature above 44°C (threshold temperature for necrosis). It was noted that the further increase in cutting rate has minimal effect on temperature reduction in Zone 2 and Zone 3 away from the cutting blade.

6. From a one way Anova conducted on the data it was observed that a p-value of less than 0.05 supported the hypothesis that the cutting rate affects the magnitude of the temperature generated in the cutting process.
7. Assuming blade wear (as was observed in our experiments) occurs at a typically constant rate we conclude that the cutting blade should be replaced after each use as they are frequently used more than once in operating theatres.
8. No attempt was made to cool down the cutting site using saline solution or any coolant during either in Experiment 1 or Experiment 2. It has previously been shown to be beneficial to use coolant while cutting bone during drilling studies and further research should be conducted to investigate the effect of this process on bone cutting using reciprocating saws.
9. Previous researchers have proposed the interruption of the cutting process and application of intermittent load rather than continuous load while cutting bone. The interruption would reduce the time the cortical temperature is elevated (Sharawy et al., 2002; Wachter and Stoll, 1991). This study has not considered the effect of intermittent loading during sawing but some experiments conducted where the bone saw stuck and had to be freed showed that temperature dropped during the process of saw extrication suggesting that this merits further investigation.

10. A detailed study of a greater range of cutting rate effects could provide a greater insight to the effect of cutting rate on cutting forces, cutting temperatures and optimized sawing conditions and this should be conducted with a range of controlled specimen sizes and specimen cross sectional areas.

References

- Abouzia, M. B., James, D. F., (1997). Temperature rise during drilling through bone. *The International Journal Of Oral & Maxillofacial Implants* 12, 342-353.
- Abouzia, M. B., Symington, J. M., (1996). Effect of drill speed on bone temperature. *International Journal Of Oral And Maxillofacial Surgery* 25, 394-399.
- Allan, W., Williams, E. D., Kerawala, C. J., (2005). Effects of repeated drill use on temperature of bone during preparation for osteosynthesis self-tapping screws. *British Journal of Oral and Maxillofacial Surgery* 43, 314-319.
- Ark, T. W., Neal, J. G., Thacker, J. G., Edlich, R. F., (1998). Influence of irrigation solutions on oscillating bone saw blade performance. *Journal Of Biomedical Materials Research* 43, 108-112.
- Ark, T. W., Thacker, J. G., McGregor, W., Rodeheaver, G. T., Edlich, R. F., (1997a). A technique for quantifying the performance of oscillating bone saw blades. *Journal Of Long-Term Effects Of Medical Implants* 7, 255-270.
- Ark, T. W., Thacker, J. G., McGregor, W., Rodeheaver, G. T., Edlich, R. F., (1997b). Durability of oscillating bone saw blades. *Journal Of Long-Term Effects Of Medical Implants* 7, 271-278.
- Ark, T. W., Thacker, J. G., McGregor, W., Rodeheaver, G. T., Edlich, R. F., (1997c). Innovations in oscillating bone saw blades. *Journal Of Long-Term Effects Of Medical Implants* 7, 279-286.
- Arnett, T., (2005). Bone structure and bone remodelling [online]. Available from: <http://www.biochem.ucl.ac.uk/teaching-resources/course-information/c41/Arnett%20Bone%20Structure%20&%20Remodelling%20Chapter.pdf> [Accessed 14 August 2005]
- Bachus, K. N., Rondina, M. T., Hutchinson, D. T., (2000). The effects of drilling force on cortical temperatures and their duration: an in vitro study. *Medical Engineering & Physics* 22, 685-691.
- Balasubramaniam, T. A., Bowman, H. F., (1977). Thermal conductivity and thermal diffusivity of biomaterials: A simultaneous measurement technique. *Journal Of Biomechanical Engineering* 99, 148-154.
- Baumgart, R., Kettler, M., Zeiler, C., Weiss, S., Schweiberer, L., (1998). Indications and technique of bone cutting. *Der Chirurg; Zeitschrift Fur Alle Gebiete Der Operativen Medizin* 69, 1188-1196.
- Biyikli, S., Modest, M. F., Tarr, R., (1986). Measurements of thermal properties for human femora. *Journal Of Biomedical Materials Research* 20, 1335-1345.

Bonfield, W., Li, C. H., (1968). The temperature dependence of the deformation of bone. *Journal of Biomechanics* 1, 323-329.

Boyne, P. J., (1966). Histologic response of bone to sectioning by high-speed rotary instruments. *Journal Of Dental Research* 45, 270-276.

Bragger, U., Wermuth, W., Torok, E., (1995). Heat generated during preparation of titanium implants of the ITI®; Dental Implant System: an in vitro study. *Clinical Oral Implants Research* 6, 254-259.

Brisman, D. L., (1996). The effect of speed, pressure, and time on bone temperature during the drilling of implant sites. *The International Journal Of Oral & Maxillofacial Implants* 11, 35-37.

Chato, J. C., (1965). A survey of thermal conductivity and diffusivity data on biological materials. In: 5th Conference on Thermal Conductivity 2, session IV-VI, Denver, CO.

Christie, J., (1981). Surgical heat injury of bone. *Injury* 13, 188-190.

Collins, D. H., (1953). Structural changes around nails and screws in human bones. *The Journal Of Pathology And Bacteriology* 65, 109-121.

Cordioli, G., Majzoub, Z., (1997). Heat generation during implant site preparation: an in vitro study. *The International Journal Of Oral & Maxillofacial Implants* 12, 186-193.

Costich, E. R., Youngblood, P. J., Walden, J. M., (1964). A study of the effects of high-speed rotary instruments on bone repair in dogs. *Oral Surgery, Oral Medicine, And Oral Pathology* 17, 563-571.

Cowin, S. C., (1989). *Bone Mechanics*. CRC Press, Boca Raton.

Currey, J. D., (2002). *Bones: Structure and Mechanics*. Princeton University Press, New Jersey.

Currey, J. D., Butler, G., (1975). The mechanical properties of bone tissue in children. *The Journal Of Bone And Joint Surgery.American* Volume 57, 810-814.

Davidson, S. R., James, D. F., (2000). Measurement of thermal conductivity of bovine cortical bone. *Medical Engineering & Physics* 22, 741-747.

Eriksson, A., Albrektsson, T., Grane, B., McQueen, D., (1982). Thermal injury to bone. A vital-microscopic description of heat effects. *International Journal Of Oral Surgery* 11, 115-121.

Eriksson, A. R., Albrektsson, T., (1983). Temperature threshold levels for heat-induced bone tissue injury: a vital-microscopic study in the rabbit. *Journal Of Prosthetic Dentistry* 50, 101-107.

Eriksson, A. R., Albrektsson, T., Albrektsson, B., (1984). Heat caused by drilling cortical bone. Temperature measured in vivo in patients and animals. *Acta Orthopaedica Scandinavica* 55, 629-631.

Eriksson, R. A., Albrektsson, T., (1984). The effect of heat on bone regeneration: an experimental study in the rabbit using the bone growth chamber. *Journal Of Oral And Maxillofacial Surgery: Official Journal Of The American Association Of Oral And Maxillofacial Surgeons* 42, 705-711.

Firoozbakhsh, K., Moneim, M. S., Mikola, E., Haltom, S., (2003). Heat generation during ulnar osteotomy with microsagittal saw blades. *The Iowa Orthopaedic Journal* 23, 46-50.

Giraud, J. Y., Villemin, S., Darmana, R., Cahuzac, J. P., Autefage, A., Morucci, J. P., (1991). Bone cutting. *Clinical Physics And Physiological Measurement: An Official Journal Of The Hospital Physicists' Association, Deutsche Gesellschaft Fur Medizinische Physik And The European Federation Of Organisations For Medical Physics* 12, 1-19.

Hall, R. M., (1959). Surgical removal of impacted teeth using air turbine unit. *Journal Of Oral Surgery, Anesthesia, And Hospital Dental Service* 17, 3-7.

Hall, R. M., (1965). The effect of high-speed bone cutting without the use of water coolant. *Oral Surgery, Oral Medicine, And Oral Pathology* 20, 150-153.

Hillery, M. T., Shuaib, I., (1999). Temperature effects in the drilling of human and bovine bone. *Journal of Materials Processing Technology* 92-93, 302-308.

Horner, D. B., (1961). A self-powered low-speed surgical drill: presentation of thermal necrosis. *American Journal of Orthopedics* 3, 278-283.

Jacob, C. H., Berry, J. T., Pope, M. H., Hoaglund, F. T., (1976). A study of the bone machining process: Drilling. *Journal of Biomechanics* 9, 343-349.

Jacobs, C. H., Pope, M. H., Berry, J. T., Hoaglund, F., (1974). A study of the bone machining process: Orthogonal cutting. *Journal of Biomechanics* 7, 131-132.

Jacobs, R. L., Ray, R. D., (1972). The effect of heat on bone healing. A disadvantage in the use of power tools. *Archives Of Surgery (Chicago, Ill.: 1960)* 104, 687-691.

Jowsey, J., (1966). Studies of Haversian systems in man and some animals. *Journal Of Anatomy* 100, 857-864.

Khambay, B. S., Walmsley, A. D., (2000). Investigations into the use of an ultrasonic chisel to cut bone. Part 1: Forces applied by clinicians. *Journal Of Dentistry* 28, 31-37.

Khanna, A., Plessas, S. J., Barrett, P., Bainbridge, L. C., (1999). The thermal effects of Kirschner wire fixation on small bones. *Journal Of Hand Surgery (Edinburgh, Lothian)* 24, 355-357.

Kirkland, R. W., (1967). In vivo thermal conductivity values for bovine and caprine osseous tissue. In: *Proceedings of the 20th Annual Conference on Engineering in Medicine and Biology* 20.4, Boston, MA.

Krause, W., (1977). Bone cutting: mechanical and thermal effects. *Bulletin Of The Hospital For Joint Diseases* 38, 5-7.

Krause, W. R., Bradbury, D. W., Kelly, J. E., Lunceford, E. M., (1982). Temperature elevations in orthopaedic cutting operations. *Journal of Biomechanics* 15, 267-275.

Labosky, D. A., Waggy, C. A., (1996). Oblique ulnar shortening osteotomy by a single saw cut. *The Journal Of Hand Surgery* 21, 48-59.

Larsen, S. T., Ryd, L., (1989). Temperature elevation during knee arthroplasty. *Acta Orthopaedica Scandinavica* 60, 439-442.

Lavelle, C., Wedgwood, D., (1980). Effect of internal irrigation on frictional heat generated from bone drilling. *Journal Of Oral Surgery (American Dental Association: 1965)* 38, 499-503.

Lundskog, J., (1972). Heat and bone tissue. An experimental investigation of the thermal properties of bone and threshold levels for thermal injury. *Scandinavian Journal Of Plastic And Reconstructive Surgery* 9, 1-80.

Lurie, R., Cleaton-Jones, P., Vieira, E., Sam, C., Austin, J., (1984). Effects of water and saline irrigation during bone cutting on bone healing. *International Journal Of Oral Surgery* 13, 437-444.

Majno, G., (1975). *The healing hand*. Harvard University Press, Cambridge.

Martin, R. B., Boardman, D. L., (1993). The effects of collagen fiber orientation, porosity, density, and mineralization on bovine cortical bone bending properties. *Journal of Biomechanics* 26, 1047-1054.

Martin, R. B., Burr, D. B., Sharkey, N. L., (1998). *Skeletal Tissue Mechanics*. Springer-Verlag, New York.

Matthews, L. S., Hirsch, C., (1972). Temperatures measured in human cortical bone when drilling. *The Journal Of Bone And Joint Surgery.American Volume* 54, 297-308.

McFall, T. A., Yamane, G. M., Burnett, G. W., (1961). Comparison of the cutting effect on bone of an ultrasonic cutting device and rotary burs. *Journal Of Oral Surgery, Anesthesia, And Hospital Dental Service* 19, 200-209.

Merchant, E., (1945a). Mechanics of metal cutting process 2. Orthogonal cutting and a type 2 chip. *Journal of Applied Physics* 16, 318-324.

Merchant, E., (1945b). Mechanics of metal cutting process 1. Orthogonal cutting and a type 2 chip. *Journal of Applied Physics* 16, 267-275.

Moses, W. M., Witthaus, F. W., Hogan, H. A., Laster, W. R., (1995). Measurement of the thermal conductivity of cortical bone by an inverse technique. *Experimental Thermal and Fluid Science* 11, 34-39.

Moss, R. W., (1964). Histopathologic reaction of bone to surgical cutting. *Oral Surgery, Oral Medicine, And Oral Pathology* 17, 405-414.

Pallan, F. G., (1960). Histological changes in bone after insertion of skeletal fixation pins. *Journal Of Oral Surgery, Anesthesia, And Hospital Dental Service* 18, 400-408.

Plaskos, C., Hodgson, A., Cinquin, P., (2003). Modelling and optimization of bone-cutting forces in orthopaedic surgery. In: *Proceedings of the 6th International Conference on Medical Image Computing and Computer-Assisted Intervention. Lecture Notes in Computer Science* 2878, 254-261, Montréal, Canada.

Ranu, H. S., (1987). The thermal properties of human cortical bone: an in vitro study. *Engineering In Medicine* 16, 175-176.

Reingewirtz, Y., Szmukler-Moncler, S., Senger, B., (1997). Influence of different parameters on bone heating and drilling time in implantology. *Clinical Oral Implants Research* 8, 189-197.

Rho, J. Y., Kuhn-Spearing, L., Zioupos, P., (1998). Mechanical properties and the hierarchical structure of bone. *Medical Engineering & Physics* 20, 92-102.

Rouiller, C., Majno, G., (1953). Morphologische und chemische Untersuchungen an Knochen nach Hitzeinwirkung [German] [Morphological and chemical studies of bones after the application of heat]. *Beitrage Zur Pathologischen Anatomie Und Zur Allgemeinen Pathologie* 113, 100-120.

Sambrook, P., (2004). Bone structure and function in normal and disease states [online]. Available from: <http://www.fleshandbones.com/readingroom/pdf/113.pdf> [Accessed 14 August 2005]

Sharawy, M., Misch, C. E., Weller, N., Tehemar, S., (2002). Heat generation during implant drilling: the significance of motor speed. *Journal Of Oral And Maxillofacial Surgery: Official Journal Of The American Association Of Oral And Maxillofacial Surgeons* 60, 1160-1169.

Shin, H. C., Yoon, Y. S., (2006). Bone temperature estimation during orthopaedic round bur milling operations. *Journal of Biomechanics* 39, 33-39.

Tetsch, P., (1974). Development of raised temperature after osteotomies. *Journal Of Maxillofacial Surgery* 2, 141-145.

Thompson, H. C., (1958). Effect of drilling into bone. *Journal Of Oral Surgery, Anesthesia, And Hospital Dental Service* 16, 22-30.

Toksvig-Larsen, S., Ryd, L., Lindstrand, A., (1991). On the problem of heat generation in bone cutting. Studies on the effects on liquid cooling. *The Journal Of Bone And Joint Surgery. British Volume* 73, 13-15.

Toksvig-Larsen, S., Ryd, L., Lindstrand, A., (1992). Temperature influence in different orthopaedic saw blades. *The Journal Of Arthroplasty* 7, 21-24.

Toksvig-Larsen, S., Ryd, L., Lindstrand, A., (1990). An internally cooled saw blade for bone cuts. Lower temperatures in 30 knee arthroplasties. *Acta Orthopaedica Scandinavica* 61, 321-323.

Tortora, G. J., Derrickson, B. H. (2005). *Principles of Anatomy and Physiology*. John Wiley & Sons Inc., New Jersey.

Turner, C. H., Burr, D. B., (1993). Basic biomechanical measurements of bone: a tutorial. *Bone* 14, 595-608.

Vachon, R. I., Walker, F. J., Walker, D. F., Nix, G. H., (1967). In vivo determination of thermal conductivity of bone using the thermal comparator technique. In: *Digest of the seventh International Conference on Medical and Biological Engineering Session 37*, 502-Stockholm, Sweden.

Wachter, R., Stoll, P., (1991). Increase of temperature during osteotomy. In vitro and in vivo investigations. *International Journal Of Oral And Maxillofacial Surgery* 20, 245-249.

Watanabe, F., Tawada, Y., Komatsu, S., Hata, Y., (1992). Heat distribution in bone during preparation of implant sites: heat analysis by real-time thermography. *The International Journal Of Oral & Maxillofacial Implants* 7, 212-219.

Wevers, H. W., Espin, E., Cooke, T. D., (1987). Orthopedic sawblades. A case study. *The Journal Of Arthroplasty* 2, 43-46.

Wiggins, K. L., Malkin, S., (1976). Drilling of bone. *Journal of Biomechanics* 9, 553-559.

Wiggins, K. L., Malkin, S., (1978). Orthogonal machining of bone. *Journal Of Biomechanical Engineering* 100, 122-130.

Yacker, M. J., Klein, M., (1996). The effect of irrigation on osteotomy depth and bur diameter. *The International Journal Of Oral & Maxillofacial Implants* 11, 634-638.

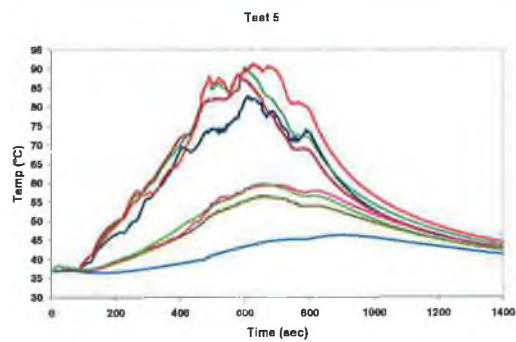
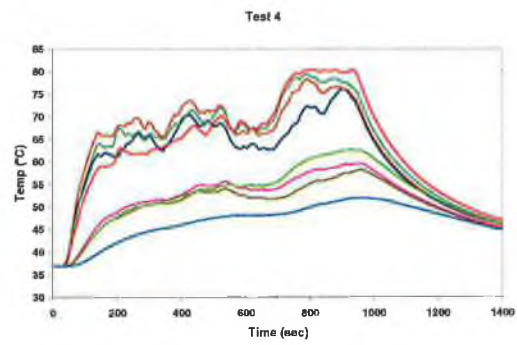
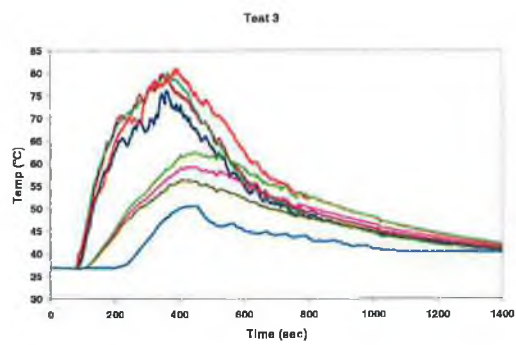
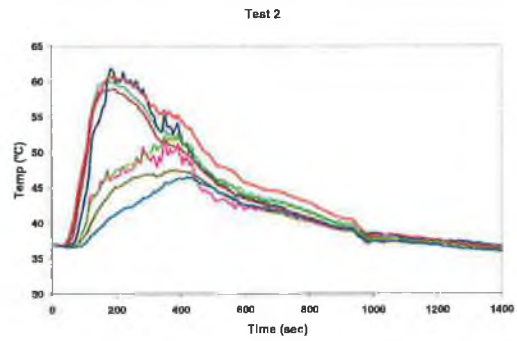
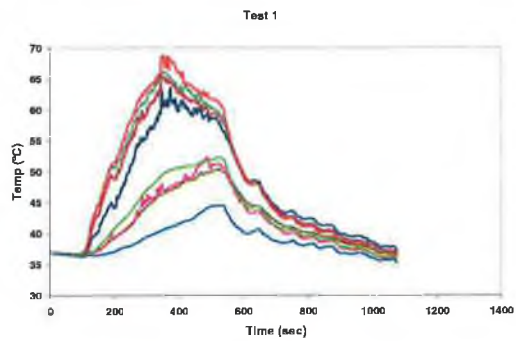
Zelenov, E. S., (1985). Experimental investigation of the thermophysical properties of compact bone. *Mechanics of Composite Materials* 21, 759-762.

Appendix A

(Experiment 1 Graphs)

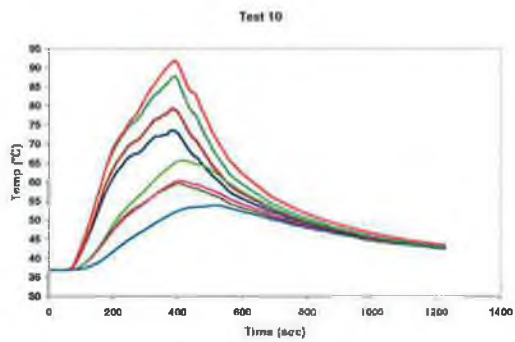
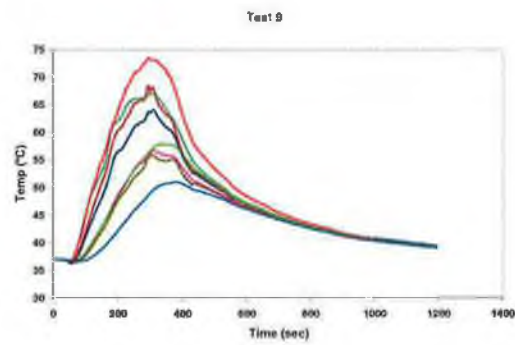
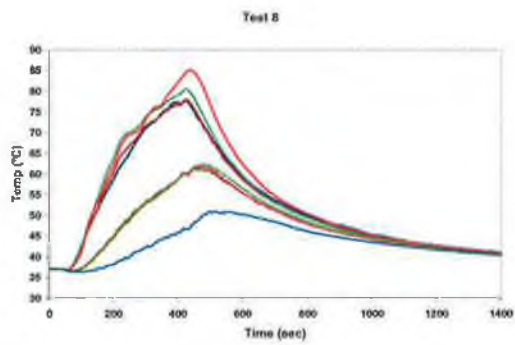
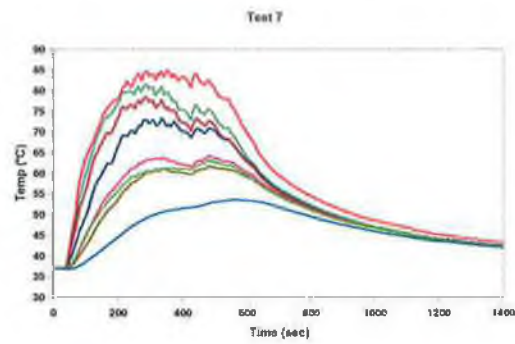
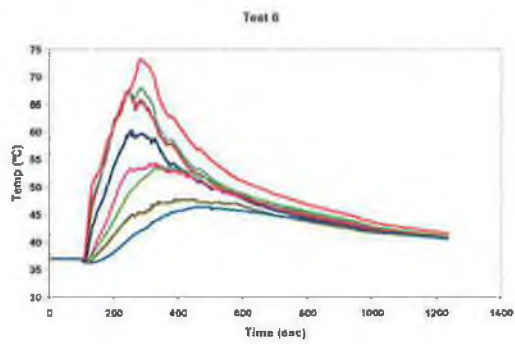
Temperature Measurement Graphs

(Experiment 1, Blade 1)



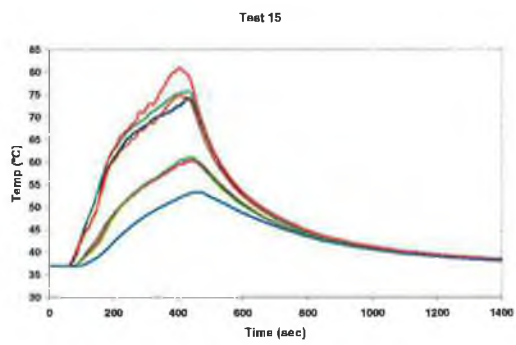
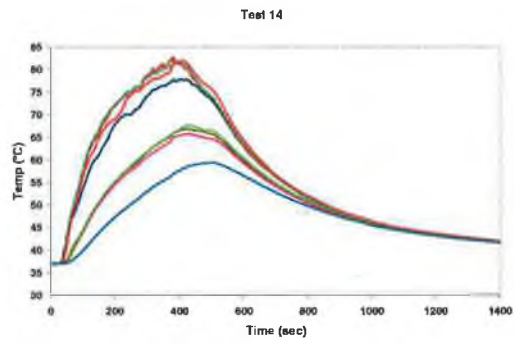
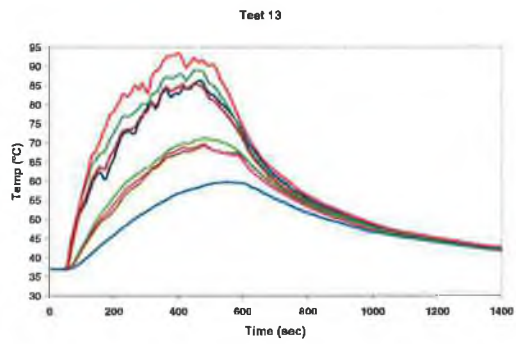
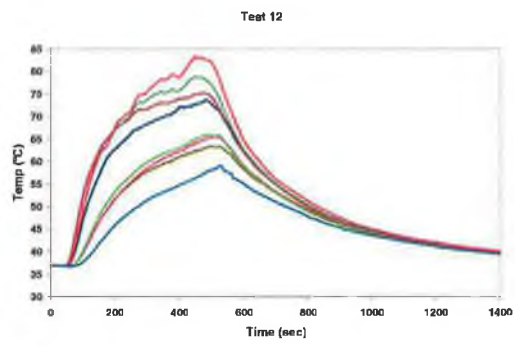
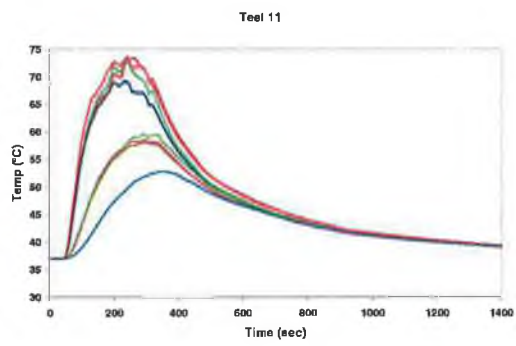
Temperature Measurement Graphs

(Experiment 1, Blade 2)



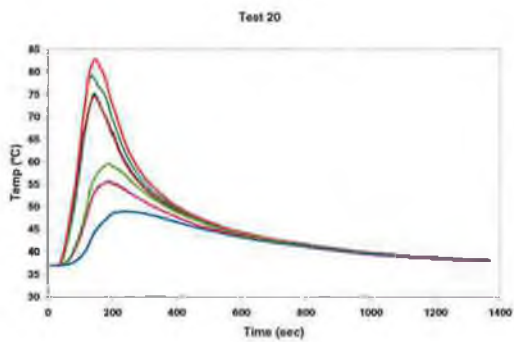
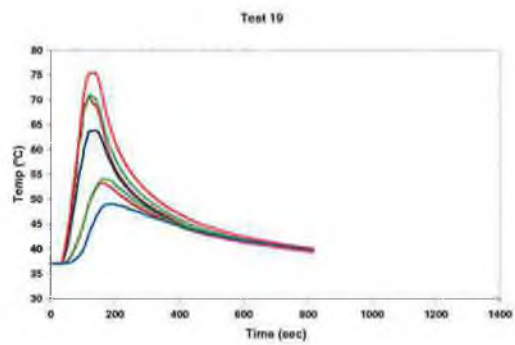
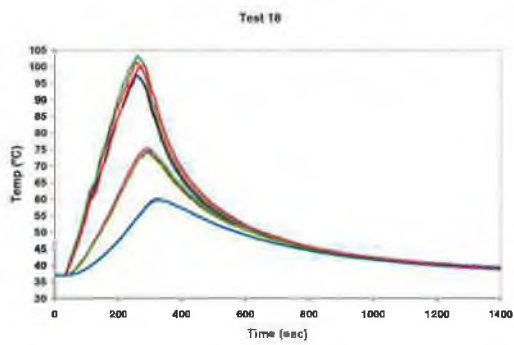
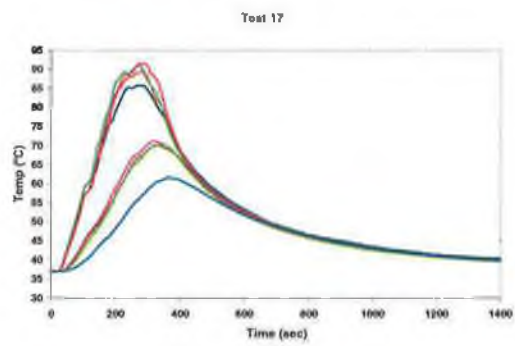
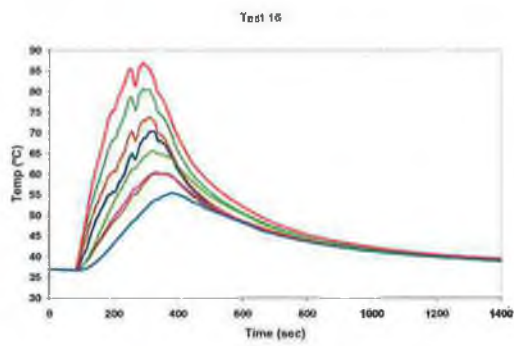
Temperature Measurement Graphs

(Experiment 1, Blade 3)



Temperature Measurement Graphs

(Experiment 1, Blade 4)

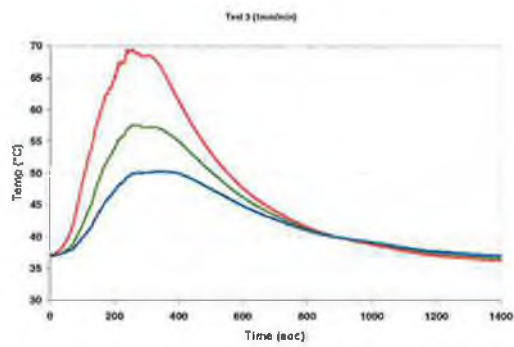
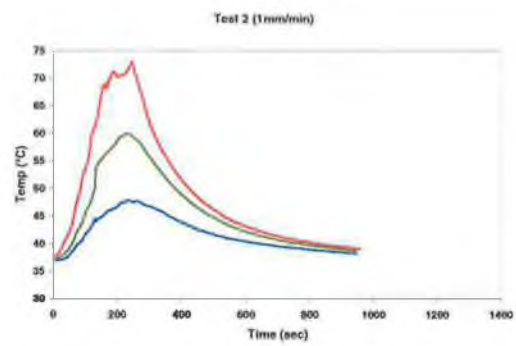
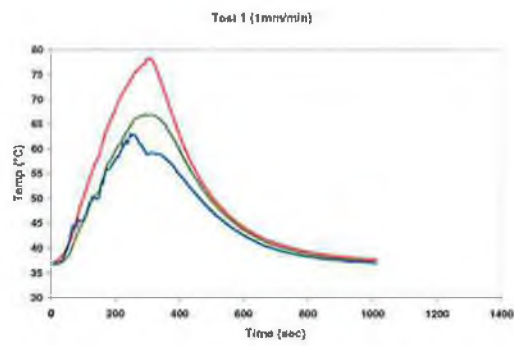


Appendix B

(Experiment 2 Graphs)

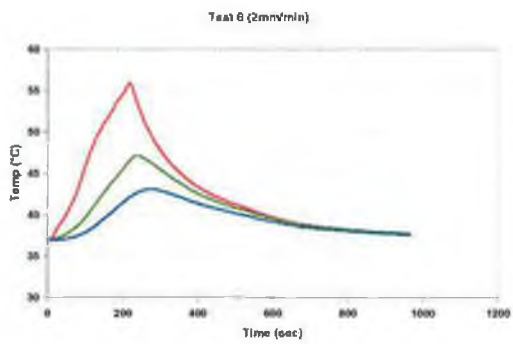
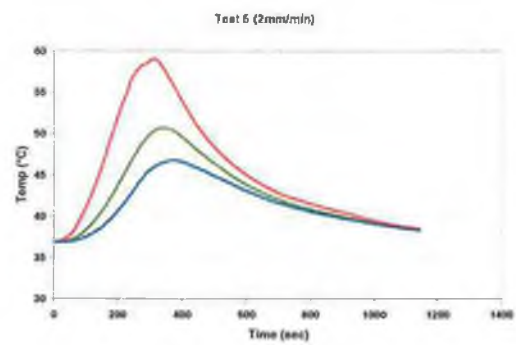
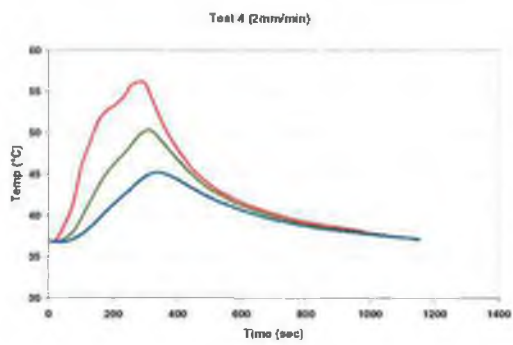
Temperature Measurement Graphs

(Experiment 2, Blade 5) Cutting Rate=1 mm/min



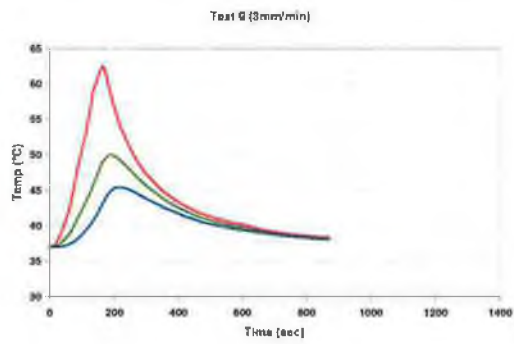
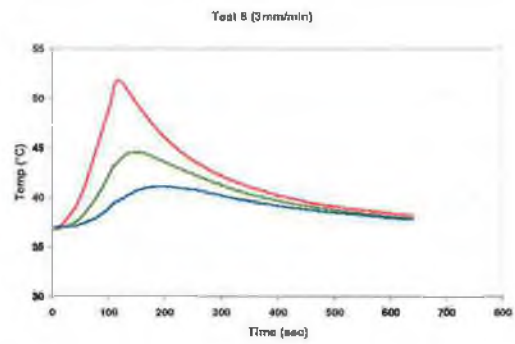
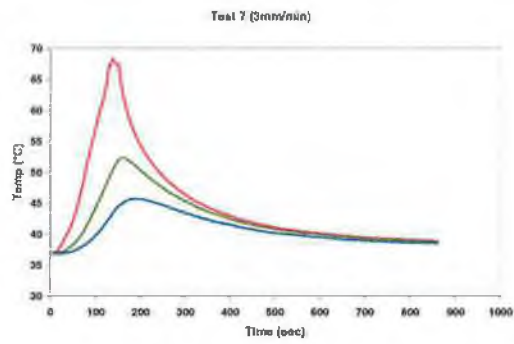
Temperature Measurement Graphs

(Experiment 2, Blade 6) Cutting Rate=2 mm/min



Temperature Measurement Graphs

(Experiment 2, Blade 7) Cutting Rate=3 mm/min



Appendix C

(Technical Sheets)

Squirrel 2020 DATA LOGGERS



System Specification

Input channels:								
2020 TYPE	ADCs	ANALOG INPUT CHANNEL OPTIONS			PULSE	ADDITIONAL CHANNELS		
		DIFFERENTIAL	SINGLE ENDED	3 OR 4 WIRE		EVENT/DIGITAL	HIGH VOLTAGE	INTERNAL CHANNELS
1F8	x 1	8	16	0	(2 x fast - 64kHz) & (2 x slow -100Hz)	8 State inputs or 1 x 8 bit Binary	2	1 Temperature
2F8	x 2	8	16	4	(2 x fast - 64kHz) & (2 x slow -100Hz)	8 State inputs or 1 x 8 bit Binary	2	1 Temperature

Standard ranges for temperature channels:

Each channel can be individually set to any of the ranges listed below. Pt100 to IEC751 and JIS1604 and Pt1000 to IEC751.

INPUT TYPE	RANGES °C	RANGES °F	INPUT TYPE	RANGES °C	RANGES °F
Y & U: Thermistor	-50 to 150	-58 to 302	K: Thermocouple	-200 to 1372	-328 to 2501
S: Thermistor	-30 to 150	-22 to 302	T: Thermocouple	-200 to 400	-328 to 752
			J: Thermocouple	-200 to 1200	-328 to 2192
Pt100/Pt1000	-200 to 850	-328 to 1562	N: Thermocouple	-200 to 1300	-328 to 2372
			R & S: Thermocouple	-50 to 1768	-58 to 3214

Standard ranges for d.c. voltage/current and resistance channels:

Each voltage/current channel can be any of the voltage or current ranges below. Mixed differential and single ended configurations are permitted.

Note: current ranges use differential input channels.

VOLTAGE RANGE	VOLTAGE RANGE	HIGH VOLTAGE RANGE	CURRENT RANGE (Ext 100 μ SHUNT)	RESISTANCE RANGE 2 WIRE	RESISTANCE RANGE 3 AND 4 WIRE (2F8 VERSION)
-0.075 to 0.075V	-3.0 to 3.0V	4.0 to 20.0V	-30.0 to 30.0mA	0.0 to 1250.0 Ω	0.0 to 500.0 Ω
-0.15 to 0.15V	-6.0 to 6.0V	4.0 to 40.0V	4 to 20mA	0.0 to 5000.0 Ω	0.0 to 4000.0 Ω
-0.3 to 0.3V	-6.0 to 12.0V	4.0 to 60.0V		0.0 to 20000.0 Ω	
-0.6 to 0.6V	-6.0 to 25.0V			0.0 to 300000.0 Ω	
-0.6 to 1.2V					
-0.6 to 2.4V					

ANALOG INPUTS

Accuracy: (at 25°C) voltage and resistance

\pm (0.05% readings + 0.025% range)

Common mode rejection: 100dB

Input impedance: > 1M Ω

Linearity: 0.015%

Series mode line rejection: 50/60Hz 100dB

ANALOG-DIGITAL CONVERSION

Type: Sigma-Delta

Resolution: 24bit

Sampling rate: up to 10, 20* or 100* readings

per second per ADC. No 100Hz on 1F8.

ALARM OUTPUTS

4 x open drain FET (18V 0.1A)

POWER OUTPUT FOR EXTERNAL DEVICE

Regulated 5 VDC at 50mA or logger supply voltage at 100mA

TIME AND DATE

In built clock in 3 formats

SCALING DATA

Displays readings in preferred engineering units.

MEMORY

Internal: 16Mb (Up to 1,800,000 readings)

External: Up to 64Mb - removable MMC

(For transferring internal memory and storing setups only)

* With mains rejection off

CALCULATED CHANNELS

Up to 16 virtual channels derived from physical input channels

RESOLUTION

Up to 6 significant digits

PROGRAMMING/LOGGER SETUP

SquirrelView or SquirrelView Plus software

COMMUNICATION

Standard: RS232 (Auto bauding to 115k baud)

USB 1.1 and 2.0 compatible

External options: Ethernet, GSM and PSTN Modems

POWER SUPPLY

Internal: 6 x AA Alkaline batteries

External: 10-18VDC

Reverse polarity and over-voltage protected

POWER CONSUMPTION @ 9V

Sleep mode: 600 μ A

Logging: 40-80mA

DIMENSIONS AND WEIGHT

Dimensions: W235 x D175 x H55mm

Weight: Approx 1.2kgs

Enclosure material: ABS

MEMORY MODES (internal only)

Stop when full or overwrite

DISPLAY AND KEYPAD

2 line x 40 character LCD display

Battery state and external power indicator

Keypad lock

Navigate to:

Arm/disarm/pause/continue

Meter any channel or alarm

Select from up to 6 x pre-stored setups

Status/diagnostics/memory/time and date

Download to MMC

OPERATING ENVIRONMENT

-30°C to +65°C

Humidity: 90% at 40°C non condensing

ACCESSORIES

MPU 12V: Universal (97-263V AC) power supply

LC76: DC lead

SQ20RB12-6: External rechargeable battery (12V, 6Ah)

SB102: 25 way digital I/O connector

CS202: Current shunt kit (8 x 10 Ω 0.125W)

PEL4: Rugged weather proof enclosure

CAL2020: Test and Calibration certificates

SQ20A802: External GSM communications kit

SQ20A801: External Ethernet adaptor kit

MMC64: Multi Media Card

(Please see price list for additional accessories)

Please note: SQ2020 is supplied with software, manual, USB cable, wall bracket and batteries.

Due to our policy of continuous improvements, specifications may change without prior notice. Grant believe that all information declared is correct at the time of issue. No liability is accepted for errors and omissions.



Grant Instruments
(Cambridge) Ltd
Shepreth
Cambridgeshire
SG8 6GB England

Tel: +44 (0) 1763 260811

Fax: +44 (0) 1763 262410

www.grant.co.uk

loggersales@grant.co.uk

Printed in England-2020/0205UK/V3

Software

SquirrelView - supplied with 2020

2020 logger setup, download and data export to Excel or CSV application for Windows 98, 2000 and XP. Features include metering and support for Modem, Ethernet and GSM communications.

SquirrelView Plus

As SquirrelView with additional features including on-line or historical graphing of data with manual and automatic scaling of charts. Readings can be listed in tabular format with timestamps and statistics.

Warranty: Equipment manufactured by Grant Instruments is warranted against faulty materials or workmanship for three years. For repairs carried out under warranty, no charge is made for labour, materials or return carriage.

CE mark: The Grant 2020 data acquisition system bears a CE mark and meets relevant European directives.

Quality Statement: Grant Instruments operates a Quality Management System complying with ISO9001:2000.

It is Grant's policy to supply customers with products which are fit for their intended purpose, safe in use, perform reliably to published specification and are backed by a fast and efficient customer support service.

Manufactured and designed in Cambridge, England.



Loctite Corporation
 1001 Trout Brook Crossing
 Rocky Hill, CT 06067-3910
 Telephone: (860) 571-5100
 FAX: (860) 571-5465

Technical Data Sheet

Product 454

Worldwide Version, December 1995

PRODUCT DESCRIPTION

LOCTITE® Product 454 is fast curing, single component gel cyanoacrylate adhesive. It is specifically formulated for difficult to bond substrates. The gel consistency prevents adhesive flow even on vertical surfaces.

TYPICAL APPLICATIONS

Rapid bonding of a wide range of metal, plastic or elastomeric materials, particularly suited for bonding porous or absorbent materials such as wood, paper, leather or fabric.

PROPERTIES OF UNCURED MATERIAL

	Value	Typical Range
Chemical Type	Ethyl cyanoacrylate	
Appearance	Clear, translucent	
Specific Gravity @ 25°C	1.1	
Viscosity @ 25°C, mPa.s (cP)	Gel	
Flash Point (TCC), °C	>80	

TYPICAL CURING PERFORMANCE

Under normal conditions, the surface moisture initiates the hardening process. Although full functional strength is developed in a relatively short time, curing continues for at least 24 hours before full chemical/solvent resistance is developed.

Cure speed vs. substrate

The rate of cure will depend on substrate used. The table below shows the fixture time achieved on different materials at 22°C, 50% relative humidity. This is defined as the time to develop a shear strength of 0.1 N/mm² (14.5 psi) tested according to ASTM D1002.

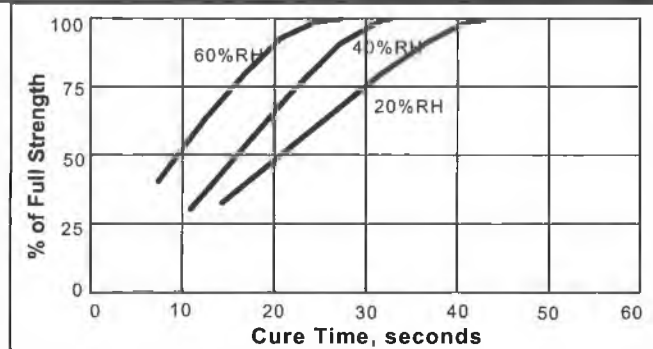
Substrate	Fixture Time, seconds
Steel (degreased)	5 to 20
Aluminum	2 to 10
Zinc dichromate	10 to 20
Neoprene	<5
Nitrile rubber	<5
ABS	2 to 10
PVC	2 to 10
Polycarbonate	10 to 40
Phenolic materials	2 to 10

Cure speed vs. bond gap

The rate of cure will depend on the bondline gap. High cure speed is favored by thin bond lines. Increasing the bond gap will slow down the rate of cure.

Cure speed vs. humidity

The rate of cure will depend on the ambient relative humidity. The following graph shows the tensile strength developed with time on Buna N rubber at different levels of humidity.



Cure speed vs. activator

Where cure speed is unacceptably long due to large gaps or low relative humidity applying activator to the surface will improve cure speed. However, this can reduce the ultimate strength of the bond, therefore testing is recommended to confirm effect.

TYPICAL PROPERTIES OF CURED MATERIAL

Physical Properties

Coefficient of thermal expansion, ASTM D696, K ⁻¹	80 x 10 ⁻⁶
Coefficient of thermal conductivity, ASTM C177, W.m ⁻¹ K ⁻¹	0.1
Glass transition temperature, ASTM, E228, °C	120

Electrical Properties

	Constant	Loss	
Dielectric constant & loss, 25°C, ASTM D150 measured at	100Hz	2.65	<0.02
	1kHz	2.75	<0.02
	10kHz	2.65	<0.02
Volume resistivity, ASTM D257, Ω.cm		1 x 10 ¹⁶	
Surface resistivity, ASTM D257, Ω		1 x 10 ¹⁶	
Dielectric strength, ASTM D149, kV/mm		25	

PERFORMANCE OF CURED MATERIAL

(After 24 hr at 22°C)

	Value	Typical Range
Shear Strength, ASTM D1002/DIN 53283		
Grit Blasted Steel, N/mm ²	22	18 to 26
(psi)	(3200)	(2600 to 3800)
Etched Aluminum, N/mm ²	15	11 to 19
(psi)	(2200)	(1600 to 2800)
Zinc dichromate, N/mm ²	7	4 to 10
(psi)	(1000)	(600 to 1500)
ABS, N/mm ²	13	6 to 20
(psi)	(1900)	(900 to 3000)
PVC, N/mm ²	13	6 to 20
(psi)	(1900)	(900 to 3000)
Polycarbonate, N/mm ²	12.5	5 to 20
(psi)	(1800)	(700 to 3000)
Phenolic, N/mm ²	10	5 to 15
(psi)	(1500)	(700 to 2200)
Neoprene rubber, N/mm ²	10	5 to 15
(psi)	(1500)	(700 to 2200)
Nitrile rubber, N/mm ²	10	5 to 15
(psi)	(1500)	(700 to 2200)
Tensile Strength, ASTM D2095, DIN 53282		
Grit Blasted Steel, N/mm ²	18.5	12 to 25
(psi)	(2700)	(1700 to 3600)
Buna N rubber, N/mm ²	10	5 to 15
(psi)	(1500)	(700 to 2200)

NOT FOR PRODUCT SPECIFICATIONS.

THE TECHNICAL DATA CONTAINED HEREIN ARE INTENDED AS REFERENCE ONLY.

PLEASE CONTACT LOCTITE CORPORATION QUALITY DEPARTMENT FOR ASSISTANCE AND RECOMMENDATIONS ON SPECIFICATIONS FOR THIS PRODUCT.

ROCKY HILL, CT FAX: +1 (860)-571-5473

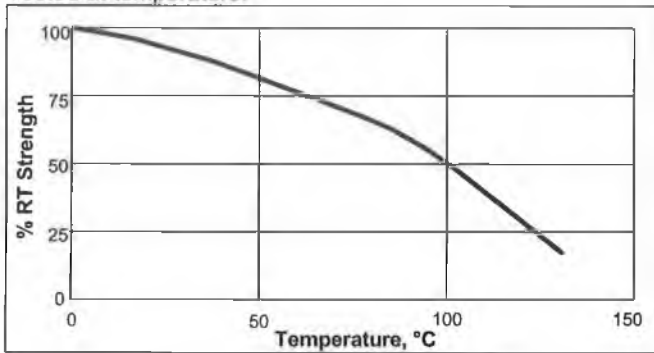
DUBLIN, IRELAND FAX: +353-(1)-451-9959

TYPICAL ENVIRONMENTAL RESISTANCE

Test Procedure : Shear Strength ASTM D1002/DIN 53283
 Substrate: Grit blasted mild steel laps
 Cure procedure: 1 week at 22°C

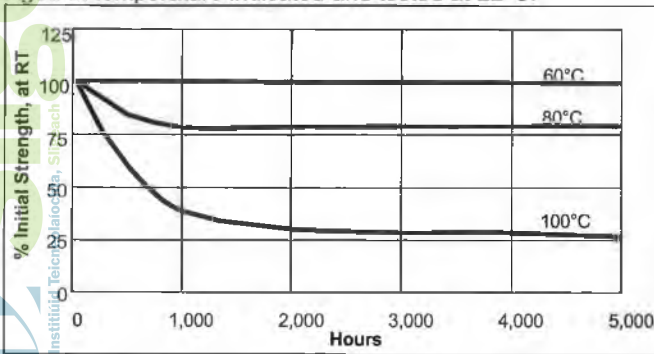
Hot Strength

Tested at temperature.



Heat Aging

Aged at temperature indicated and tested at 22°C.



Chemical / Solvent Resistance

Aged under conditions indicated and tested at 22°C.

Solvent	Temp.	% Initial strength retained at		
		100 hr	500 hr	1000 hr
Motor Oil	40°C	85	85	75
Leaded Petrol	22°C	100	100	100
Ethanol	22°C	100	100	100
Isopropanol	22°C	100	100	100
Freon T.A.	22°C	100	100	100
Humidity 95% RH	40°C	65	55	50
Humidity 95% RH polycarbonate	40°C	100	100	100

GENERAL INFORMATION

This product is not recommended for use in pure oxygen and/or oxygen rich systems and should not be selected as a sealant for chlorine or other strong oxidizing materials.

For safe handling information on this product, consult the Material Safety Data Sheet, (MSDS).

Directions for use

For best performance surfaces should be clean and free of grease. This product performs best in thin bond gaps, (0.05mm). Excess adhesive can be dissolved with Loctite clean up solvents, nitromethane or acetone.

Storage

Product shall be ideally stored in a cool, dry location in unopened containers at a temperature between 8°C to 21°C (46°F to 70°F) unless otherwise labeled. Optimal storage conditions for unopened containers of cyanoacrylate products are achieved with refrigeration: 2°C to 8°C (36°F to 46°F). Refrigerated packages shall be allowed to return to room temperature prior to opening and use. To prevent contamination of unused product, do not return any material to its original container. For specific shelf life information contact your local Technical Service Center.

Data Ranges

The data contained herein may be reported as a typical value and/or range (based on the mean value ±2 standard deviations). Values are based on actual test data and are verified on a periodic basis.

Note

The data contained herein are furnished for information only and are believed to be reliable. We cannot assume responsibility for the results obtained by others over whose methods we have no control. It is the user's responsibility to determine suitability for the user's purpose of any production methods mentioned herein and to adopt such precautions as may be advisable for the protection of property and of persons against any hazards that may be involved in the handling and use thereof. In light of the foregoing, **Loctite Corporation specifically disclaims all warranties expressed or implied, including warranties of merchantability or fitness for a particular purpose, arising from sale or use of Loctite Corporation's products. Loctite Corporation specifically disclaims any liability for consequential or incidental damages of any kind, including lost profits.** The discussion herein of various processes or compositions is not to be interpreted as representation that they are free from domination of patents owned by others or as a license under any Loctite Corporation patents that may cover such processes or compositions. We recommend that each prospective user test his proposed application before repetitive use, using this data as a guide. This product may be covered by one or more United States or foreign patents or patent applications.